Interaction Notes
Note 506
16 November 1993

An Application of the Electromagnetic Topology Theory on the Test-Bed Aircraft, EMPTAC

J.P. Parmantier, V. Gobin, F. Issac

**Office National d'Etudes et de Recherches
Aérospatiales**
8, rue des vertugadins
9290 Meudon,France
Tel: (33) 1 46 23 50 64
Fax: (33) 1 46 23 50 61

I. Junqua, Y. Daudy, J.M. Lagarde

Centre d'Etude de Gramat
46500, Gramat, France
Tel: (33) 65 10 53 34
Fax: (33) 65 10 54 09

Abstract

This note presents an experiment carried out in October, November 1993 on the electromagnetic pulse test-bed aircraft (EMPTAC), available at the Kirtland Air Force Base, Albuquerque, New Mexico, in collaboration with the Phillips Laboratory.

The document presents the analysis of the coupling to a wiring running inside the cockpit and the forward shielding volumes. Local excitations with current probe and global illumination with an Ellipticus antenna are presented. The note also points out how a topological data bank, constituted in France, on cables and electrical boxes of a test wiring, can be used to characterize the topology of the wiring and sources induced in each volume.

Comparison results between CRIPTE code calculations and measurements are presented on the test wiring and on the actual wiring of the aircraft.

1

Contents

1 - INTRODUCTION

1.1) Context

This report reviews a common experimentation between the Office National d'Etudes et de Recherches Aérospatiales (ONERA), the Centre d'Etudes de Gramat (CEG) and the Phillips Laboratory (PL). This experiment has been performed as a part of the DEA, MWDDEA 7336 on the atmospheric environment.

The objectives of this collaboration, defined in October 1992 during a technical meeting involving the three laboratories, were to apply the topological approach (both experimentally and numerically) to a cable network installed in the EMPTAC test-bed aircraft, with a view to the analysis of coupling phenomenon on the aircraft when it is submitted to a global illumination supplied by the Ellipticus antenna.

In order to achieve this program, two weeks of preliminary experimentation had been performed in France involving ONERA and CEG, in January and September 1993, and three weeks in the Phillips Laboratory, in November 1993, involving the three laboratories.

1.2) A few recalls on Electromagnetic Topology

The Electromagnetic Topology (EMT) is a method to analyse complex coupling problems, originally developed during the 70's in the U.S.A. The objective of this theory is to break down a complex system into elementary sub-systems, in order to find proper rules for the design of hardened structures.

Until 1987, the great majority of the scientific publications on EMT were based on a theoretical approach and a lot of interesting concept have been defined or developed: description of complex structure by means of E.M. interaction graphs, definition of shielding levels, description of wire interactions with transmission line theory, ...

In 1987, ONERA decided to complete former studies on EMC, by taking into account the EMT methodology (both on the experimental and theoretical point of view). The final purpose is to improve the potentiality of the method, in order to be able to understand E.M. interactions on actual structures, such as aircraft submitted to various kinds of E.M. aggressions. An important point is to be able to predict both qualitatively (by understanding the coupling processes) and quantitatively (by calculating field, voltage and current levels) the final interference on equipment.

A numerical code, named CRIPTE, based on the "BLT equation" derived by Baum, Liu and Tesche has been continuously developed to achieved this purpose. This tool comes from the multiconductor transmission line modelling ("tubes"). The interaction between tubes is calculated by means of topological scattering parameters (S-parameters) at "junctions". First experiments on canonical structures first, becoming more and more complex, have validated the methodology. Since 1990, a permanent collaboration between ONERA and CEG have improved the quality of the results on more and more realistic structures (modular built structures, industrial type problems ...). Results have been achieved both in the frequency and time domains, using local EM sources and full scale EMP simulators, available at Gramat. In 1993, studies were carried out with success on a full 1 scale Mirage III aircraft wing. A recent synthesis of our researches on EMT is reproduced in this report (see annex C)

1.3) Objectives of the experiment on the EMPTAC test-bed aircraft

The objective of the 1993 French/American collaboration is to reach further qualitative and quantitative results on a full 1 scale aircraft which was originally designed using topological rules.

1.4) EMPTAC test-bed aircraft presentation

The studies performed by the Phillips Laboratory intend to develop and validate hardening methods for E.M. design and maintenance. Following former studies on this aircraft, two series of major modifications of the structure have been carried out on the EMPTAC.

The first modification dealt with the building of two new shielded zones in the existing structure according to the geometry of the B1B bomber aircraft (see Fig. 1.1):

- The aft shielded volume

- The forward shielded volume

The second modification has consisted in introducing a cable network in the EMPTAC, representative of the one existing in the B1B aircraft and running throughout the previous defined shielded volumes. The scheme of the wiring concerning the forward shielded volume is presented in Fig. 1.2.

The modified structure of the EMPTAC, appears to be a perfect test-bed for the application of the EMT method, as it is developed nowadays at ONERA and CEG.

Therefore, a complete campaign and schedule has been defined, taking the availability of the involved laboratories and their facilities into account.
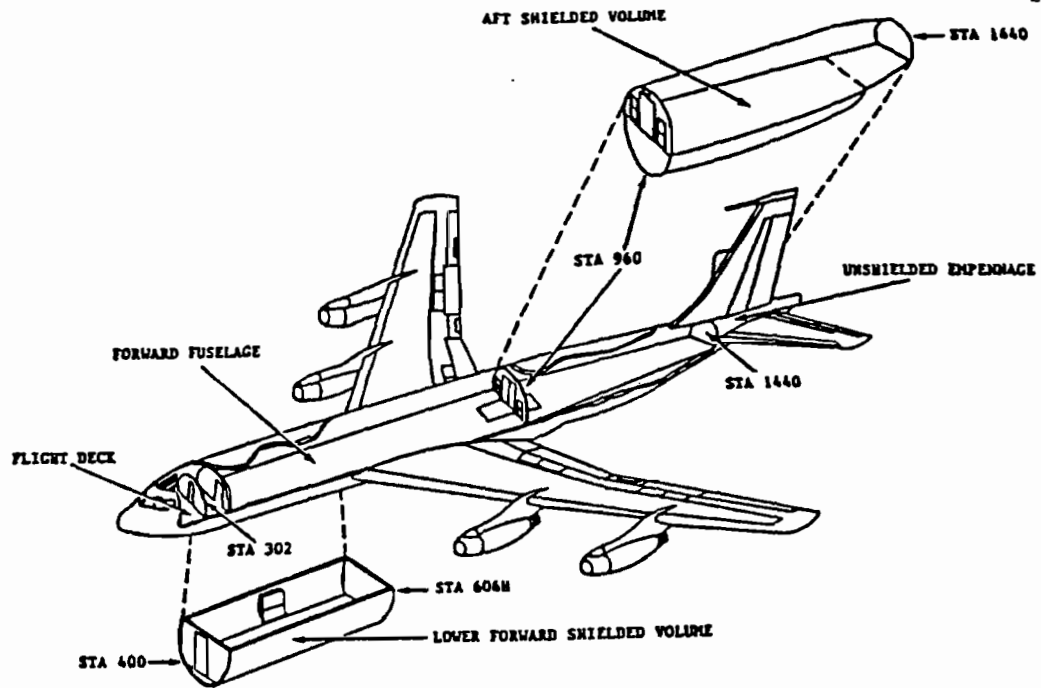
Fig. 1.1: EMPTAC sections after modifications
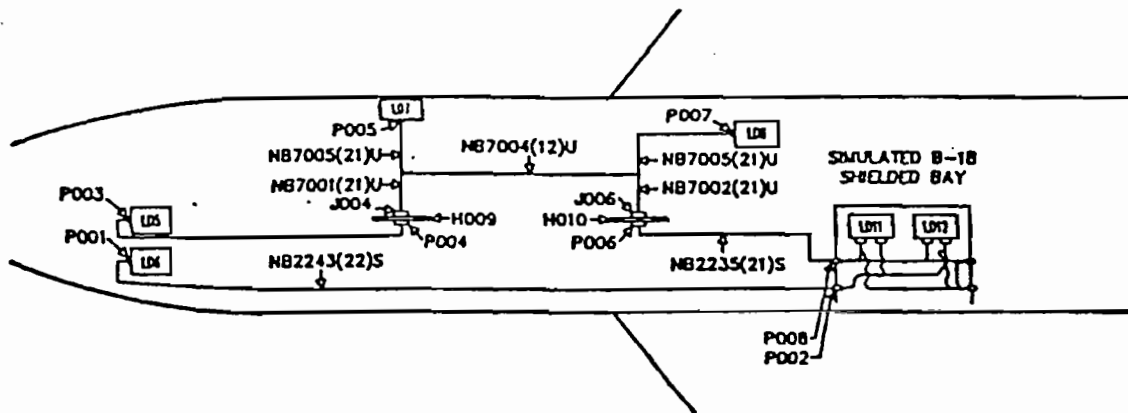
Fig. 1.2: Modified wiring in EMPTAC (part related to the forward shielded volume).

2 -DESCRIPTION OF THE PROGRAM

2.1) Introduction

The various points to consider for reaching the purpose of the experiment have been summarized in these following topics:

2.1.1) Two experiments

The experiment in Albuquerque being carried out in a limited time (3 weeks), a first experiment had to be done in France in order to obtain in advance all the parameters of the problem. During this first phase, experimental characterizations of the network under test was performed and a data base of the measured parameters was built to use in the second phase, held in Albuquerque.

2.1.2) Two networks

Although the actual whole modified EMPTAC network presents a very clean geometry (on the EMT point of view), it still remains complex for a first approach on a complex aircraft. It is the reason why the topological method has been applied by limiting the existing network to the forward shielded volume. This reduced network (network A) is constituted by the cables located in this volume and the cables connected to the cockpit.

Moreover, during the first phase in France, it was impossible to reproduce correctly the actual topology of the network and then, to qualify it experimentally. On the other hand, this network being composed of a high number of conductors (up to 22 wires per bundle), starting the experiment with a simplified configuration seemed to be a careful step. Therefore it was decided to create a simplified network (network B), made up of simple lines, up to three twisted lines, that had to be introduced in the forward shielded volume and into the cockpit. This network B had to run along the existing network A (all the geometrical parameters such as lengths, point to point connections being kept) and enabled a first qualitative topological approach of the existing network A. The objective of this phase was to apply the theory of electromagnetic topology in a case where all the electrical parameters of the signal propagation could be analysed and characterized experimentally.

In a second phase, network A has been studied to obtain quantitative results on the EMPTAC.

Note that, in France, the second network was installed on a large flat ground plane. Thus a second "in situ" characterization of this wiring, once installed in the EMPTAC, was necessary to appreciate the evolution of the various electrical parameters due to local geometrical changes.

2.2.3) Two electromagnetic sources

In order to progress with step by step procedure (former ONERA and CEG successes have been obtained with this methodology) the illumination of the whole aircraft was preceded by a local illumination phase. The decision was made to use a current injection probe as a perturbation point of entry on network B. This method had to be totally validated during the first phase.

2.2.4) Two parallel approaches

The objectives of the experimentation being to have both an experimental and a numerical analysis of the coupling processes, it was necessary to obtain the results of the modelling at the same time as the measurements. This "real time" organization of the work is the condition to be able to make decisions when unexpected observations are done.

To achieve this purpose, a lot of numerical data files were prepared in France and CRIPTE modelling were performed during the whole test phase. Because it is impossible to move the most powerful computer available at ONERA and CEG, 2 PC computers and a mobile work station were chosen. To get the results of the modelling with realistic delay, the numerical topological modelling of the networks was broken down in correlated sub networks as it will be shows in this report. The price to be paid for saving computer time is an increase of the numerical treatments (on a powerful computer, only one network file could have been used whereas 3 or more were necessary here).

2.2.5) Two analyses

The criteria for the success of the 1993 experimentation was neither a pure experimental **qualitative** analysis of the coupling on networks, neither a **quantitative** prediction of the response on each loads. What we expected was that the **complementary** aspect of both approaches would produce more interesting results than separated and independent experimental and numerical studies.

2.2) Program synopsis

The following chart sums up the different phases of studies :

preliminary works performed in french laboratories

Network B _characterization_ _on a ground plane_ - Calculations - Measurements	**_Network A_** _characterization_ - Calculations

Network B
 Current injection
 - Calculations
 - Measurements

Experiment in the Phillips Laboratory

Network B _in situ_ _Current injection_ - Calculations - Measurements	**_Network A_** _in situ_ _Current injection_ - Calculations - Measurements
Network B _in situ_ _CW Illumination_ - Calculations - Measurements	**_Network A_** _in situ_ _CW Illumination_ - Calculations - Measurements

3 - EXPERIMENT ON NETWORK B

3.1) Objectives

Two weeks of experiment were held in France, in January and October 1993, in order to prepare the final experiment in Albuquerque. The network B has only been considered in this first phase, because no sufficient electrical data were available on network A. Thus, Network B was built in France, and has been installed in the EMPTAC cargo aircraft.

The main objective of this first experiment was to constitute a data bank on all the lines, termination boxes, current probes, and then have the first predictive response on the Network, in a canonical geometrical case.

During the experiment in Albuquerque, these data have been directly introduced into our network numerical simulations and only a few lines, boxes or probes further characterization had to be carried out, to take local variation of the EMPTAC geometry into account.

3.2) Description of network B

Network B is made of four boxes LD5M, LD7M, LD8M, LD6M, similar to Network A boxes of (Fig 3.1)

Fig. 3.1: Electrical scheme of network B

Instead of 21 termination loads, these boxes contain only 3 output ports, terminated on SMA connectors. In the first experiment, all the loads considered have been taken equal to 50Ω. Considering that the input port of the network analyser is also equal to 50 Ω, it is possible to make direct voltage and S-parameter measurements on these ports. The SMA connectors are then connected to a multiconductor connector with coaxial 50Ω cables (fig 3.2).
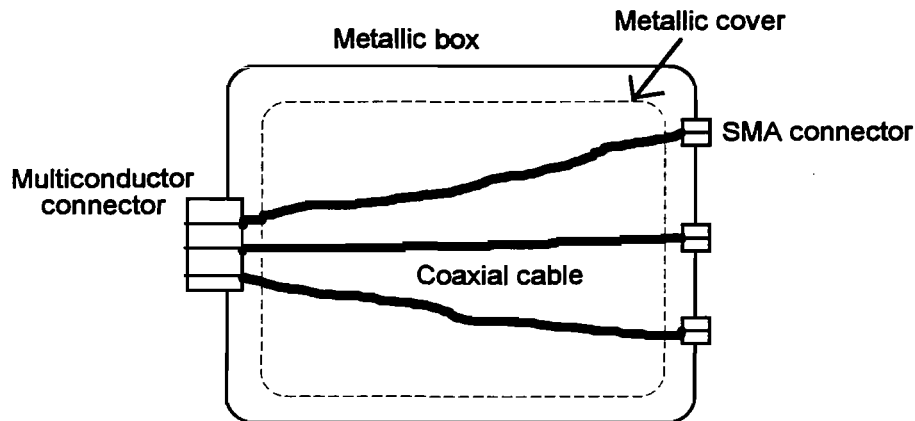
Fig. 3.2: top view of Network B' metallic box

In the aircraft, LD5M is located inside the cockpit, screwed on the separation wall in place of Network A' LD5 box. LD7M, LD8M are located inside the lower shielded volume in place of network A' LD7 and LD8. LD6M does not represent a real box, but a connector with 3 coaxial cables, connected at the J006 point of network A, inside the fuselage.

Network B' harness can easily be disconnected at J004 and J006. Inside the cockpit, a 3 wire shielded cable connects LD5M box and J004 interface connector.

During the first experiment, network B was placed on a metallic ground plane, reproducing the running of cables inside the forward shielding volume. The dimensions of the various sections of the harness are similar to Network A ones. The only difference between the network B tested in France and the network B tested in Albuquerque comes from the length of the shielded cable. In France, it has been chosen equal to 3.10 meters whereas it is 6.1 meters in the EMPTAC aircraft (the geometrical documents mentioned 3.10 meters).

The electrical connections between the various wires are presented on figure 3.3.

3 wires are connected on each box:
- L59, L56, L55 on LD5M box
- L79, L76, L75 on LD7M box
- L85, L86, L89 on LD8M box
- P65, P66, P69 on LD6M box

Some wires connect directly LD5M and LD7M boxes on the left side of the network, as in the actual network A:

- wire from port L55 to port L75
- wire from port L56 to port L76.

Some wires connect directly LD6M and LD8M on the right side:

- wire from port P65 to port L85
- wire from port P66 to port L86.

Other wires connect boxes of the left and right sides:

- wire from port L59 on LD5M to port L89 on LD8M
- wire from port L79 on LD7M to port L69 on LD6M

During their common running from the left to the right, these two wires are twisted, constituting a two wire cable. Figure 3.3 also precises the different wire numbers and the different ports of the junction equivalent to the lower shielded volume.
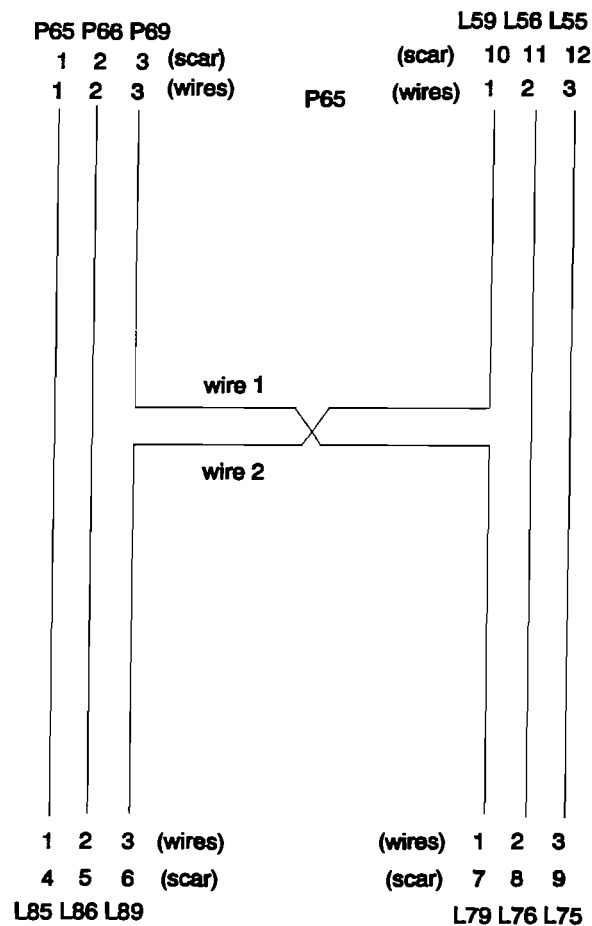
Fig. 3.3: electrical scheme of network B

3.3) First experiment performed in France on Network B

During the first experiment, an effort was made to flatten the cables on the metallic plane. Near the boxes, the cable is running from the connector, at a 5 cm average height, to the ground, making a discontinuity, that we'll call further a "coude" (elbow in English).
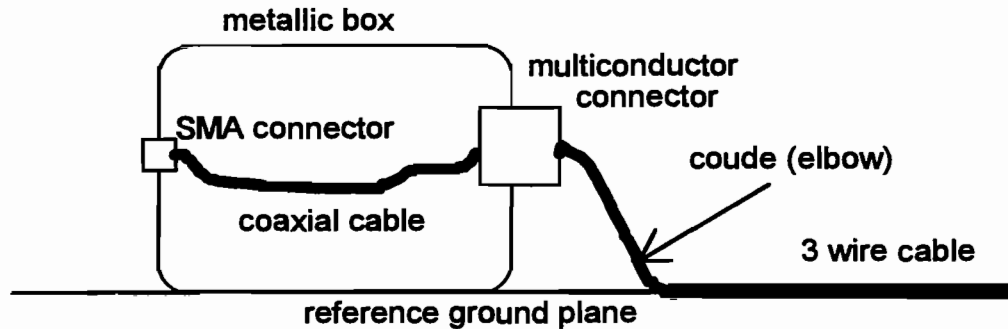
Fig. 3.4: side view of the connection of the 3 wire cable to a box in the first experiment

3.3.1) Network B characterization

3.1.1.1) Internal coupling: network "empb"

Figure 3.5 is an exhaustive description of the network dealing with the internal coupling between wires. This network contains:

- the structure of the network with tubes and junctions,

- the characteristics of tubes (data files with extension ".t"),

- the characteristics of the connections at the junctions ports,

- the characterization of S-parameters of the junctions (data files with extension ".s"),

- the characterization of the lower volume sub-network.

External boxes are modelled with 3 terminal 50 Ω loads (junction 12, 15, 13, 14) with the S-parameter file "ter50_3.s". These loads are connected to a tube made of the 3 coaxial cables (data file "coax3.t" and tubes 11, 12, 13, 14).

Tubes 1, 2, 4, 5 describe the 3 wire cable connecting LD6M, LD8M, LD7M, J004 respectively (files "trifnbf.t").

Tube 7 represents the 3 wire shielded cable inside the cockpit (file "trifbf.t")

Tube 3 represents the 2 wire cable made of the 2 wires connecting LD5M to LD8M from one side and LD7M to LD6M from the other side.

Tubes 10, 9, 8, 6 represent the "coude" at the level of the boxes.

The doted lines contains the sub-network associated to the lower shielded volume. The equivalent S-parameters will be saved as "soute.s50". "Soute" means "bay" in French.
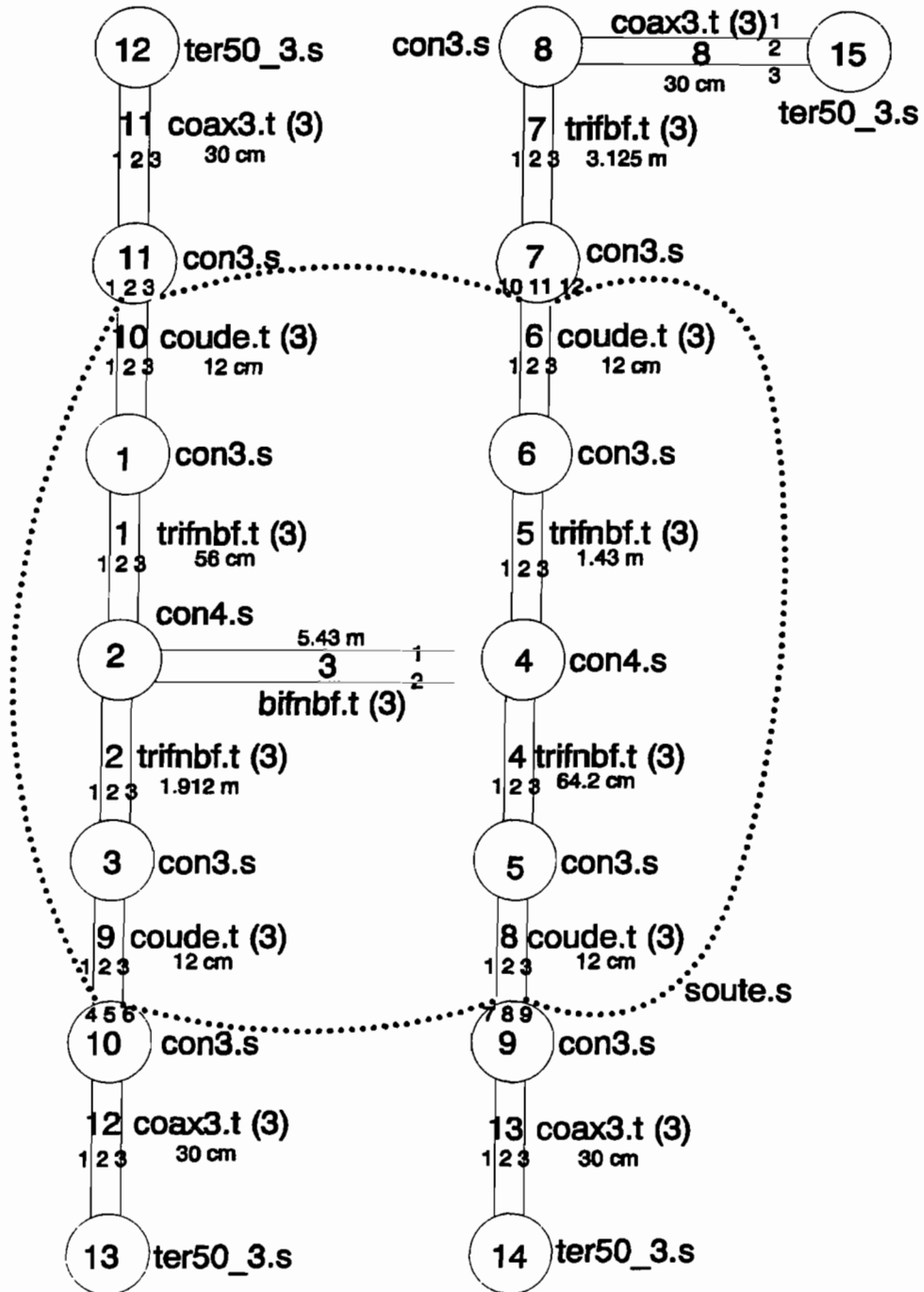
Fig. 3.5: Network B topological modelling (internal coupling - network "emptacb")

3.3.1.2) external coupling: network "injblind"

This network is useful to study the coupling on the shielded wire, due to a current probe. In this case, the voltage equivalent source is applied on all the wires and on the shield which constitutes tube 5 (file trifb4f.t).

This network uses the junction 2, equivalent to the lower shielded volume (file soute.s50). Tube 4 is a small tube of zero length assuring the connection between junction 2 and junction 5.
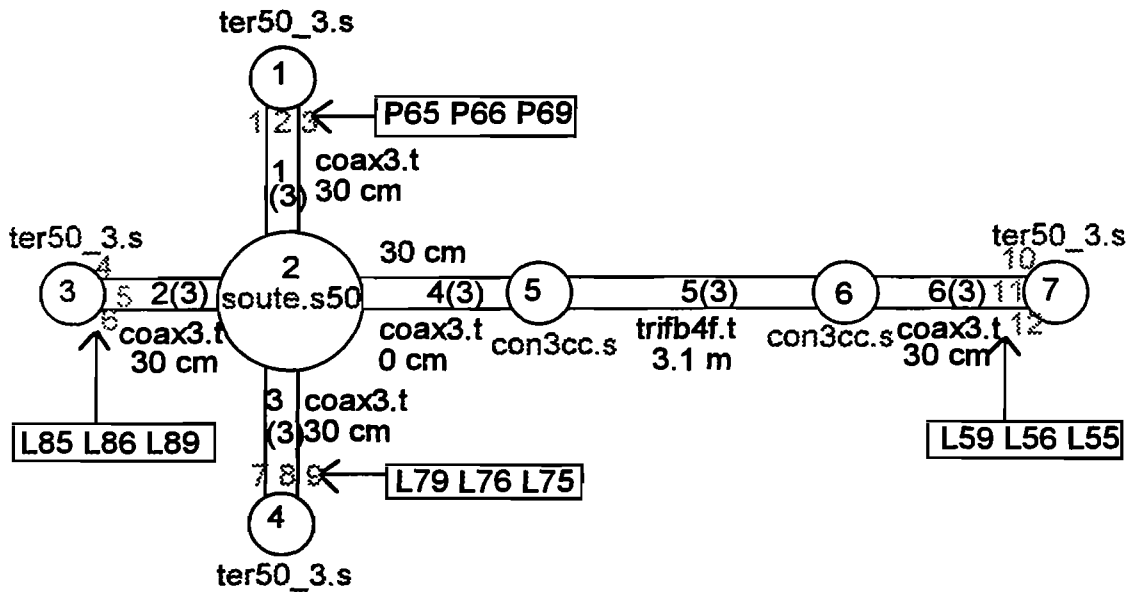
Fig. 3.6: Network B topological modelling (external coupling - network "injblind")

3.3.1.3) Test on the shielded cable: network "test_trifb"

This network is used for testing the current probe injection model on the shielded wire. Tube 2 and tube 5 have 0. m length: they are used to assure the connection between the 3 ports of the terminal boxes and the 4 ports of the shielded cable which includes the shield as a wire (file "trifb4f.t").
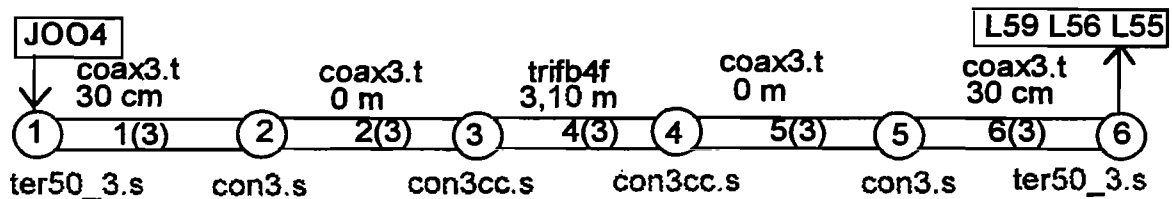
Fig. 3.7: network for testing the current probe injection (network "test_trifb")

3.3.2) Cables

In the first experiment, all the tubes of the previous network have been determined separately. It has been shown that it can be very useful to describe the R, L, C parameters of the multiconductor transmission line as a function of frequency. Here are given the average values of these matrices for each type of lines (obtained at 300 kHz):

two twisted wire line:
R11= 0.1 Ω/m M11= 0.55 μH/m   M12= 0.24 μH/m
              C11= 60 pF/m   C12= -30 pF/m

three twisted line:
R11= 0.1 Ω/m M11= 0.48 μH/m   M12= 0.23 μH/m
              C11= 12 pF/m   C12= -5 pF/m

three wire shielded line:
R11= 0.1 Ω/m M11= 0.32 μH/m   M12= 0.1 μH/m
              C11= 15 pF/m   C12= -4 pF/m

shield of the three wire line:
R11= 0.1 Ω/m M11= 6.4 μH/m
              C11= 1.7 pF/m

Transfer impedance of the three wire shielded line:: Rt= 9 mΩ/m   Lt= 1.25 nH/m

"coude" equivalent tube:
R11= 0.1 Ω/m M11= 1.25 μH/m   M12= 0.67 μH/m
              C11= 100 pF/m   C12= -43 pF/m

3.3.3) Junctions

This section presents the different junction models which are introduced in the network models.

a) connection junctions:

These junctions allow the wire to wire connection between two different tubes.
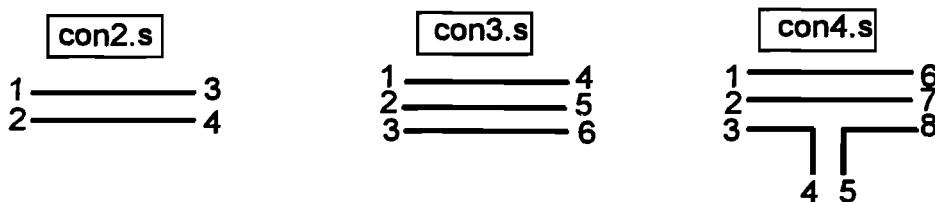
"con2.s" makes the connection between 2. wires

"con3.s" makes the connection between 3 wires. It may also represents the measured scattering parameters of the 3 wire connector (in this case the file is "connecteur.s")

"con4.s" makes the connection between 4 wires. It is specially used in the lower volume sub-network to connecti two three wire cables with the two wire cable.

b) connection junctions for shielded cables

"con3-4cc" is used to connect a three wire cable from one side with a four wire cable whose fourth wire is short circuited.

"con3-4co" is used for connecting a three wire cable from one side with a four wire cable whose fourth wire is in open circuit.

The interesting point with these two junctions is that the fourth conductor may be the wire equivalent to the shield. By this way, it is easy to simulate a perfect connection to the ground or a disconnection from the ground.

c°) terminal junctions:

These junctions represent the loads located at the extremity of the harness.
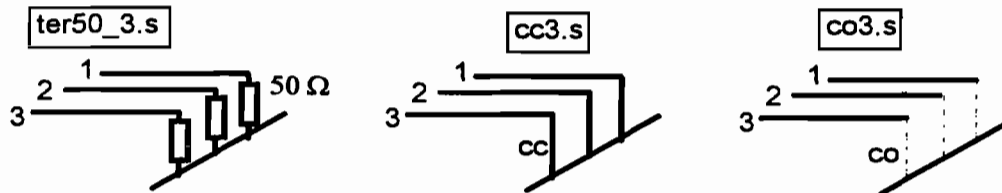
"ter50_3.s" represents three common loads equal to 50 Ω.

"cc3.s" represents three short-circuit loads

"co3.s" represents three open circuit loads.

3.3.4) Global S-parameter validation on the network

To verify that the values of R, L, C parameters introduced in tubes were correct, a comparison between measured and computed parameters on the inner coupling network (network "emptacb") has been performed.

Curve 3.8 to 3.11 show the different results which were obtained by introducing more and more accurate data into emptacb network, on the example of the S-parameter between L55 and L76 ports.

Figure 3.8 was obtained with R, L, C parameters independent of the frequency for all the tubes. The general aspect of the curve is satisfactory, but the amplitudes are not well fitted on the whole frequency range.

Figure 3.9 was obtained by adding R, L, C parameters dependent from frequency in the model of the three wire shielded cable (tube 7 in emptacb network). The amplitude is now well fitted until 40 MHz.

In Figure 3.10, the frequency dependence of R, L, C parameters has been applied on the three wire cable models (tubes 1, 2,, 4, 5 in emptacb network). The global amplitude is well fitted on the whole frequency range. Particularly, the previously calculated peak around 70 MHz has now disappeared.

Finally, Figure 3.11 shows the result with the introduction of frequency dependant R, L, C parameters on the two wire cable (tube 3 on emptacb network). As if it doesn't bring a consistent amelioration, it must be noticed that the amplitude is perfectly fitted until 30 MHz.
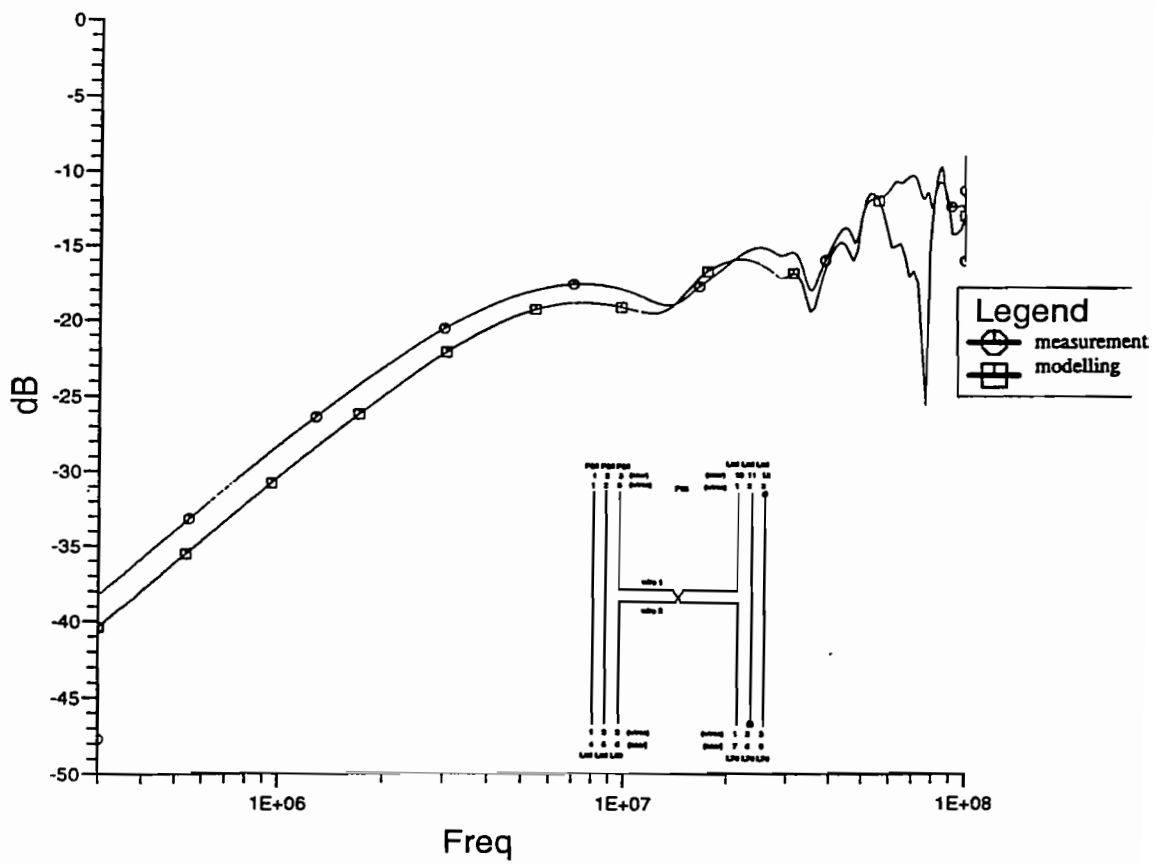
Fig. 3.8: S55_76 modelling with R, L, C independent of the frequency
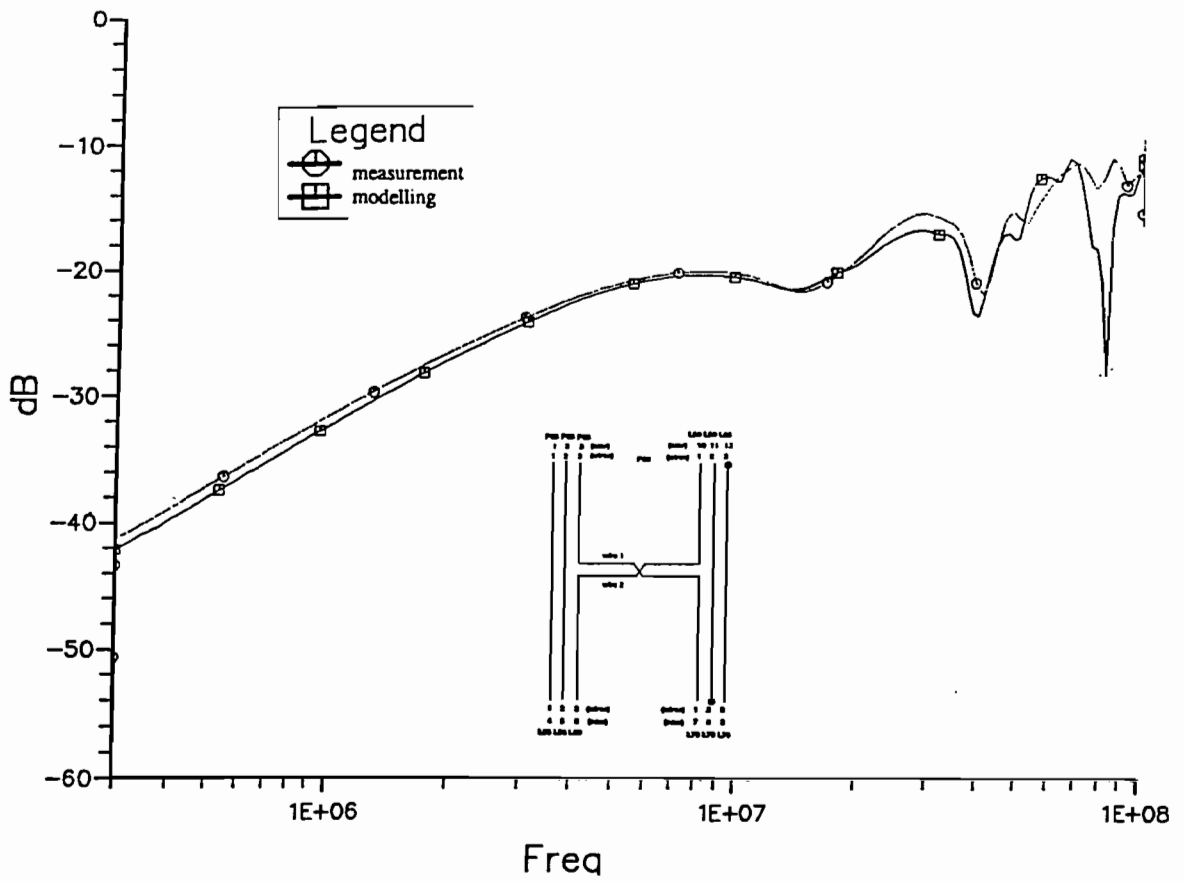
Fig. 3.9: S55_76 modelling with frequency dependent R, L, C parameters on the shielded cable

22
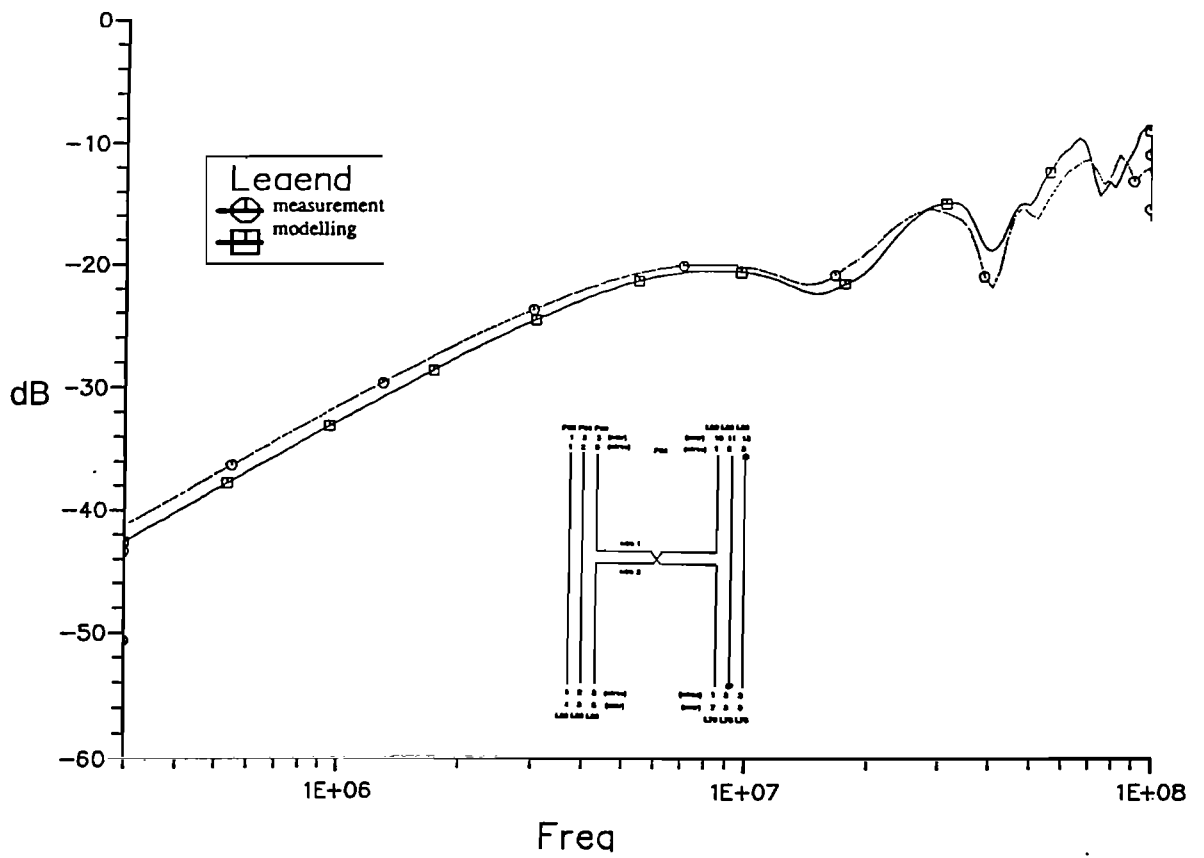
Fig. 3.10: S55_76 modelling with frequency dependent R,L,C parameters on the 3 wires cables
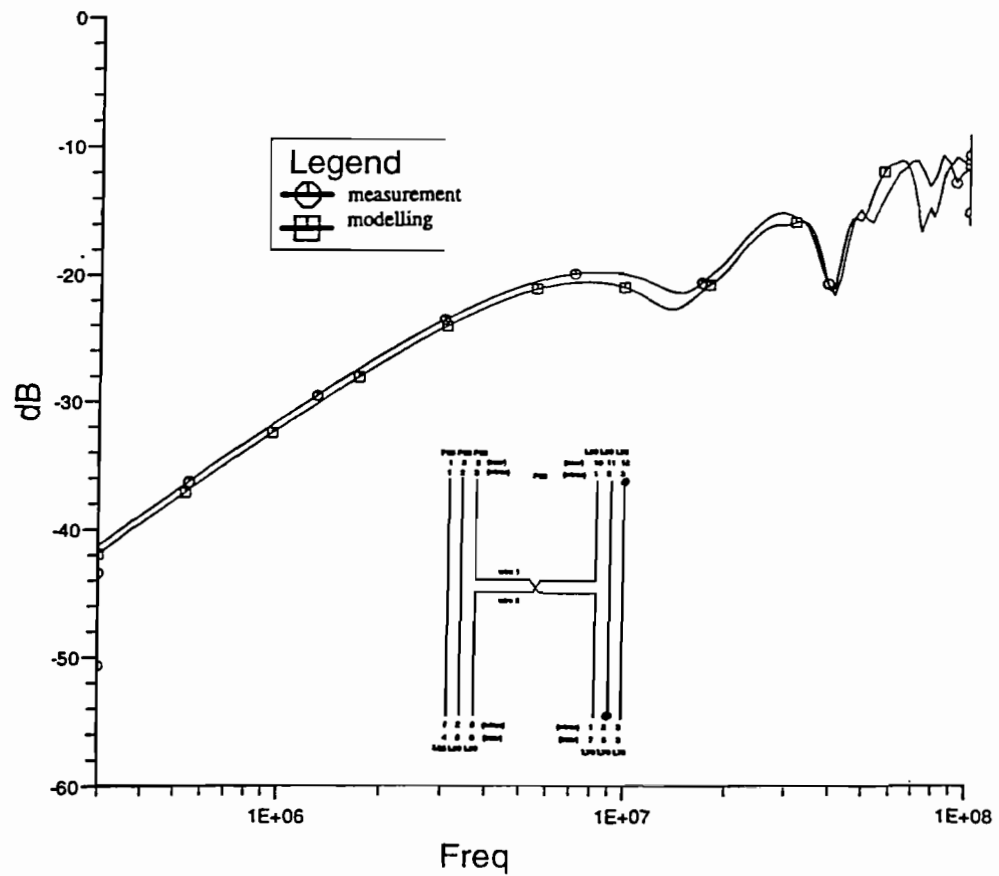
Fig. 3.11: S55_76 modelling with frequency dependent R, L, C parameters on the 2 wires cables

3.3.5) Current probe injection

3.3.5.1) Current injection on the shielded cable alone

This phase was necessary to validate the current probe injection model. Measurements were performed on a reduced wiring made of the three wire shielded cable connected to two boxes (Fig. 3.12).
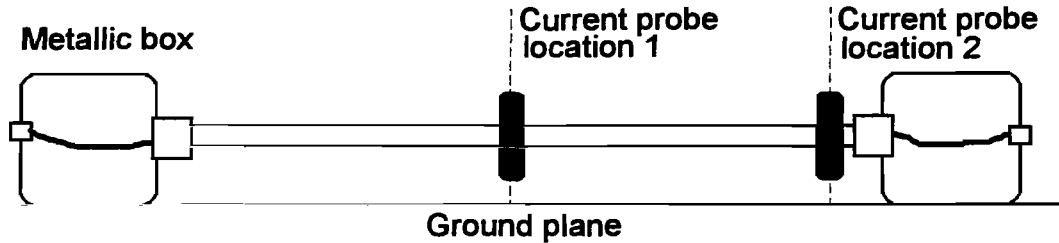
Fig. 3.12: experimental device for the characterization of the current probe injection

Two positions of the current probe have been considered. The first position was in the middle of the cable. The second position was at one extremity of the cable.

Fig. 3.13 and 3.14 represent a comparison of the resultant 50 Ω voltage at the extremity of the cable for both locations, 1 and 2 respectively. One must notice that the positions of the resonance peaks are correctly calculated in both situations.

3.3.5.2) Current probe injection on whole network B

The following results Fig. 3.15 to 3.16 have been obtained with the shielded cable once connected to the total network.
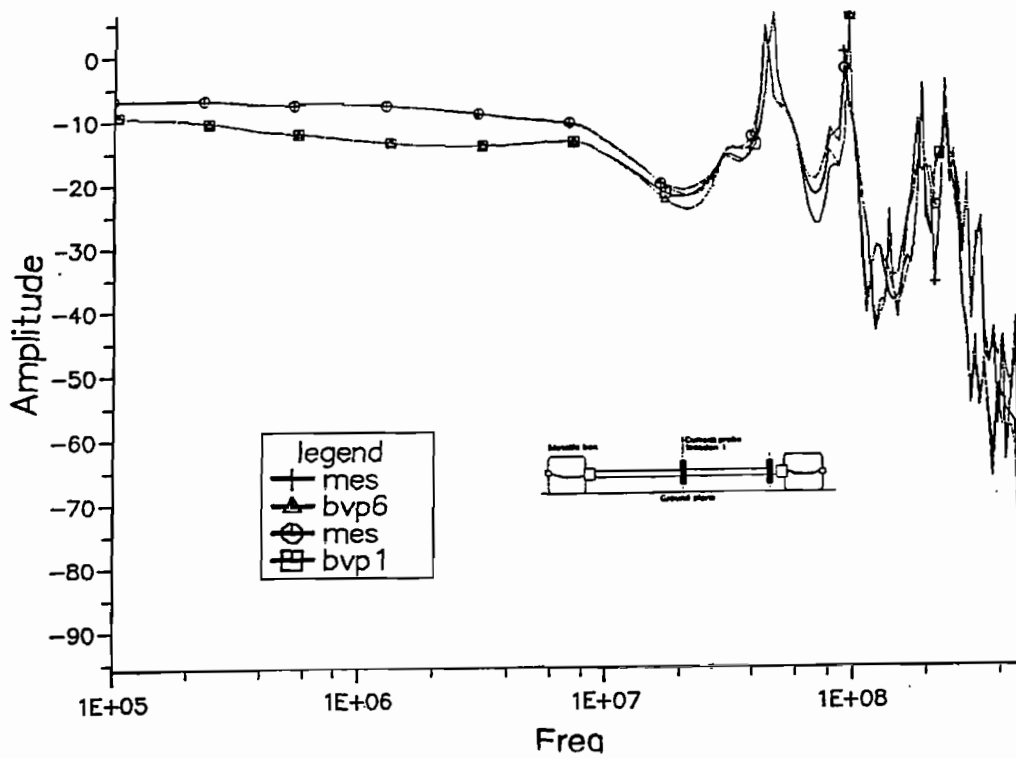
Fig. 3.13: Voltage with current injection at position1 (shielded cable alone)

Amplitude = 20 log (Voltage in Volts)

26
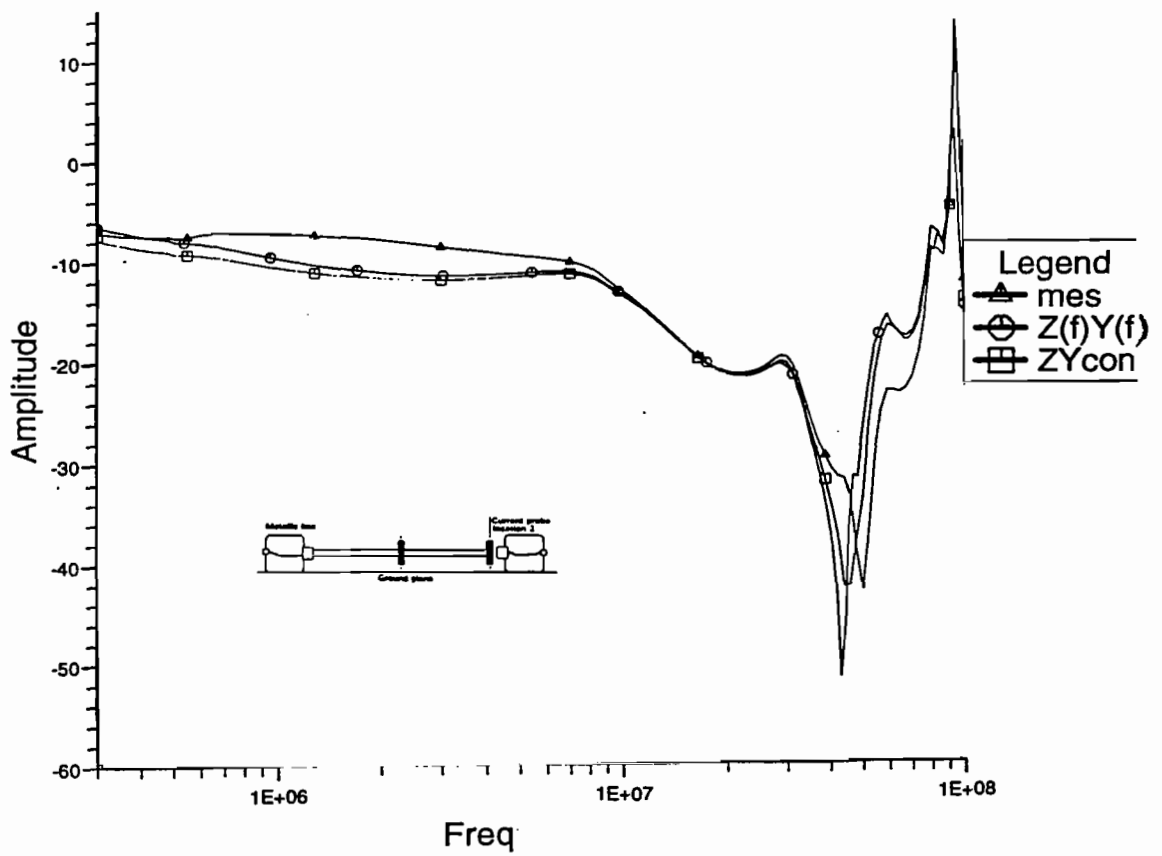
Fig. 3.14 Voltage with current injection at position 2 (shielded cable alone)

Amplitude = 20 log (Voltage in Volts)
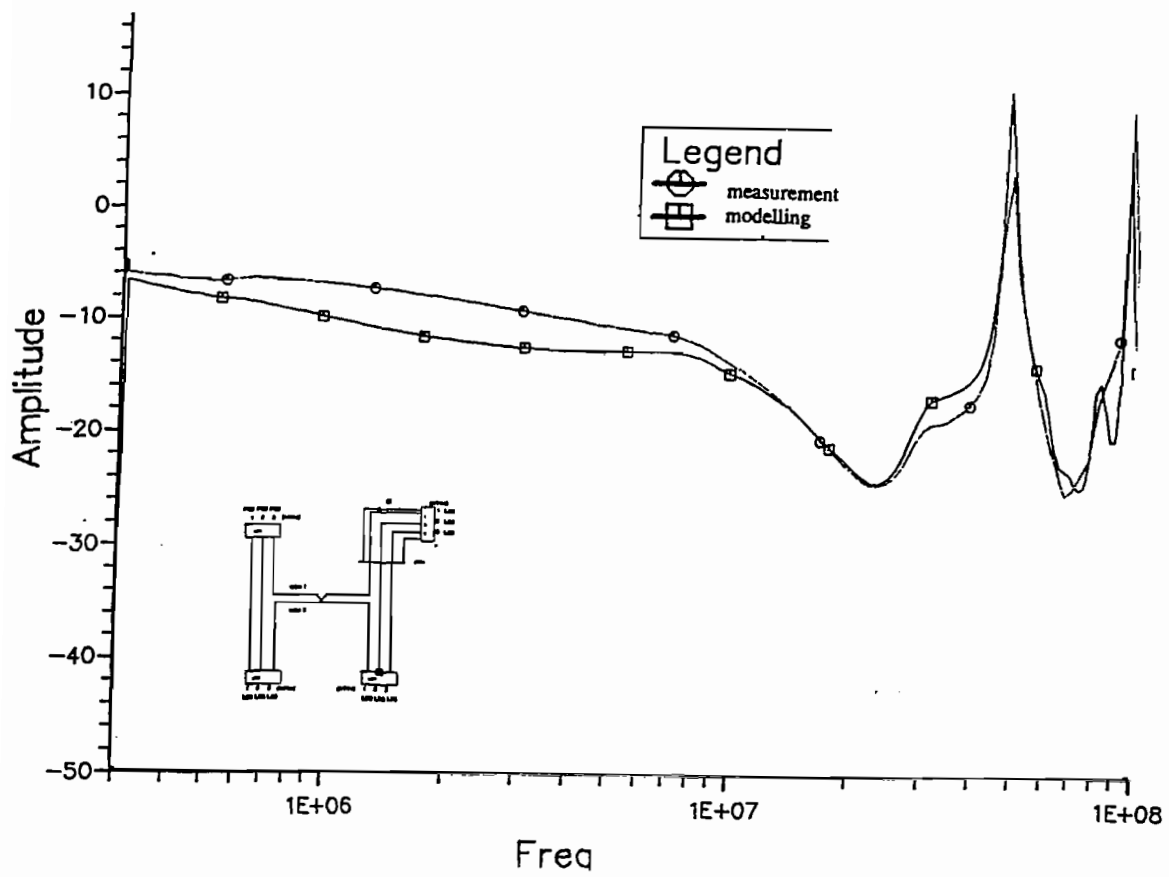
Fig. 3.15 Voltage on the port 6 of the box LD7 (current probe injection at position 1)

Amplitude =20 log (Voltage in Volts)

28
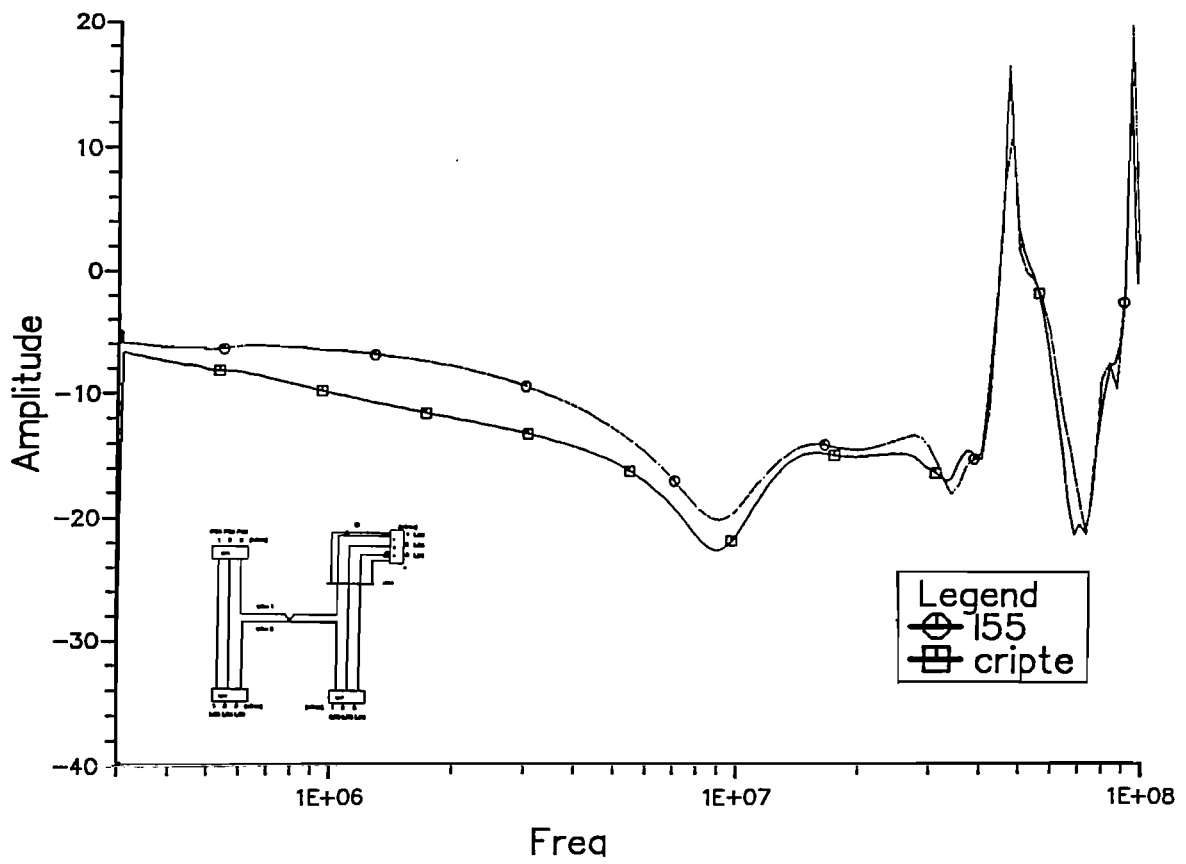
Fig. 3.16 Voltage on the port 5 of the box LD5 (current probe injection at position 1)

Amplitude =20 log (Voltage in Volts)
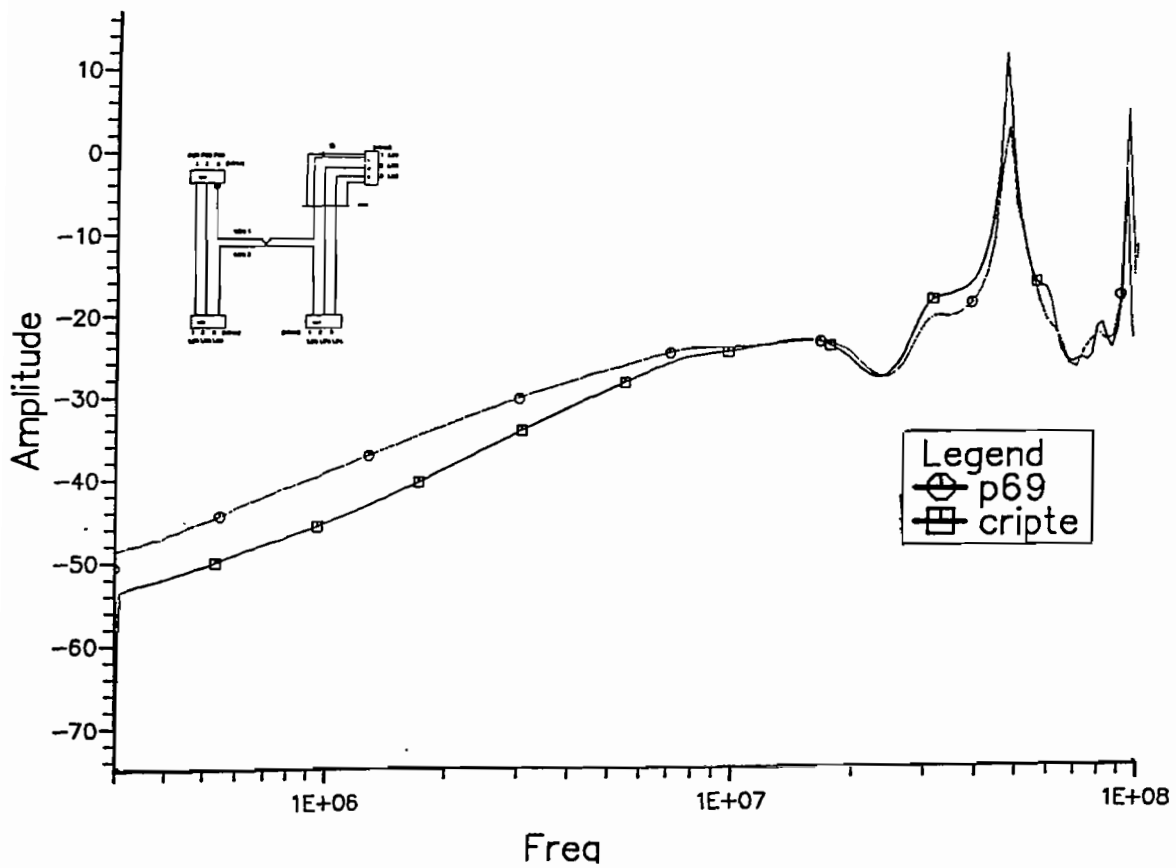
Fig. 3.17 Voltage on the port 9 of the box PD6 (current probe injection at position 1)

Amplitude $=20$ log (Voltage in Volts)

3.4).Experiment on Network B "In situ"

3.4.1) Introduction

As previously described in the program synopsis, Network B has been placed in the aircraft along the existing cable network, Network A. During the experiment held in Albuquerque, network characterization, current injection on the shielded cable located in the cockpit and illumination under the Ellipticus Antenna available at the PHILLIPS Laboratory have been performed. At each step of this experiment, different numerical simulations have been made in order to validate the network and sources characterization methods.

Moreover, this "in situ" experiment has shown that the Electromagnetic Topology approach can be used to determine the relative importance of the different points where the external aggression can enter the structure.

3.4.2) Network characterization : [S-parameters]

In order to validate the characterization of the network carried out during the first experimentation in France, S-parameters have been measured between different ports of Network B, once installed in the aircraft. At the same time, numerical simulations on Network B, introducing the line parameters directly measured in France were performed with CRIPTE code (See Fig. 3.5).

After comparisons between measurements and these first simulations, some discrepancies appeared (see Fig. 3.18 to 3.21 where the solid line is measurement and the dash line is the simulation). They can be easily explained. Indeed we can see on the figures which represent a diaphony S-parameter (Fig. 3.18 and 3.19), a reflection parameter, (Fig. 3.20), and a transmission parameter (Fig. 3.21) that the measurement has a higher level in low-frequency than the simulation. From this remark, we can deduce that the network characterization in the lower volume, as done in France does not fit totally once network B is located in the aircraft.

It can be shown that these S-parameters are proportional to the line parameters in low frequency. Thus differences noticed between measurements and simulations indicate that the line parameters introduced in numerical simulations have been under-evaluated.
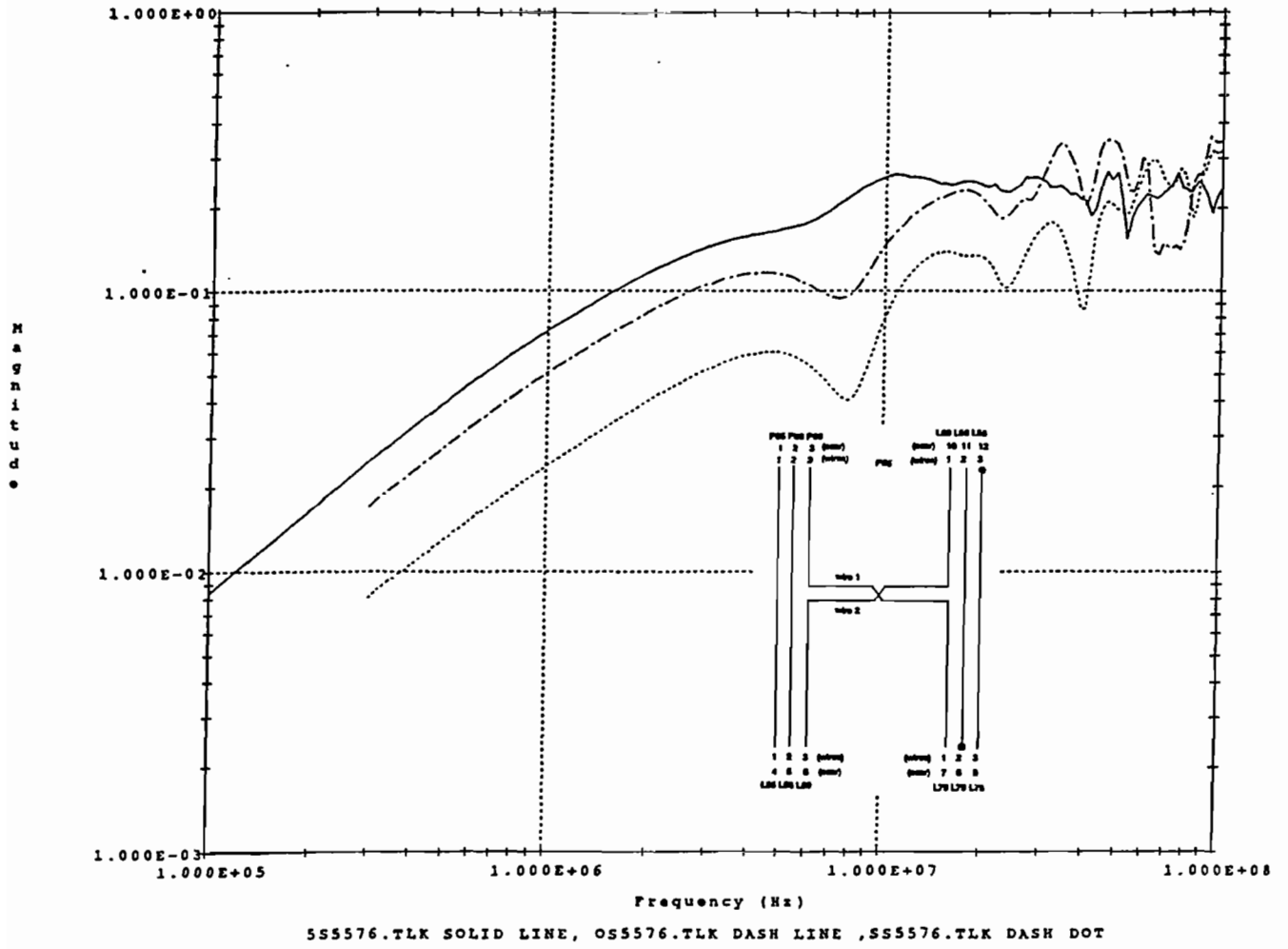
Fig 3.18: S-parameter modelling of a diaphony between two wires (s55_76)
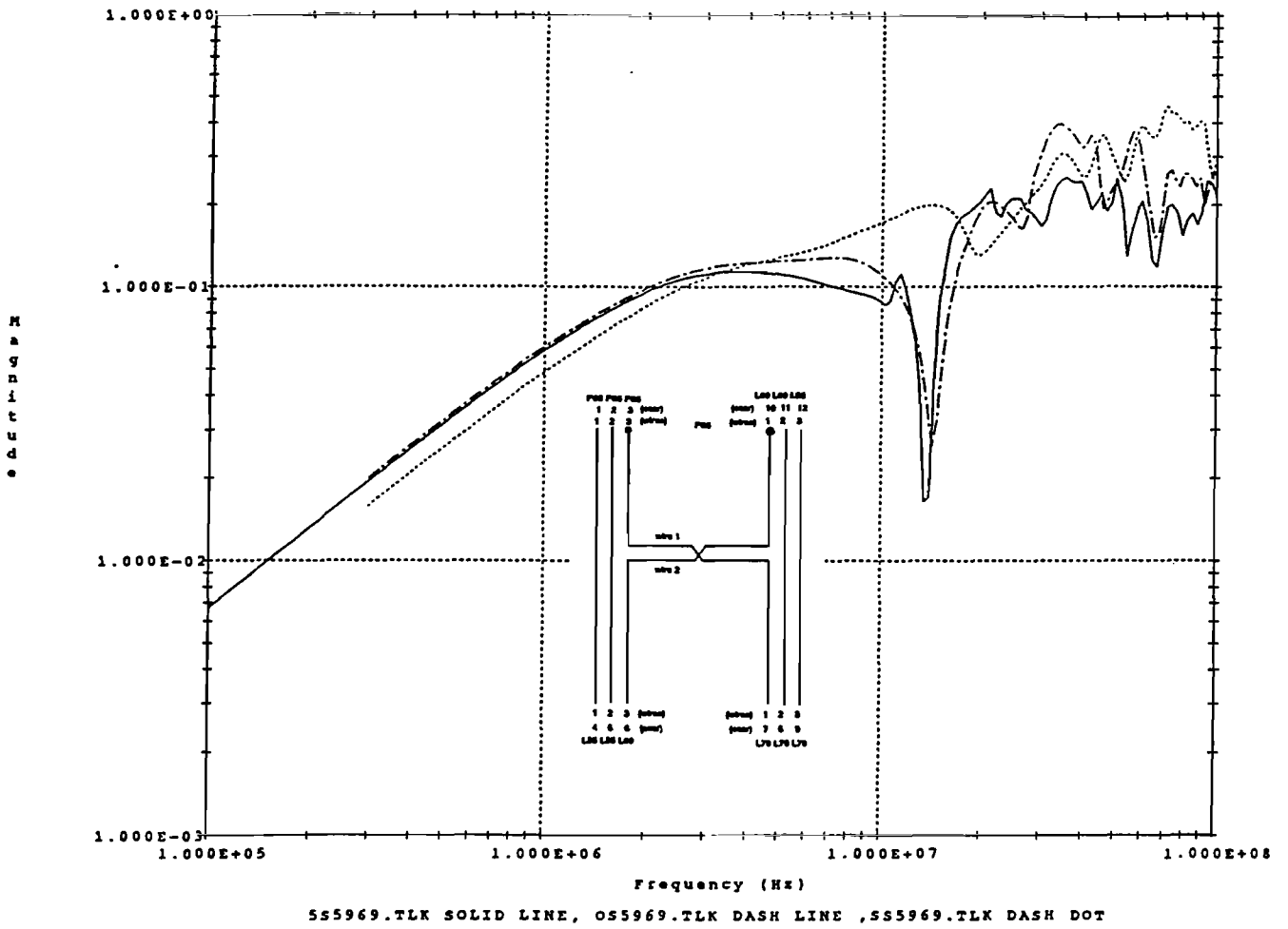
Fig 3.19: S-parameter modelling of a diaphony between two wires (s59_69)
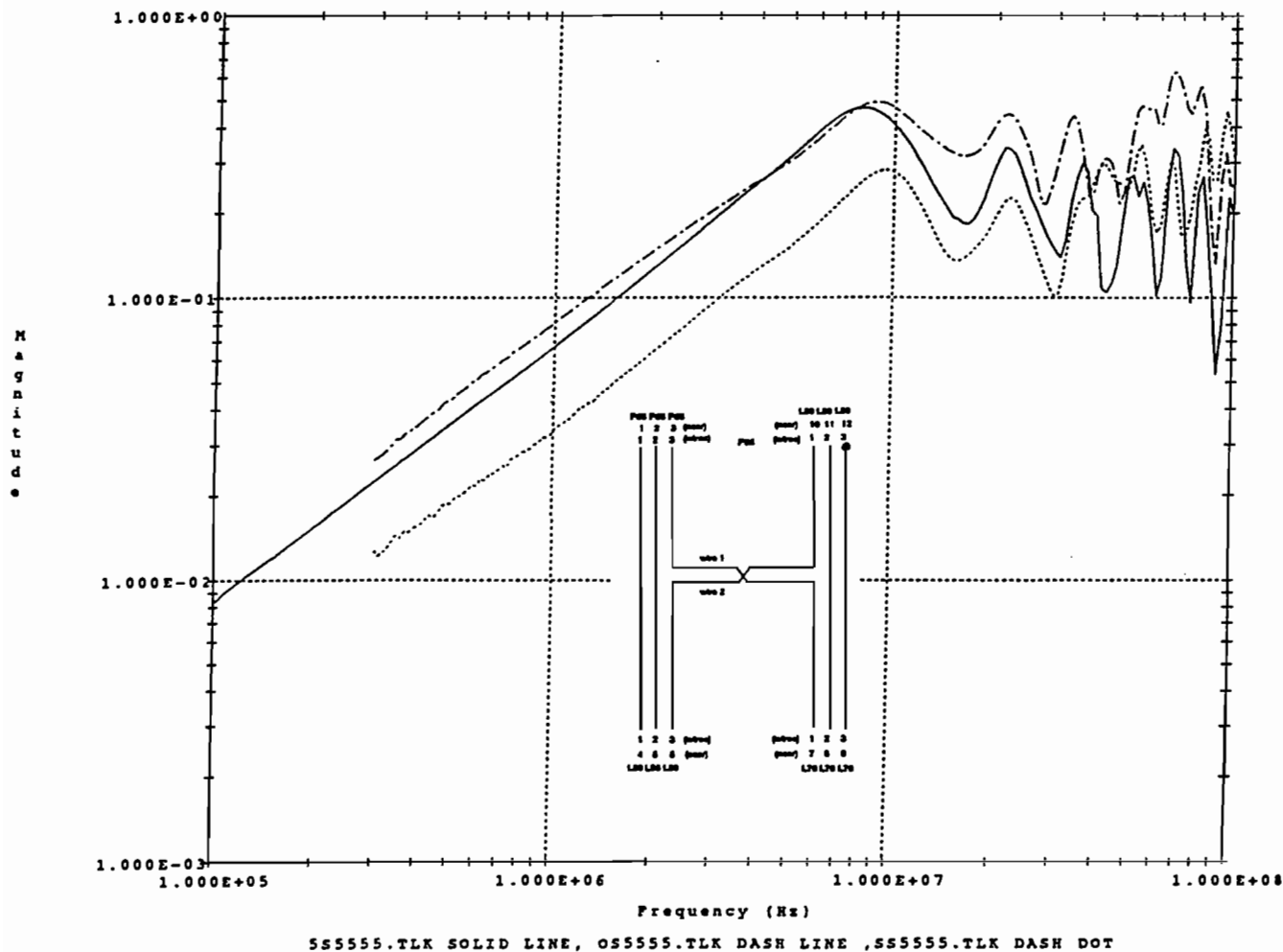
Fig 3.20: S-parameter modelling of a reflection on a wire (s55_55)
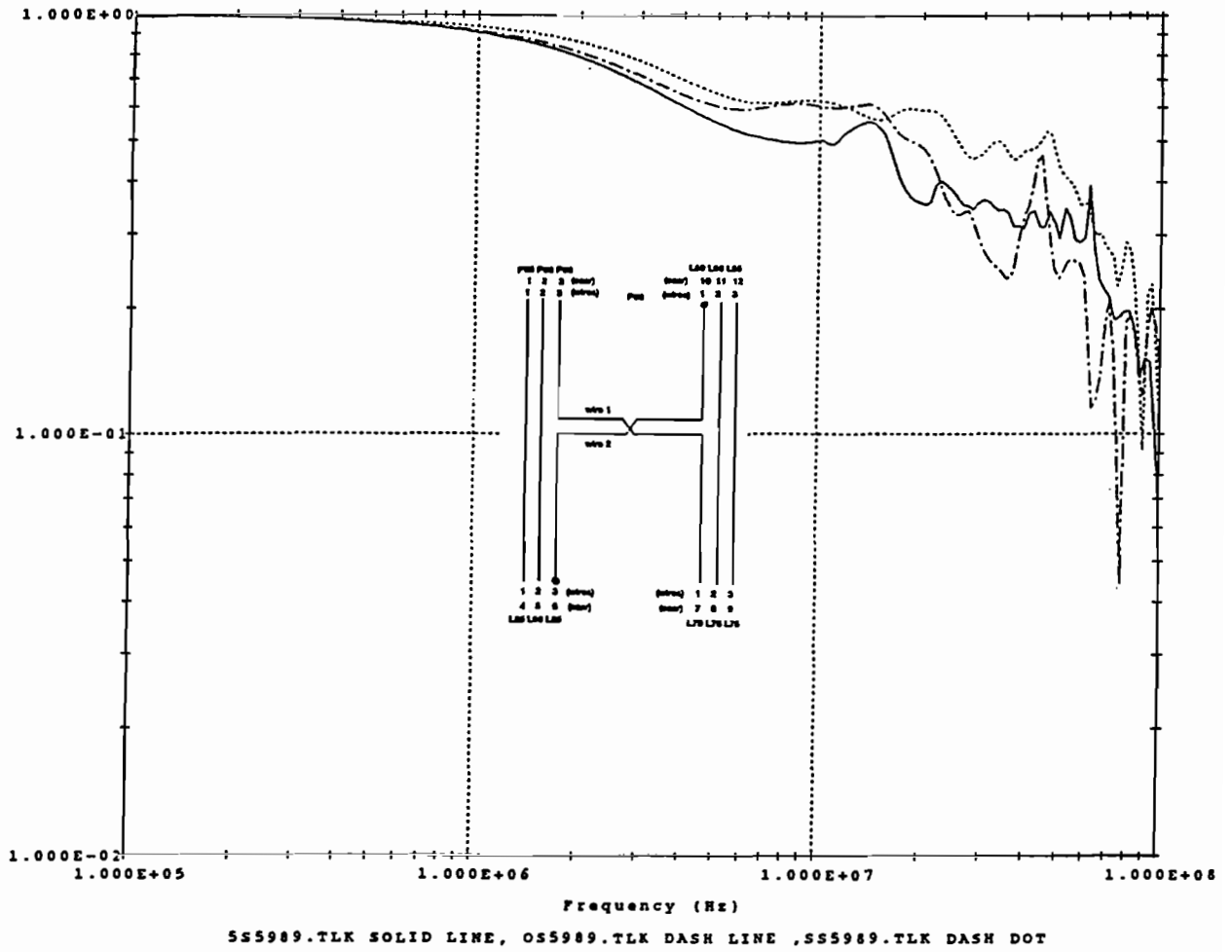
Fig 3.21: *S-parameter modelling of a direct transmission on a wire (s59_89)*

Indeed this can be easily explained by the fact that Network B, once installed in the aircraft, is not flattened against the ground reference as done in France. Therefore, by setting Network B inside the aircraft, the average height of the cables over the structure has increased compared with the flattened network studied in France. The line parameters such as inductances, capacitances are function of the distance of the bundle over the reference. Thus new numerical simulations on Network B have been performed, optimizing cable parameters in the lower shielded volume by assuming that the bundle is about 5 cm over the structure along its running through the aircraft.

Once optimized, Network B has the following structure (Fig. 3.22):
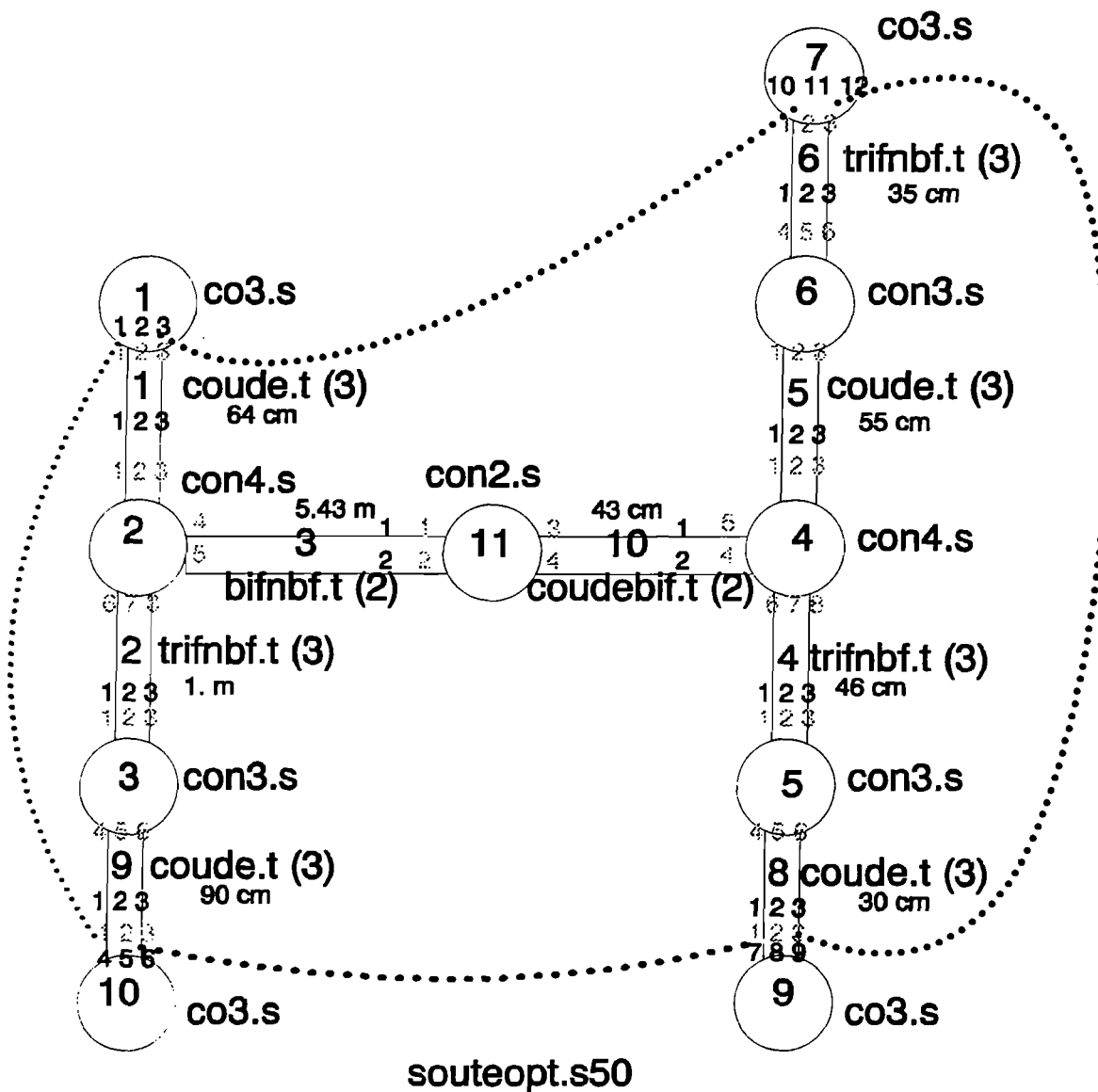
Fig. 3.22: optimized in situ Network B

where trifnbf.t and bifnbf.t represent the characterization of the bundles flattened against the ground plane and where coude.t and coudebif.t represent the characterization of the bundles located 5 cm above the ground plane.

We can now compare S-parameters measurements and simulations with this optimized Network B, represented on Fig. 3.18 to 3.22 by dash dot lines. From this comparison, it is obvious that optimized simulations represent correctly coupling phenomenon of the network located inside the real structure.

This first part of experiment enables us to characterize correctly Network B in the lower volume. This optimization has been made from the experience we had acquired during the pre-experiment held in France. So, we pointed out the interest to built a data base of line parameters, function of the average height of the bundles over the reference plane.

All along the following experiment, numerical simulations have been made with this optimized Network B in the lower shielded volume.

3.4.3) Current injection on the shielded cable located in the cockpit

The second step of the experiment on Network B consisted in injecting a current on the shielded cable located in the cockpit, 1 meter from box LD5M, by means of a current probe connected to an amplifier and to a network analyser, as previously done in the pre-experiment in France (see annex B).

3.4.3.1) Experimental set-up for current injection

Fig. 3.23 represents the experimental set-up used for the current injection inside the cockpit.
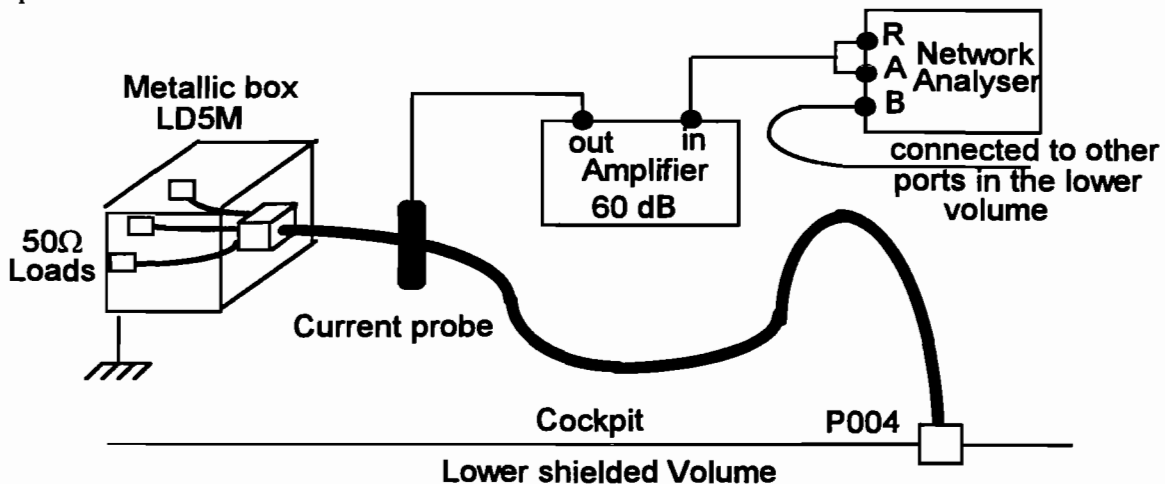
Fig. 3.23: Set-up for current injection on the shielded bundle in the cockpit

37

Different voltage responses to this current injection on wires connected to LD7M, LD8M, LD6M and LD5M have been measured in order to compare them with the numerical simulations using several methods of introducing source terms (See Annex B).

3.4.3.2) Introduction of sources terms in numerical simulations

As described in Annex B, two methods for introducing source terms in numerical simulation were studied:

- Introduction of Voltage generators on each internal wire of the shielded cable :

$$V_s = Z_t . I_b$$

where Z_t is the transfer impedance of the shielded cable measured during the pre-experimentation and I_b, the current measured on the shielded cable near the point of injection.
- Introduction of Voltage generators on each internal wire of the shielded cable and on the shield of the cable, considered as a fourth conductor, where the voltage generator comes from the characterization of the amplifier and the current probe measured during the pre-experiment.

3.4.3.3) Comparisons between numerical simulations and measurements of the current on the shield

In order to see if the topography of the current was correctly reproduced on the shield by numerical simulations, several currents were measured along the shielded cable located in the cockpit:

- Near the box LD5M

- 1.8m from the box LD5M

- Near the connector P004

The first calculation carried out to evaluate the topography of the shield current along the cable is represented in Fig. 3.24. The line parameters of the shield are the ones measured during pre-experiment, that is to say :

$$R = 2\,m\Omega/m \quad L = 0.67\,\mu H/m \quad C = 170\,pF/m$$

Network : Blind_situ_injh
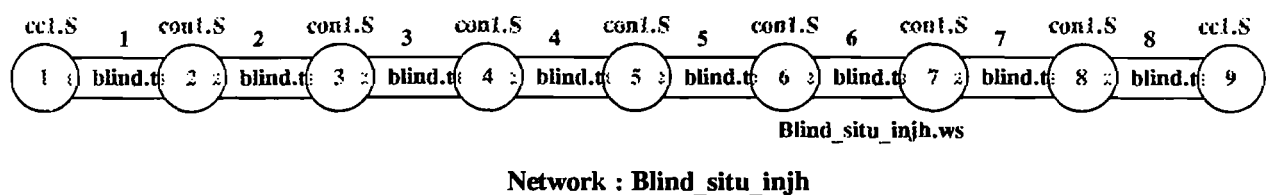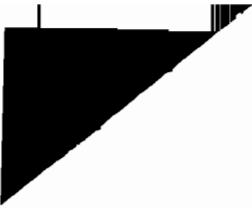
Fig. 3.23: Network with shield characterisation evaluated during pre-experimentation

38

On Fig. 3.24 to 3.26 are drawn the measured shield currents (solid line) at the different locations described previously, and the currents calculated with the parameters determined in pre-experiment (dash line). It appears that this first numerical simulation does not fit correctly the behaviour of the shielding current, especially near the resonances.

This phenomenon can be explained by the fact that the shielded cable was flattened against the ground plane during the pre-experiment whereas the shielded cable in the cockpit had not a homogeneous running.

From this remark, a reflectometry was done on the shielded cable in the cockpit in order to be able to split up the shielded cable into different tubes representing more properly its running inside the structure. We can deduce from the reflectometry that eight tubes would be more appropriate. The line parameters of these tubes have been evaluated by taking eight values of the reflection coefficient given by the reflectometry. On Fig. 2.27 is represented the shielding network optimized thanks to time domain reflectometry.

1.000E+02

1.000E+01

1.000E+00

1.000E-01

1.000E-02

1.000E+05   1.000E+06   1.000E+07   1.000E+08   1.000E+09

Frequency (Hz)
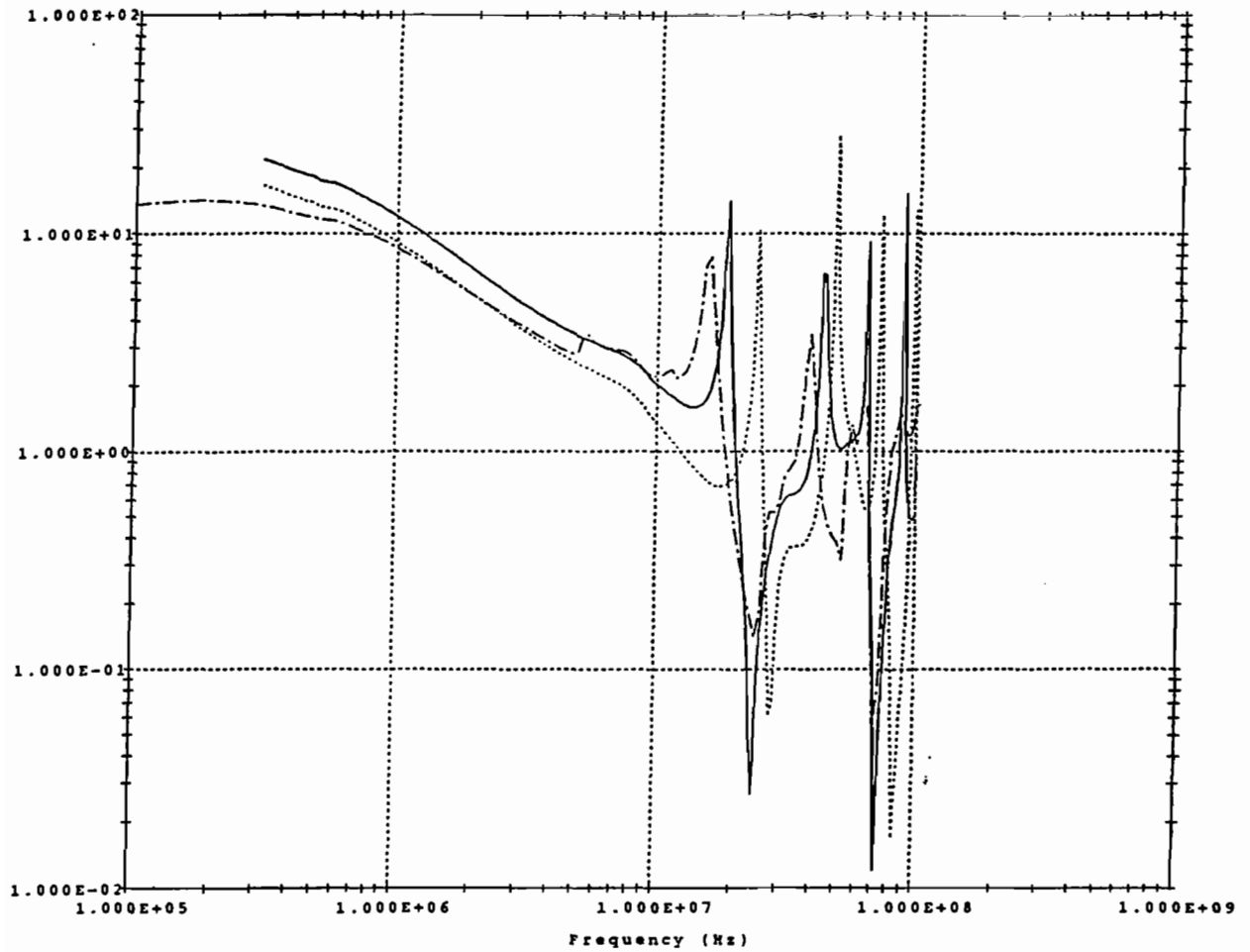
3ILD5D.TLK SOLID LINE, 3ILD5DH.TLK DASH LINE ,3ILD5DC.TLK DASH DOT

Fig. 3.24: current on the shield (0.35m from LD5)

3ILD5.TLK SOLID LINE, 3ILD5E.TLK DASH LINE ,3ILD5H.TLK DASH DOT
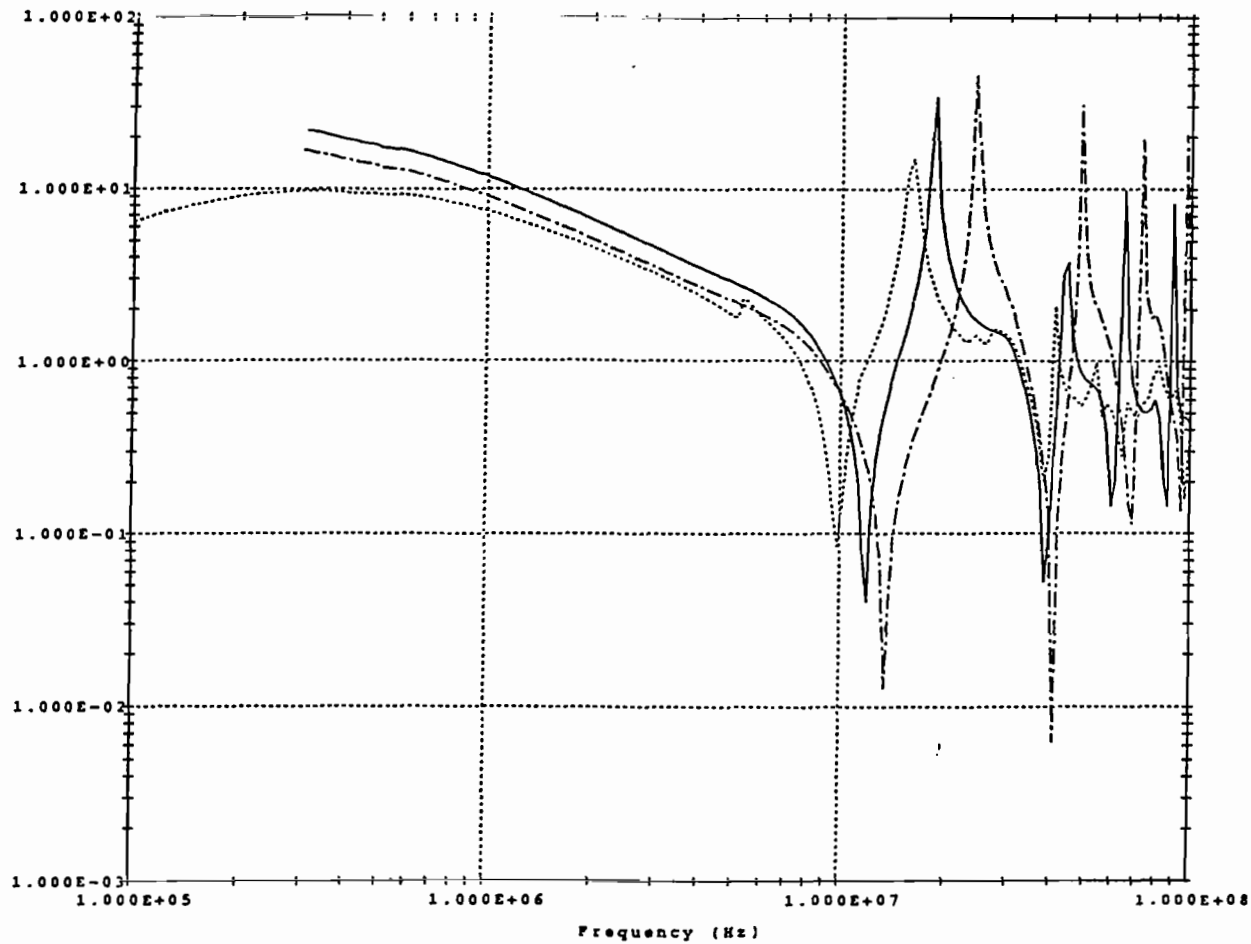
Fig. 3.25: current on the shield (2.8m from LD5)
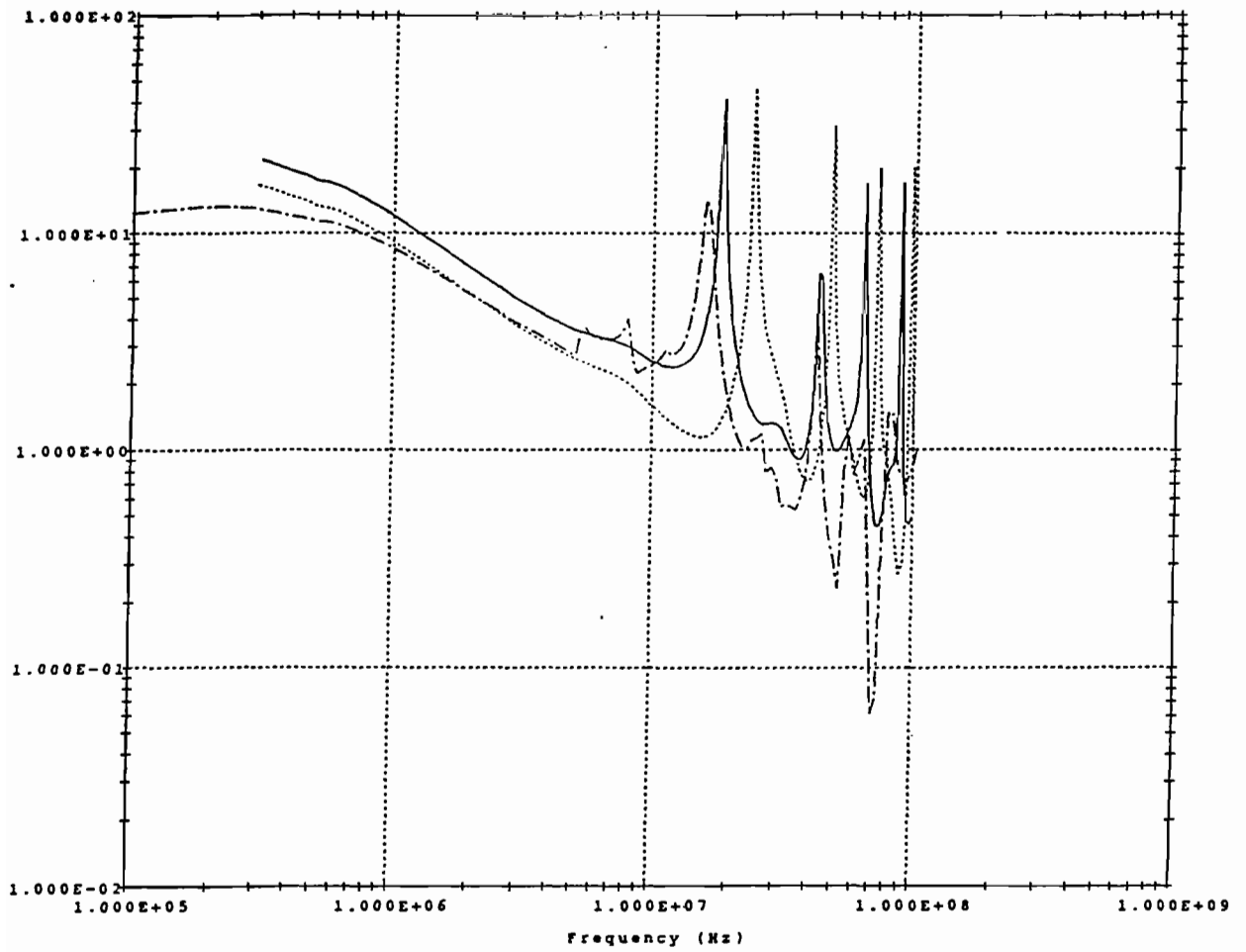
Fig. 3.26: current on the shield (near J004)

| ccl.S | 1 | conl.S | 2 | conl.S | 3 | conl.S | 4 | conl.S | 5 | conl.S | 6 | conl.S | 7 | conl.S | 8 | ccl.S |

```
1  blind1.t   2  blind2.t   3  blind3.t   4  blind4.t   5  blind5.t   6  blind6.t   7  blind7.t   8  blind8.t   9
   1.75 m       0.87 m       0.87 m       0.87 m       0.522 m      0.765 m      0.348 m      0.104 m
```

Blind_situ_injh.ws

Network : Blind_situ_inj
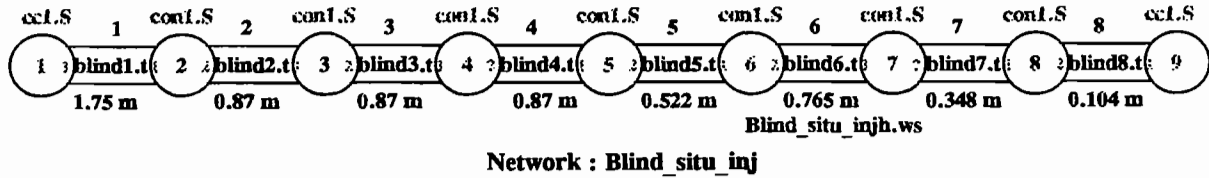
Fig. 3.27: Network with shield characterisation evaluated from the reflectometry

The average line parameters on the shielded cable once located in the cockpit are:

$$R_{av} = 2\,m\Omega/m \quad L_{av} = 0.50\,\mu H/m \quad C_{av} = 31\,pF/m$$

The average capacitance representing the cable in the cockpit appears to be much less important that the one evaluated during pre-experiment; this is easily explained by the fact that the distance between the shielded cable and the reference plane is more important at some locations in the cockpit compared to the test-bed studied in France.

On Fig. 3.24 to 3.26 the shielding currents resulting from the numerical simulation, taking into account the running of the shield inside the cockpit, are represented in dash dot line. We can notice that this last calculation reproduces correctly the topography of the current along the shielded cable in low frequency and in the frequency domain where the first resonances appear. Therefore the shielded cable was introduced in the following simulations as described on the figure 2.27 each time the whole network has been studied.

3.4.3.4) Comparisons between numerical simulations and measurements on the whole network

Different numerical simulations of the response of the whole network to a current injection on the shielded cable located in the cockpit were performed using both methods to introduce sources terms on the shielded cable.

In order to validate each step, the whole network calculation has been divided between:

- the shielded cable in the cockpit

- the network located in the lower volume

The network located in the lower volume of the EMPTAC was characterized by its S-parameters. Then two numerical simulations of the shielded cable in the cockpit, using both methods of introducing source terms, have been made. This enables the evaluation of the voltage induced by the current injection on each internal wire of the shielded cable at the point of entry of the lower volume, the network being disconnected at P004. These signals can be compared to the voltages measured in the same conditions. These voltages are usually named as "Thevenin Voltages" seen from the lower volume.

On Fig. 3.28 and 3.29 are represented the networks related to the shielded cable in the cockpit using both methods to introduce source terms.
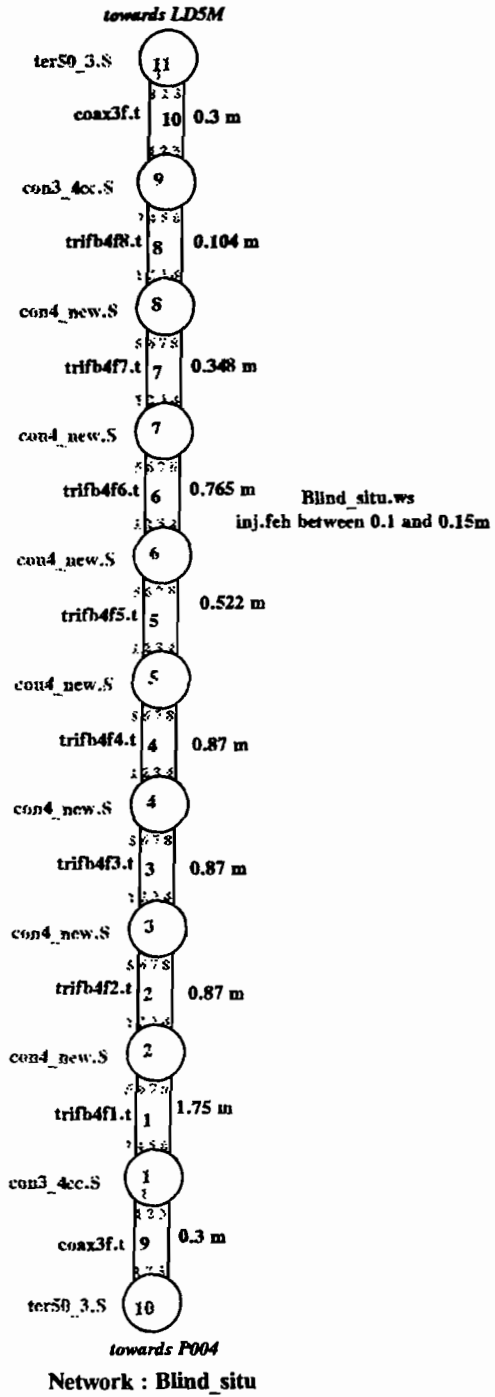
Fig. 3.28: Thevenin voltage numerical simulation using characterisation of the injector
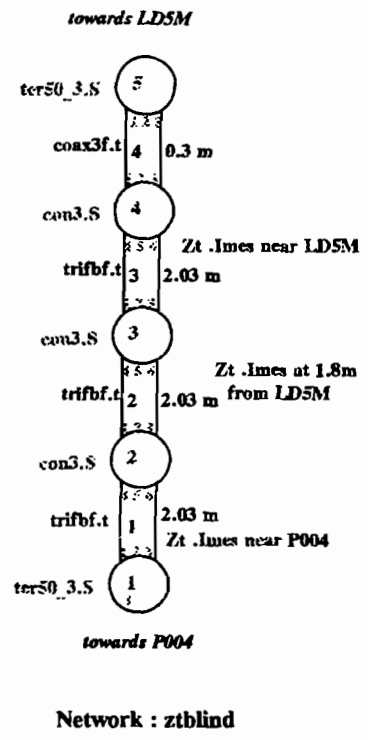
Fig 3.29 : Thevenin voltage numerical simulation using measured currents and transfer impedance concept

From the comparison between measurements and numerical simulations (Fig. 3.30), we can say that both ways to introduce in the model source terms represent correctly the coupling on the internal wires of the shielded cable and the first resonances of the shield short-circuited at each extremities.

Nevertheless, the method using the characterization of the injector appears to be more satisfactory because it can be used as a real predictive approach since no measurement of shielding current is necessary to characterise source terms in the simulations.

The next step consists now in introducing the Thevenin model, representing the perturbation at the point of entry in the lower volume, as the source term for the network constituted by the optimized lower volume (see Fig. 3.31).

Network : Thsoute
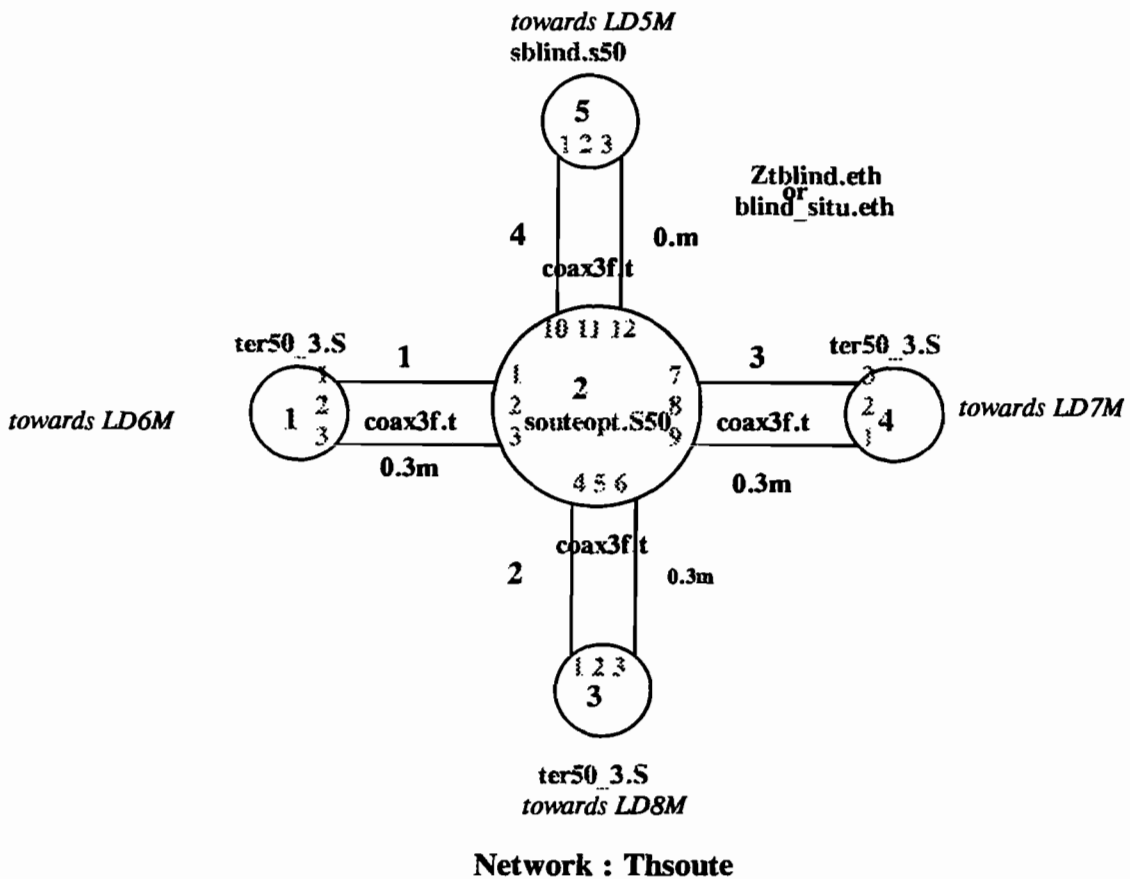
Fig. 3.31: Simulation of the whole network with a current injection

On Fig. 3.32 and 3.33, are represented the voltages measured and calculated on one port of the network in the lower volume. Comparison of these signals proves that the response of the whole network to a current injection on the shielded cable is correctly reproduced in the numerical simulation in a frequency domain including the first resonances.

45

6V5THM.TLK SOLID LINE, 6V5THS.TLK DASH LINE ,VTHZT.TLK DASH DOT
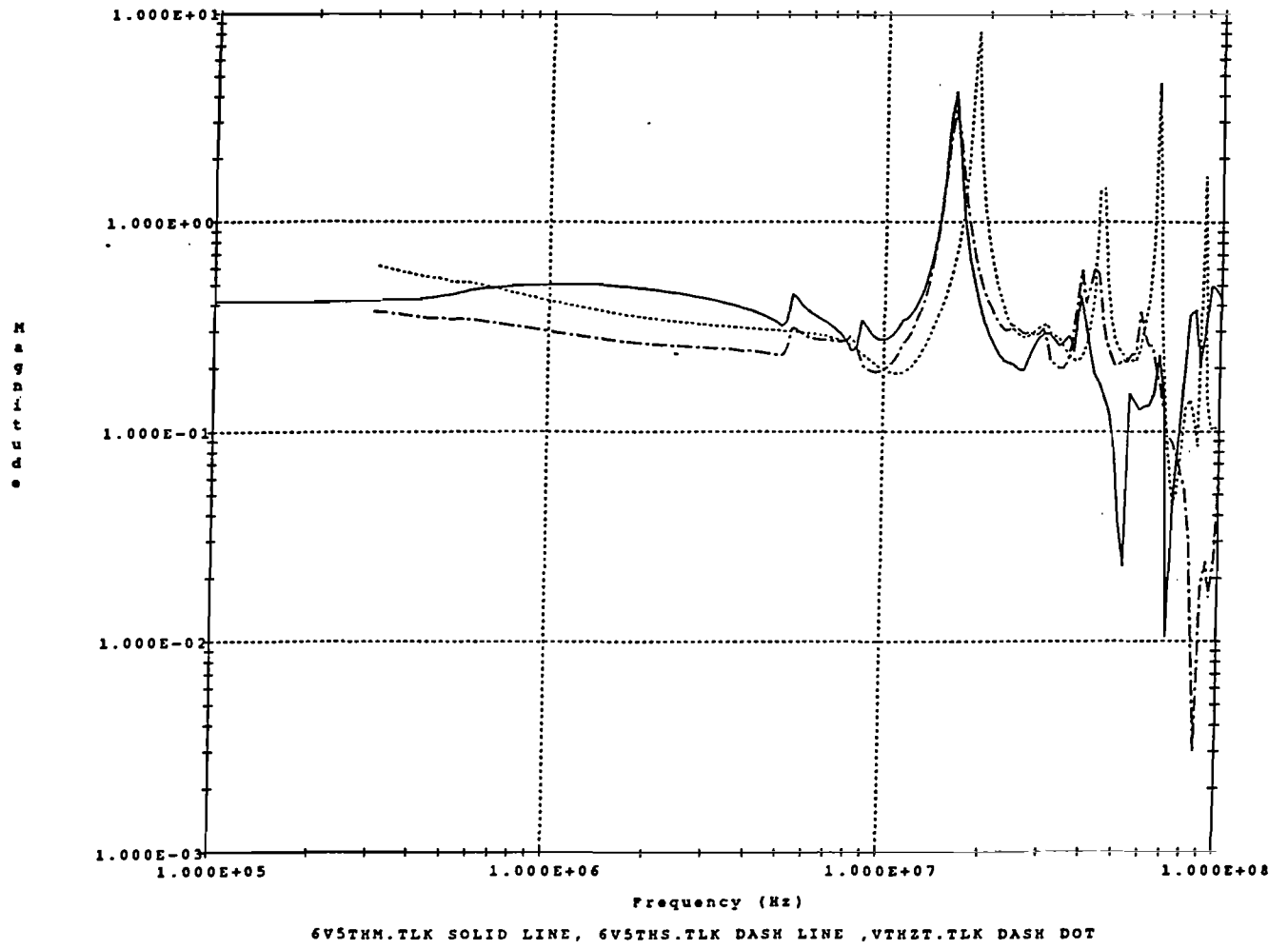
Fig. 3.30: Thevenin voltage generator on J004(measured and calculated)
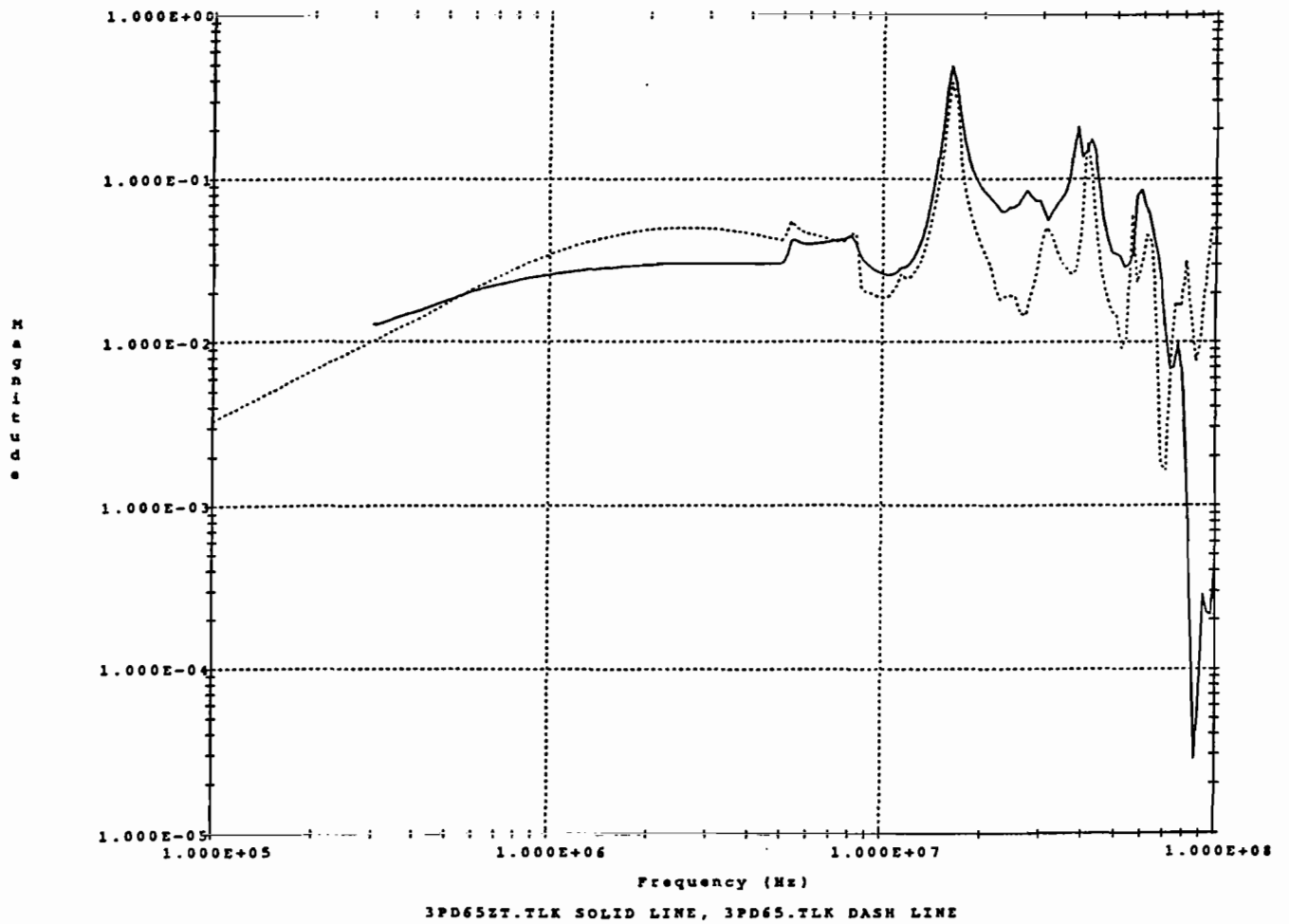
Fig. 3.32: Voltage at port 5, PD6 (measured and calculated with Zt*I)

1.000E+0

1.000E+00

M
a
g
n
i
t
u
d
e

1.000E-01

1.000E-02

1.000E-03

1.000E-04

1.000E+05   1.000E+06   1.000E+07   1.000E+08

Frequency (Hz)

3PD65S.TLK SOLID LINE, 3PD65.TLK DASH LINE
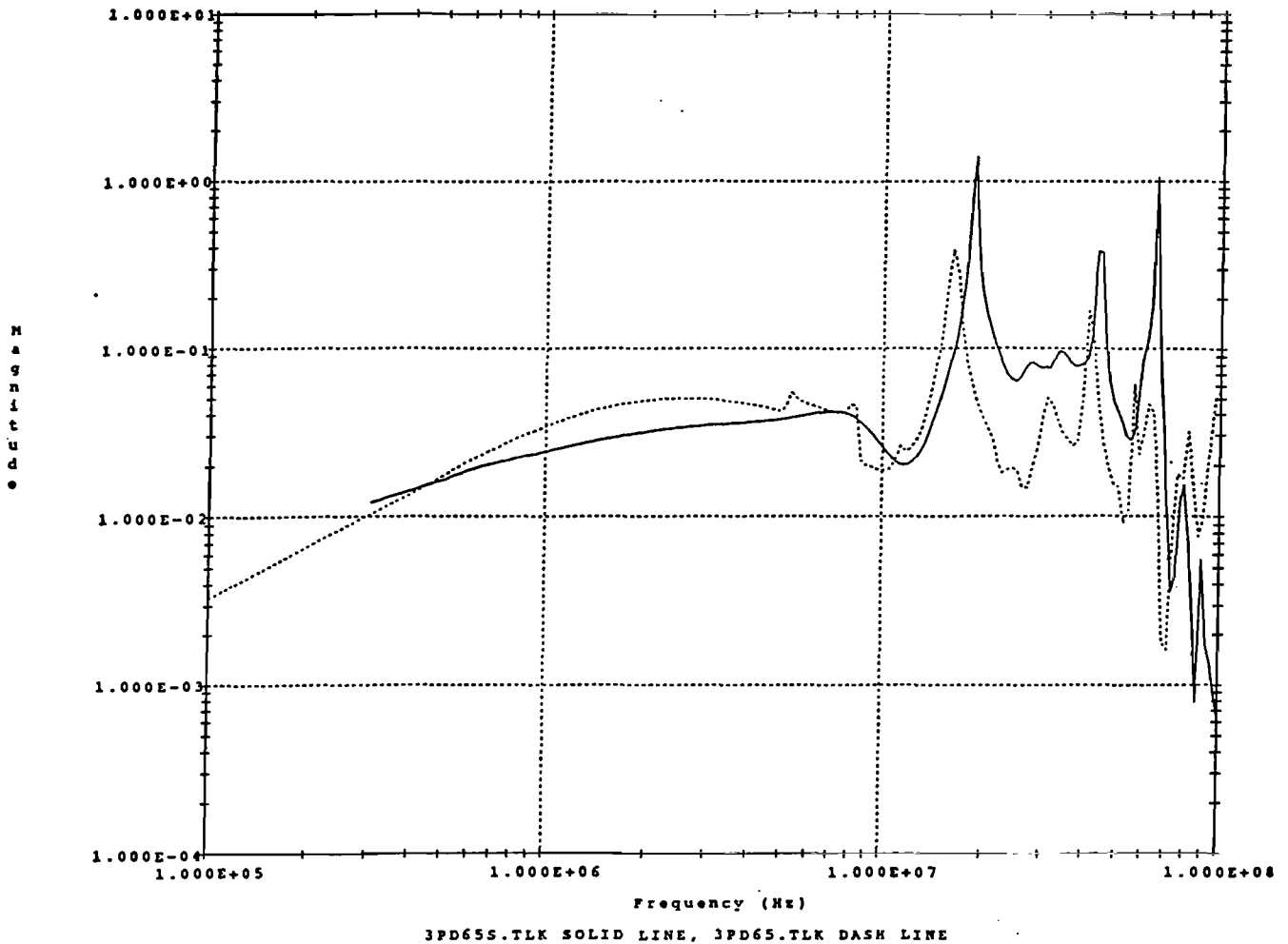
Fig. 3.33: Voltage at port 5, PD6 (measured and calculated with injector)

3.4.3.5) Conclusion on the work performed on Network B

This first step of experiment enabled the validation of the source characterization in the case of a shielded cable submitted to a current injection. Both methods to introduce source terms give satisfactory results. Therefore, they can be both used according to the experimental conditions:

- if it is impossible to characterize correctly the injector or the shield, the introduction of voltage generators as function of the measured shield currents multiplied by its transfer impedance seems more appropriate.

- on the other hand, the method of the introduction of the characterized injector is interesting when shield current measurement is impossible and enables a whole predictive approach whatever the shield connections are.

3.4.4) Network B illumination under Ellipticus antenna

3.4.4.1) Presentation of the experiment

The next step of the study on Network B was to evaluate numerically the response of the whole network located in the aircraft to a frequential illumination and to compare it to measurements.

To achieve this phase, the aircraft was placed under the Ellipticus Antenna, available on the Leslie site. This antenna is driven by an amplifier and a network analyser, in a frequency range from 300 KHz to 100 MHz for our purpose. Measurements are performed by means of sensors, current probes connected to optic fibbers and to the network analyser. A magnetic field measurement was made on the top of the aircraft and was used as a reference for the network analyser (B-channel). The measurements on the network inside the aircraft were made on the A-channel (See Fig. 3.34).
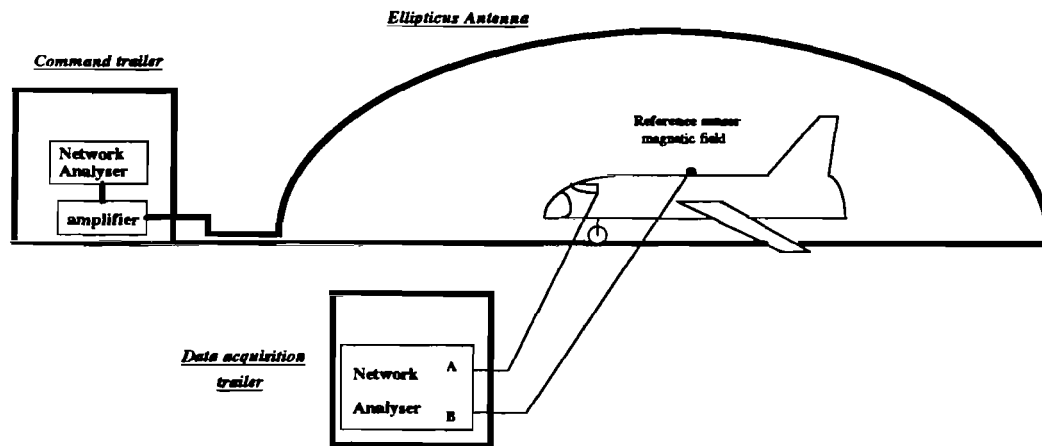
Fig. 3.34: Experiment description under Ellipticus antenna

3.4.4.2) Experiment difficulties

During the experiment, the power delivered by the amplifier following the driving network analyser was set to 100 Watt. Therefore in this configuration of illumination, the resultant voltages or currents on bundles located inside the shielded volumes of the structure was too low to be correctly measured with the instrumentation available on the site.

Thus in order to face this problem, a 30 dB amplifier was added at the extremity of the optic fibber allowing correct measurements.

3.4.4.3) Modelling of the source terms under Ellipticus antenna

In this model, we assumed that, when the aircraft is illuminated, the main point of entry for the aggression is the cockpit. The energy is captured by the shielded cable located in the cockpit and then propagates in the lower volume along the network connected to the perturbed shielded cable. In the modelling, the sources terms were applied on the topological tubes representing the shielded cable.

As described in Annex B, the method developed to model the perturbation on the shielded cable was based on the concept of transfer function. This method requires a generic numerical simulation and a current measurement on the shielded cable.

Fig. 3.35 recalls briefly the process to evaluate the voltage generator to apply on the shielded cable model.
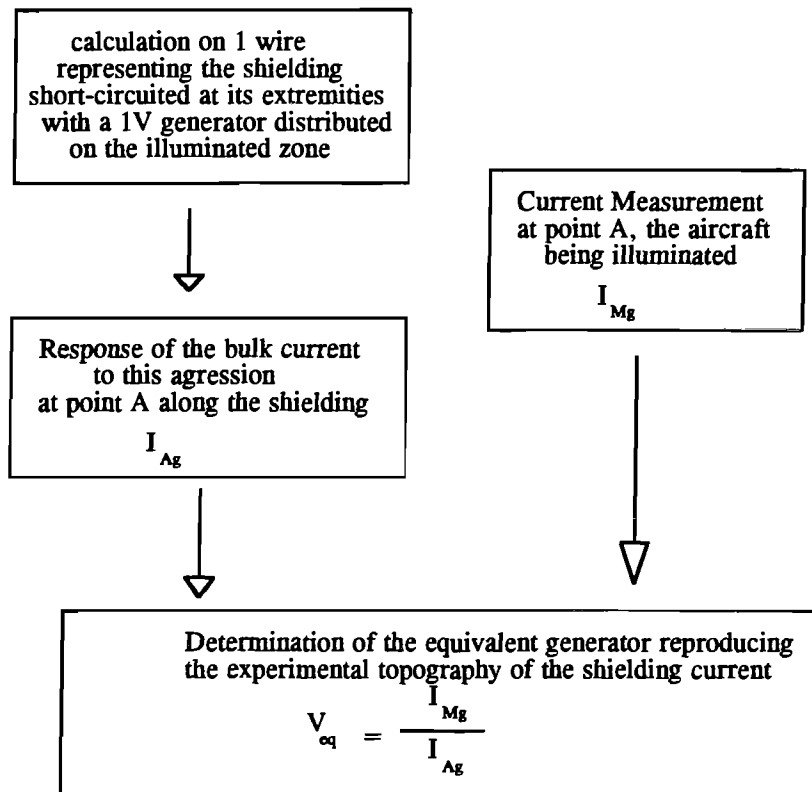
Fig 3.35: Synopsis for the determination of source terms

3.4.4.4) Numerical simulations management

The method applied to simulate the response of the whole network to an illumination is the same as the one applied to the current injection (see §3.4.3), that is to say:

- modelling of the shielded cable with the equivalent generator processed from a generic simulation and a measurement.
- determination of the Thevenin generators on each wire representing the interference at the junction between the cockpit and the lower shielded volumes.
- application of Thevenin generators on the network when modelling the lower volume.

3.4.4.5) Case 1 : shield of the shielded cable short-circuited

3.4.4.5.1) Network configuration

The network used for the determination of Thevenin generator is represented on Fig. 3.28 (where the topological source file for the code is now "blind_situ_c.ws") Fig. 3.31 represents the modelling of the lower volume network, where the source file is now "blind_situ_il.eth".

3.4.4.5.2) Comparisons simulation-measurement

On Fig. 3.36, numerical simulation and measurement of the Thevenin generator at the junction cockpit-lower volume are overlaid with a satisfactory agreement. We can notice that up to 10 MHz the signal is correctly reproduced by the modelling (it is obvious that in this frequency range the interference propagates without being disturbed by the line behaviour). This signal value is 6 dB below the Voltage generator introduced as source term since each internal wire is loaded with 50 Ω. Over 10 MHz, resonances of the shielded cable appear and deform the initial interference. The modelling reproduces correctly the first resonances and gives an average level of energy over 50 MHz comparable to the measurement.

On Fig. 3.37 are overlaid measured and simulated voltages induced on wire 5 of box LD7M. This wire is directly connected to one of the internal conductors of the illuminated shielded cable. Previous remarks are still available and the calculation is considered as being satisfactory. Fig. 3.38 and 3.39 represent the measured and calculated voltages, induced on wires 5 et 9 of box LD8M. On these figures, we also see the voltage induced on these wires when the shielded cable is disconnected from the connector, at the cockpit-lower volume junction. This curve represents the voltage induced by an interference entering this lower volume and independent of the shielded cable. This voltage is named as "residual signal".

We can notice that in the case of wire n°5 of box LD8M, this residual signal is the majority signal. This can be explained by the fact that, if we consider that the point of entry for the interference is the shielded cable, this wire is submitted to a second-order coupling (mutual inductance and capacitance coupling). The voltages level on the loads, due to this second-order coupling, can be then smaller than the ones issuing by an interference entering directly the lower volume (which is not as well shielded as we supposed initially).
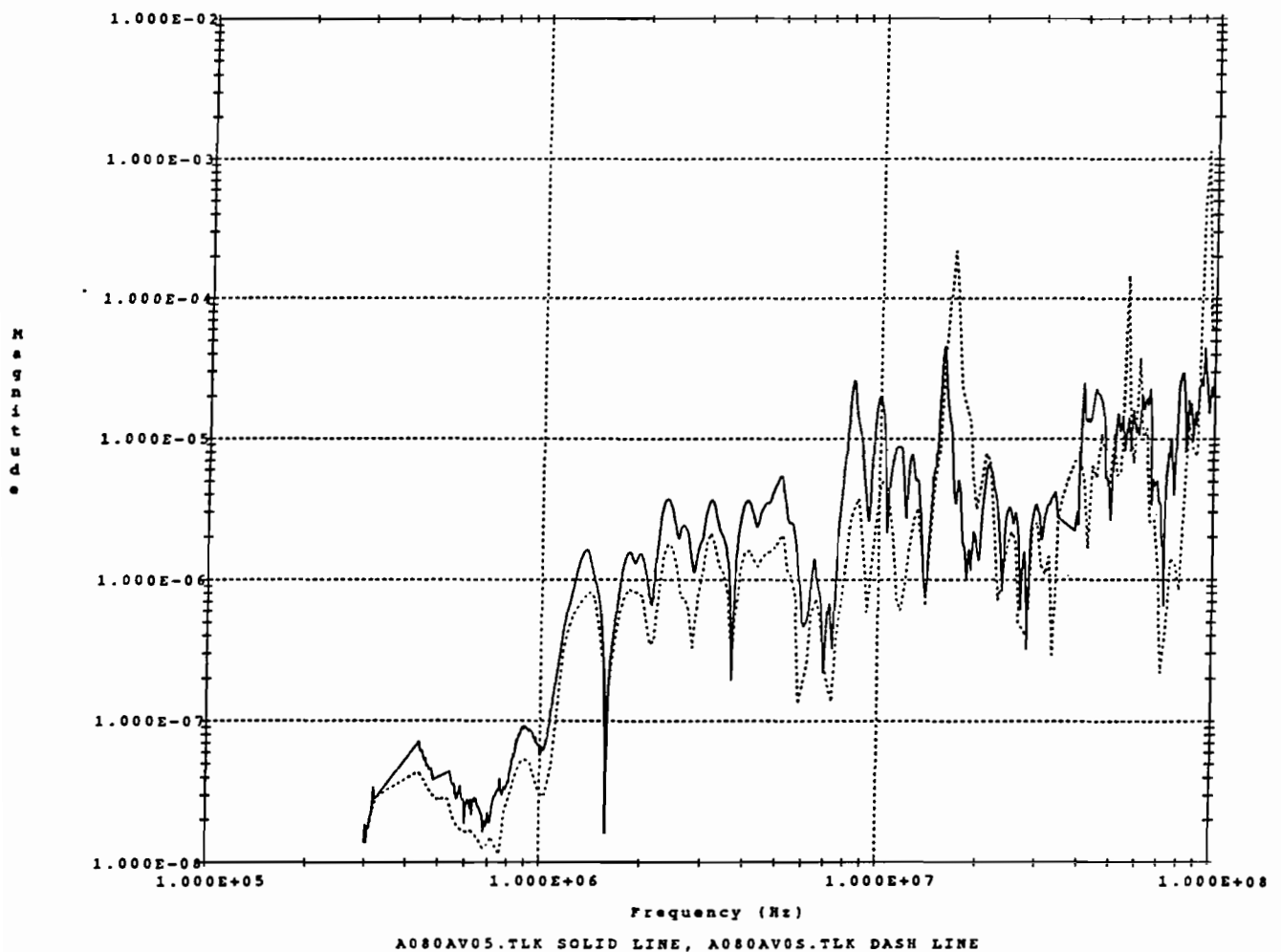
Fig. 3.36: Thevenin generator when the shield is short-circuited
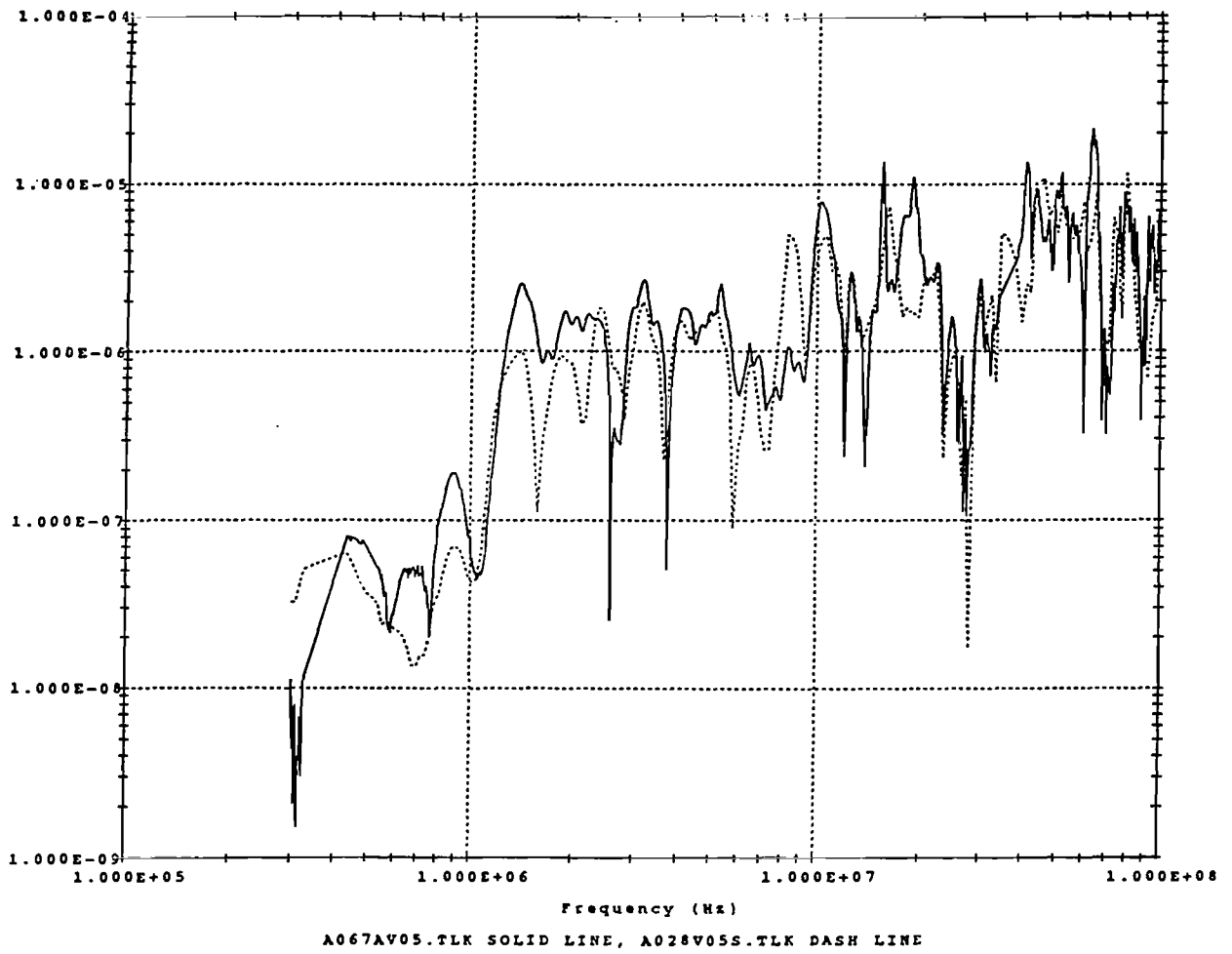
Fig. 3.37: Voltage at port 5 of ld7 with the shield short-circuited
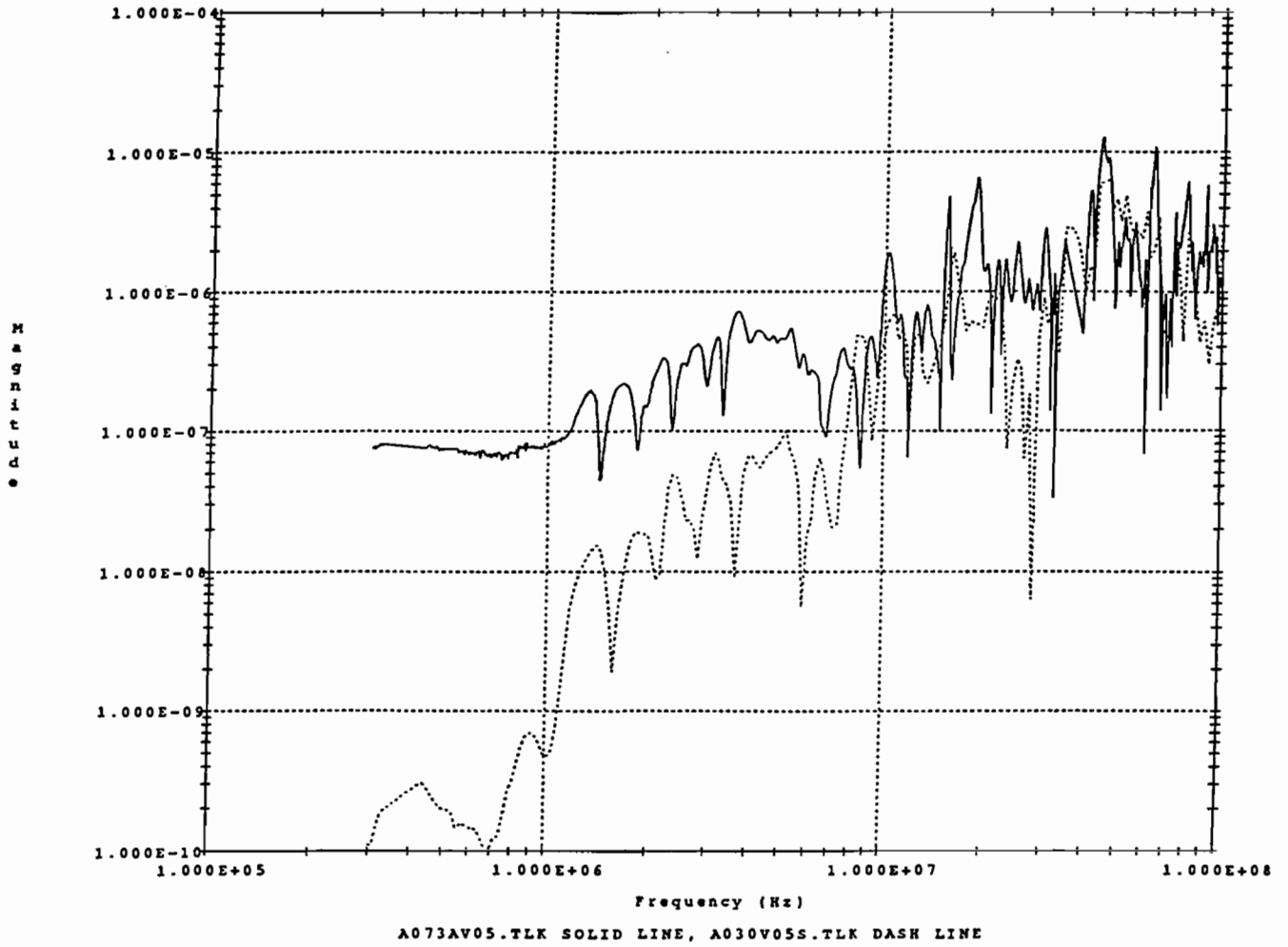
Fig. 3.38: Voltage at port 5 of ld8 with the shield short-circuited
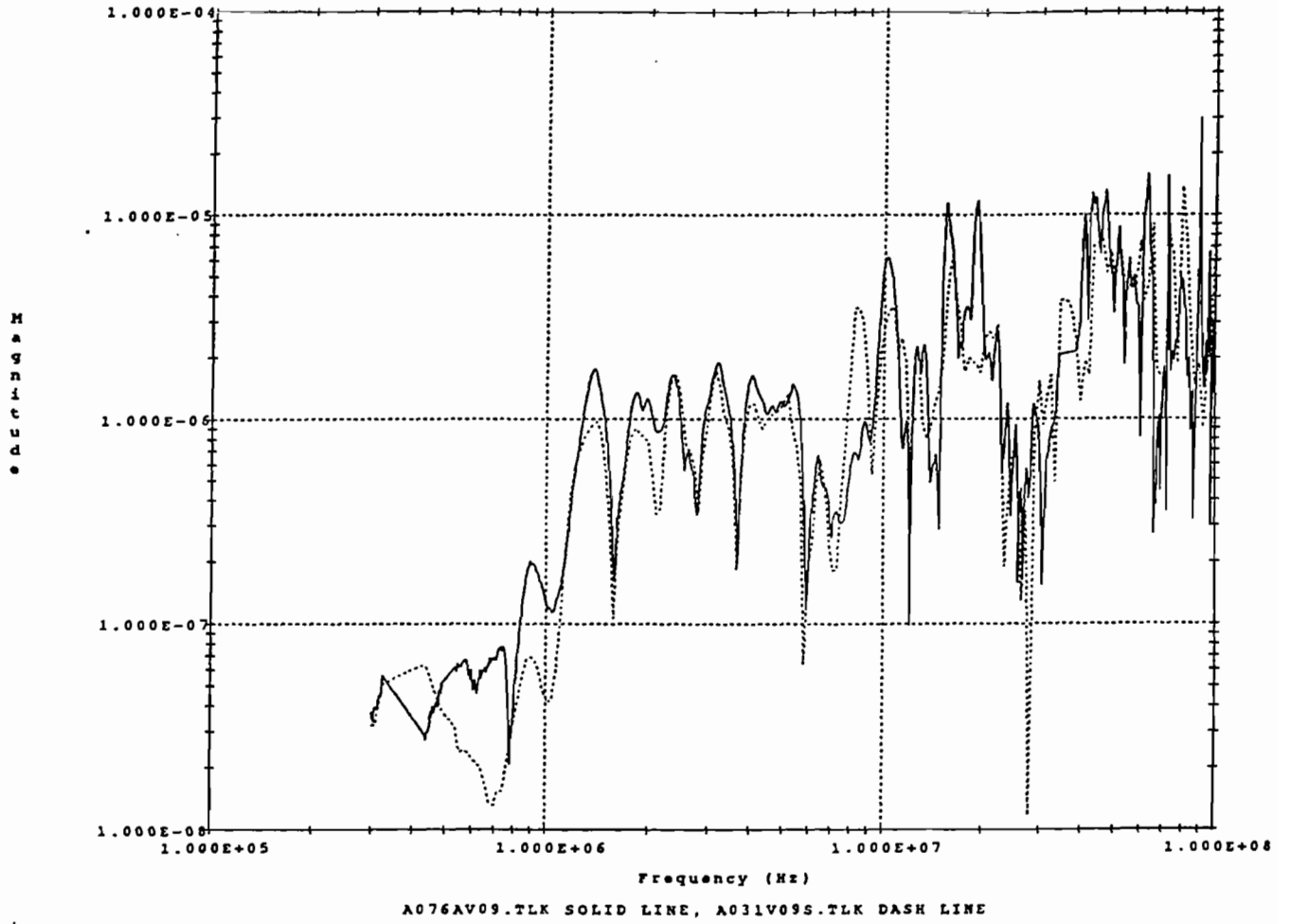
Fig. 3.39: Voltage at port 9 of ld8 with the shield short-circuited

3.4.4.6) Case 2 : shield of shielded cable open

In a second phase, in order to simulate an incorrect grounding of the wiring, the shield of the bundle inside the cockpit was disconnected at one end, near the connector J004. This configuration of study appears to be very interesting since it enables to evaluate the potentiality of a topological predictive approach in the case of a default in the tested cable network. Another advantage is that all the induced voltage levels increased and thus the measurement difficulties disappeared.

3.4.4.6.1) Experimental configuration of the shielded cable

Now, the inner conductors of the shielded cable are directly perturbed by the external aggression (Fig 3.40).
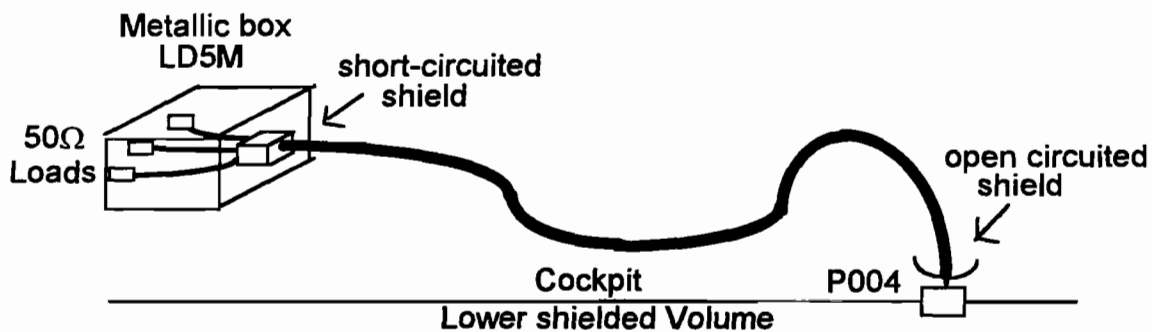
Fig. 3.40: Experimental configuration

On Fig. 3.41, different voltages measured on wire 9 of box LD8M are overlaid:
- measurement when the cable shielding is short-circuited
- measurement when the cable shielding is open-circuited
- measurement of the residual voltage when the shielded cable is disconnected from the network located in the lower volume.

We can notice that the signal measured when the cable shield is disconnected has a level much more important than in the two other cases. Therefore in the case of the cable shield disconnection, the main point of entry for the perturbation was the bundle located in the cockpit.

A105V09G.TLK SOLID LINE, A076AV09.TLK DASH LINE ,A077BV09.TLK DASH DOT
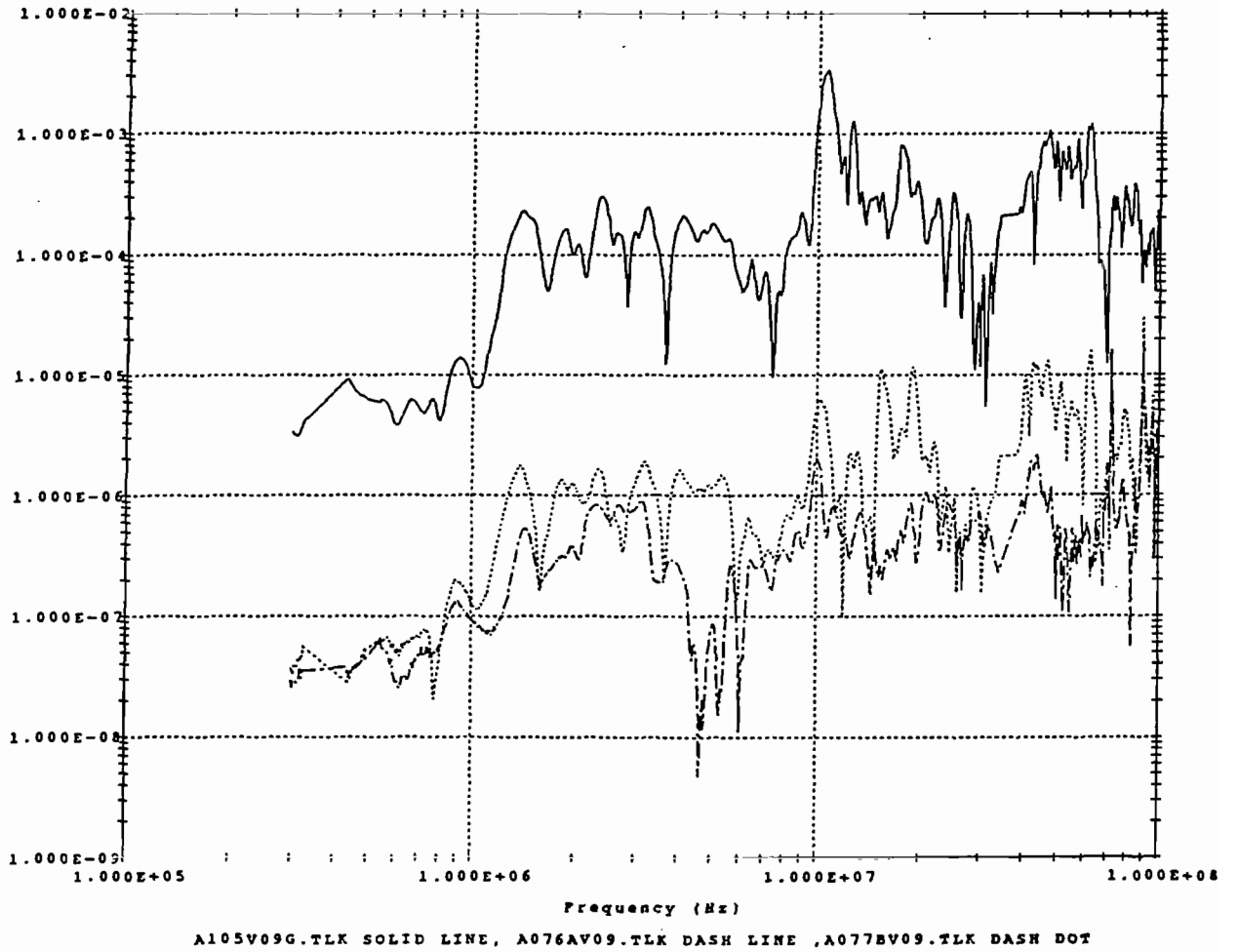
Fig. 3.41: measured voltage at port 9 of LD8 for short-circuited and open shields

3.4.4.6.2) Network configuration

The network used for the determination of Thevenin generators is the same as the one represented on Fig. 3.28 (where the source file is "blind_situ_c.ws" and junction 1 is now "con3_4co.s", modelling the disconnection at P004). Indeed the source model is the same as the one introduced in the case of the shield short-circuited, since this source represents the electromagnetic interference existing without the bundle (distribution of the electrical tangential field on the virtual running of the network).

The lower shielded volume is modelled with the same network as the one presented on Fig. 3.31: the source term is now "blind_situ_il.eth ". Junction 5, modelling the shielded cable in the cockpit, is now calculated by taking into account the shield disconnection and the file is "blind_co.s50".

3.4.4.6.3) Comparison between numerical simulation and measurement

Measurement and numerical simulation of the Thevenin voltage at the point of entry in the lower volume are overlaid on Fig. 3.42. Calculation fits correctly the measured signal up to 50 MHz. This confirms the fact that the model representing the shielded cable and its perturbation was correctly optimized and that this model can be used to determine any defect existing on the shield and creating some interference on the internal wires.

3.4.4.7) Conclusion of the study under Ellipticus antenna

During this phase of experiment, interesting points concerning the experimental and modelling studies were raised such as:

- the set-up of an instrumentation allowing noiseless correct measurements and of connection ,

- the modelling of sources terms on a shielded cable combining transfer impedance concept and measurement of only one bulk current ,

- the application of the topological approach to determine the points of entry of the energy and evaluate the consequences of a shielding default on the response of the whole network.
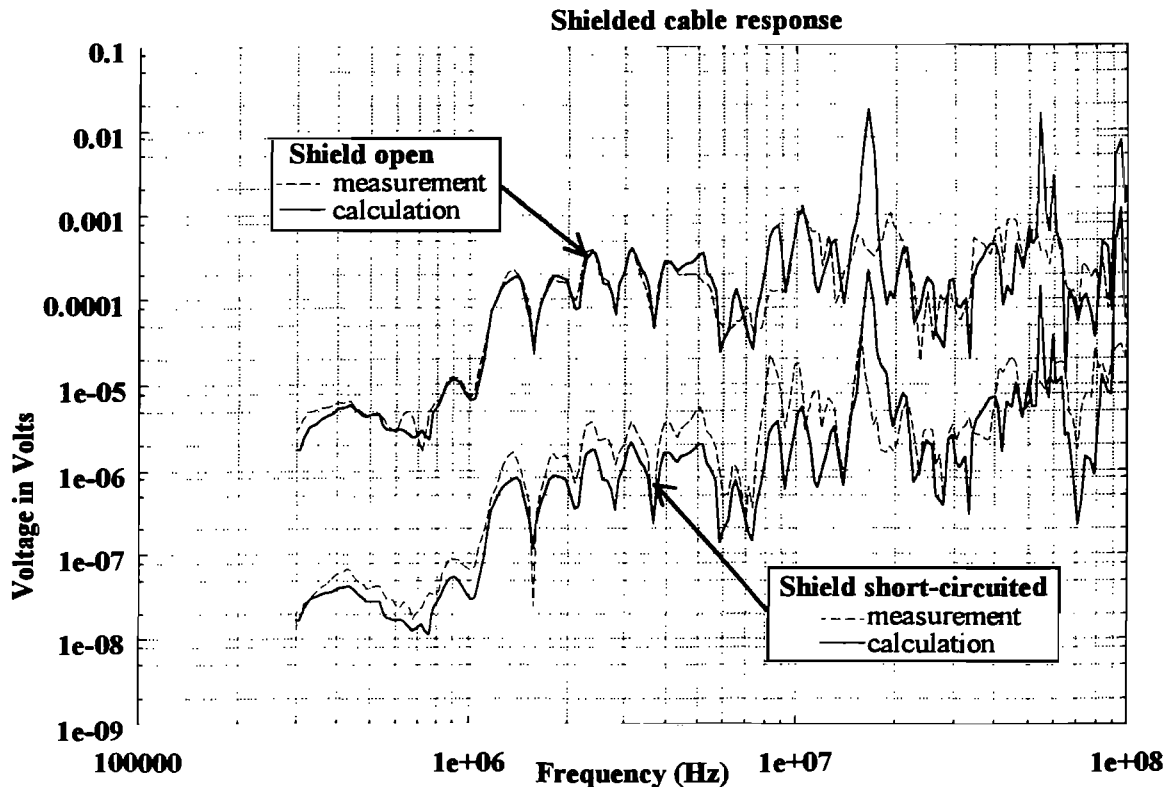
Fig. 3.42: Thevenin voltage generator with open and short-circuited shields

3.4.5).Conclusion of the study on network B:

This study on network B enabled the setting of different methods concerning the network characterization, optimization and modelling of source terms combining experiments and numerical simulations. Moreover in our study, we always tried to fit calculations and measurements in order to evaluate the influences of each parameter of the models, such as:

- the line parameters, representing the network running inside the real structure, thanks to a data base built during the pre-experiment performed in France,

- the characterization of the injector, equipment boxes, connectors,

- the characterization of a shielded cable including its transfer impedance

Once the modelling correctly validated with canonical configurations such as current injection, this topological application on network B enabled a predictive approach to evaluate the response of the cable network to an illumination and a qualitative approach allowing the determination of potential points of entry of energy inside the structure.

This approach on network B was very deterministic and essential to understand the coupling of interference on a cable network in a realistic structure and to set up and validate topological methods which can be applied on a more complex network such as the existing network A.

4 - EXPERIMENT ON NETWORK A

4.1) Introduction

The main objective of this experiment on Network A is to apply Electromagnetic Topology concepts to a realistic cable network. To achieve this aim , similar methods to the ones developed and validated on Network B have been applied.

During the first experiment in France, the whole network A was characterized by means of numerical simulations made from a few information given by the documentation of the PHILLIPS LABORATORY. The introduction of source terms is similar to the ones used during the phase on network B.

Because of a lack of time, only a single qualitative approach on network A, based on measurements and on canonical simulations, has been studied during the experiment in Albuquerque. Nevertheless, some conclusions could be given. These conclusions would be later confirmed by a quantitative work on network A performed in France. after the experiment. Indeed, all the parameters for this quantitative approach were at our disposal.

4.2) Description of network A

The existing network A presents the same topology as the network B previously studied, that is to say, the same running along the structure. It differs from network B only by the complexity of bundles, that is to say the number of conductors constituting bundles, equal to 12 or 21, and the number of loads inside each electrical box.
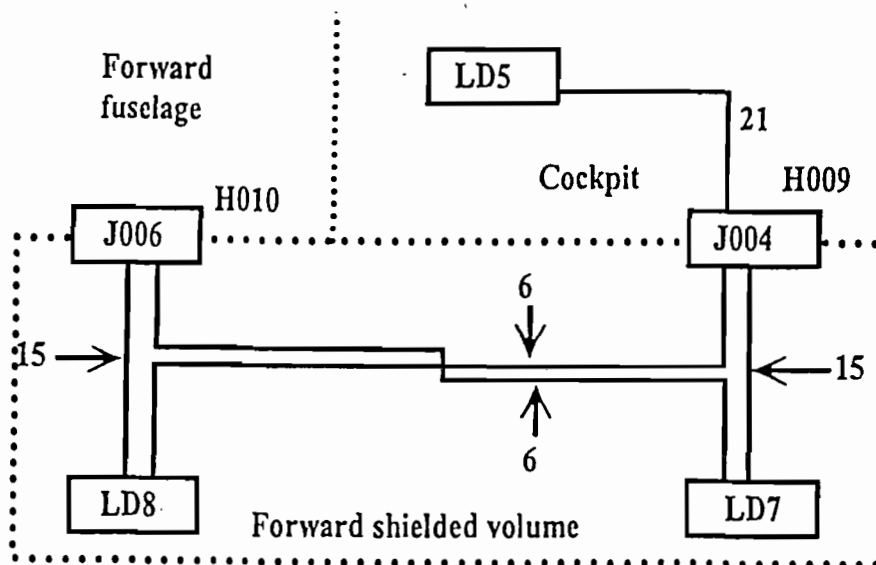
Fig. 4.1: Electrical scheme of network A

4.3) Network A topological model building

4.3.1) Introduction

Since this Network topology is similar to the previous one, Network A modelling has been performed in O.N.E.R.A. In this context , one of the problem is that we do not have any access to primary information such as electrical parameters of the bundles. Thus, this modelling was based on geometrical hypothesis which had been introduced as parameters of numerical codes allowing the characterization of the network.

4.3.2) Bundle characterization : numerical simulations

A realistic bundle running into a structure presents some characteristics such as its twisting and its position over the reference plane. In order to take into account this specificity a method has been developed, combining two kinds of numerical simulations based on:

- the use of the 2D code LAPLACE, available at O.N.E.R.A, modelling a section of the bundle, that is to say the relative position of each conductor between each other and the position of the bundle versus the reference,

- the use of CRIPTE code, modelling artificially the twisting inside the bundle along its running;

Once this achieved, each bundle can be electrically characterized and its parameters can be introduced in the topological model of the whole network.

4.3.2.1) 2D characterization

Let us recall that three kinds of bundles constitute the whole network:

- unshielded 12 conductor bundle,
- unshielded 21 conductor bundle,
- shielded 21 conductor bundle.

In the case of unshielded bundles, the electrical parameters are defined assuming the reference is the ground plane whereas for the shielded bundle, the reference is the shield.

In order to model a section of each bundle, assumptions based on geometrical description has been made such as:

- conductor dimensions: di-electric and inner conductor diameter,
- di-electric permittivity,
- bundle average diameter,
- relative position of each conductor in a section.

61

Once the geometrical description of each bundle defined, numerical simulations on each kind of bundles were performed with LAPLACE code, giving the capacitance matrix of each bundle, without di-electric and with di-electric. These simulations are based on the resolution of LAPLACE equation by means of the method of moments.

Fig 4.2 presents an example of the modelling of one section of bundle.

Fig. 4.2: Modelling of a section of bundle

The inductance matrix of each bundle was derived from the capacitance matrix calculated by removing di-electric as follows.

$$[L] = \mu_0 \cdot \varepsilon_0 \cdot [C_0]^{-1}$$

$[C_0]$ is the capacitance matrix without di-electric.

At this step, capacitance and inductance matrices, calculated as above, characterize a section of the bundle.

4.3.2.2) Application of CRIPTE code to model the twisting

The next step was to reproduce artificially the cable twisting inside the bundle and to derive, from this model, an average inductance matrix and an average capacitance matrix. To achieve this, CRIPTE code has been used by building a network constituted of tubes having the same line parameters calculated in a section as previously described and of different junctions connecting randomly ports of each tubes. Therefore, this model represents wires running randomly inside the bundle.
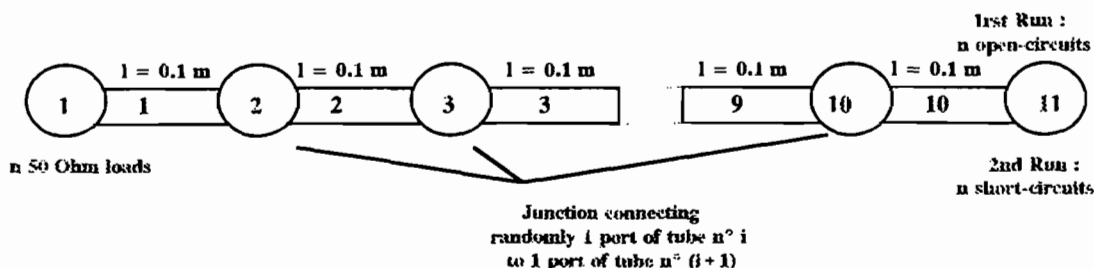
Fig. 4.3 : Topological model of a cable made of "n" twisted wires

A particularity of CRIPTE code is the option enabling the determination of sub networks scattering parameters. Therefore two numerical simulations have been performed :

- one with junction 11 being constituted of n open-circuits

- one with junction 11 being constituted of n short-circuits

The final matrices representing the average line parameters of the bundle are derived from the calculations of the [S] matrix with open-circuits and with short-circuits by means of an other code called "CALLC", available at ONERA (see Annex n°A).

4.3.3)Junction characterization

Network A is constituted of three kinds of junctions:

- Junctions connecting wires , representing cables running inside the structure and modelled with ideal junctions .On figure 4.4 is shown an example of a junction in the lower volume, at a point where the bundle is divided,

63
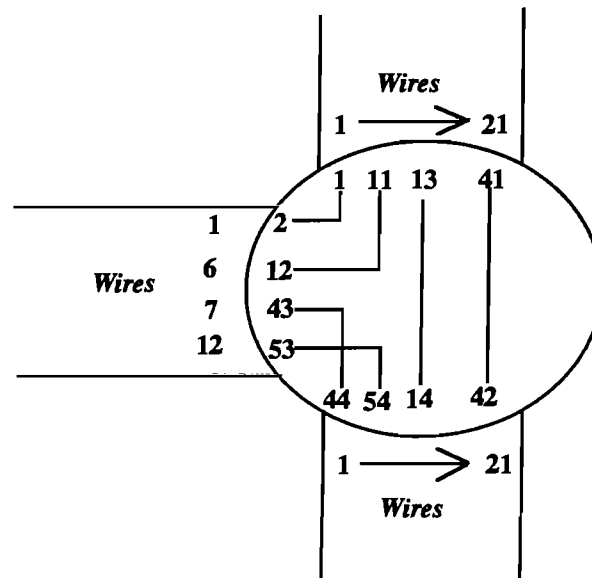
Fig. 4.4 : example of junction : J54.S

- Junctions modelling equipment and constituted of the theoretical existing loads,

- Junction modelling a fictive equipment box at P006 connector, since the studied network is limited to the lower volume.

4.3.4) Network A scheme

The final built network has the same structure as the one presented on figure 3.22 and figure 3.28. In fact, one of the big interest of Network B was to optomize the tube decomposition of the actual Network A. Of course, the tube and junction data files are now different because the number of elementary wires has changed.

The three wire shielded cable has been replaced by a 21 wire shielded cable. As the shield is treated as a wire in our model, the equivalent tube contains 22 wires. Of course, these tubes depend on the height of the cable over the ground.

The three wire unshielded cable has been replaced by a 21 wire unshielded cable. Two types of cables had to be considered as in figure 3.22: some were flattened on the ground whereas some others are unflattened.

The two wire unshielded cable is replaced by a 12 wire unshielded cable, with always the distinction between flattened tubes and unflattened.

4.4) Sources terms : experimental characterization

Since no information concerning the shielded cable located in the cockpit was available before the "in situ" experiment , no predictive simulations had been performed.

Therefore measurements related to the characterization of the shielded cable and its transfer impedance were necessary to determine correctly the interference induced by this cable.

4.4.1) Transfer impedance measurement

This measurement being done inside the structure, a correct determination of the transfer impedance is impossible because of:

- the length of the cable (6m) which does not allow a high frequency measurement

- problems related to ground reference inside the aircraft

Despite these limits, the following set-up had been used for the transfer impedance measurement:
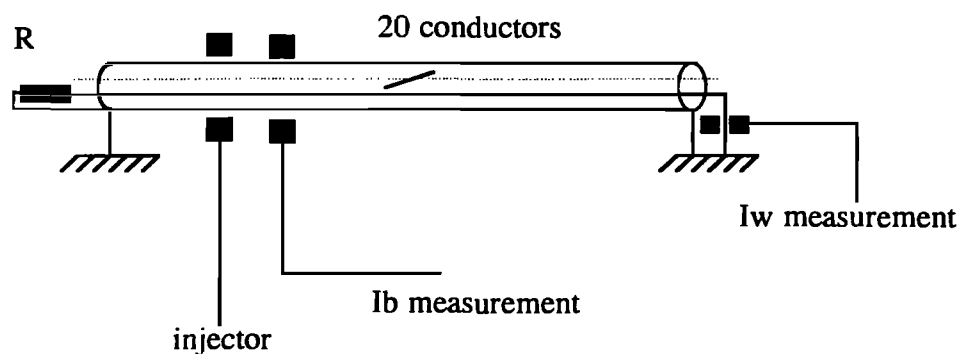
$$Zt = \frac{R\ Iw}{Ib} \qquad \text{(low frequency model)}$$

Fig. 4.5 : transfer impedance measurement set-up

From this measurement, the transfer resistance was found equal to $2m\Omega$ /m and the transfer inductance equal to 10 pH/m.

4.4.2) Cable shield characterization

As it was explained in the section relative to network B, the running of the shield along the structure influences the topography of the shield current, resulting from an external coupling. This is the reason why the shield might be correctly characterized in terms of line parameters depending on its location over the reference plane.

Therefore, a reflectometry was performed on the shield, showing that, in fact, the shielded cable could be split up in eight tubes representing significant change of location over the ground plane.

4.4.3) Introduction of source terms under illumination

When introduction of source terms on network B was studied, the aircraft being illuminated, a method based on a combination of a canonical simulation and a bundle current measurement had been developed and validated. We have shown that the equivalent voltage generator representing the perturbation coupling on the shielded cable is directly connected to the electromagnetic field existing while the absence of cables.

Therefore this equivalent generator is independent of the perturbed bundle characteristics and can be, thus, introduced as source terms on the existing network A. On fig 4.6, are represented the simulated shield current and the measured current near the box LD5. The main tendencies are correctly reproduced in the numerical simulation.
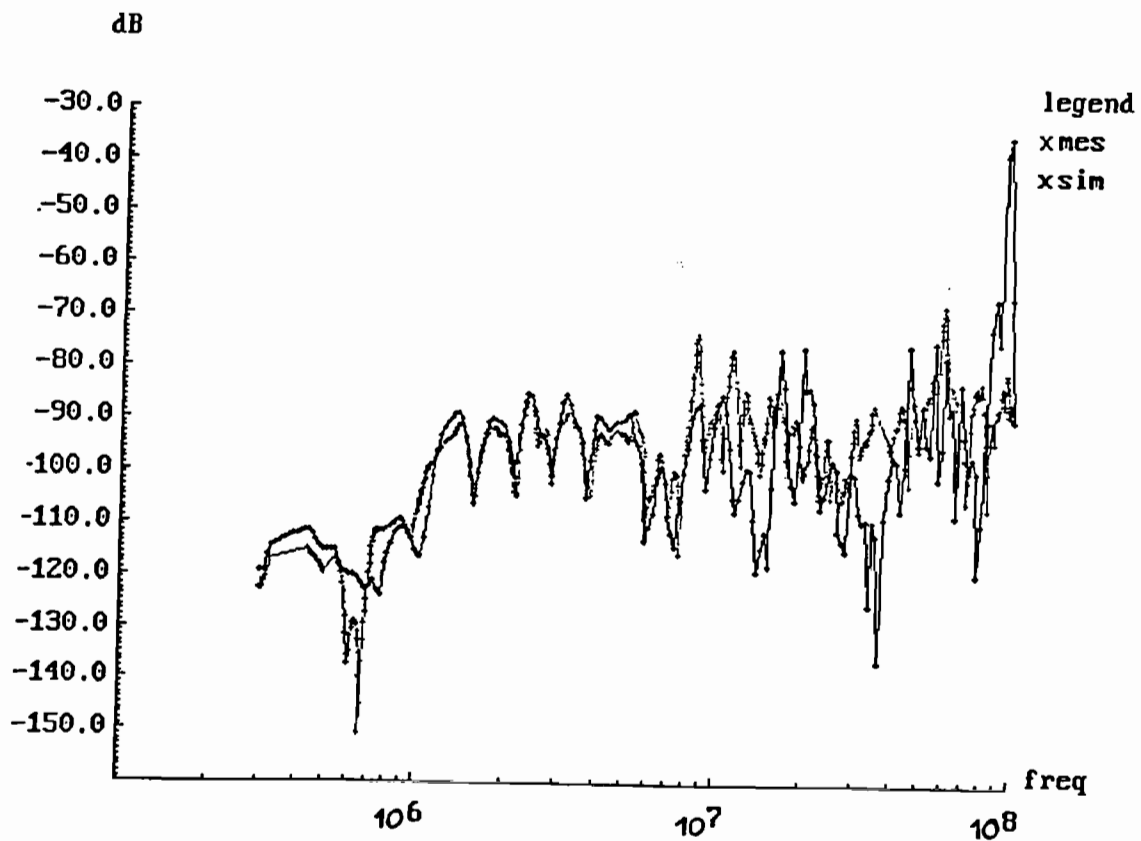
Fig. 4.6: Calculated and measured shield current

dB = 20.log(current in Ampere)

4.4.4.) Analysis of the coupling on the inner conductors of the shielded cable

The next step, once the topography of the shield current correctly simulated, was to evaluate the coupling induced on the inner conductors of the shielded cable. To achieve this purpose, the part of Network A located in the lower volume was disconnected from the shielded cable at the level of connector P004. Then a measurement and a calculation of Thevenin voltage at P004 on a conductor have been compared. In that precise case, the method used to introduce the source terms in the simulation is the one combining a shield current measurement and the transfer impedance concept (Annex B). At the extremity LD5, a configuration short-circuit, open-circuit enabled to fasten numerical simulation.
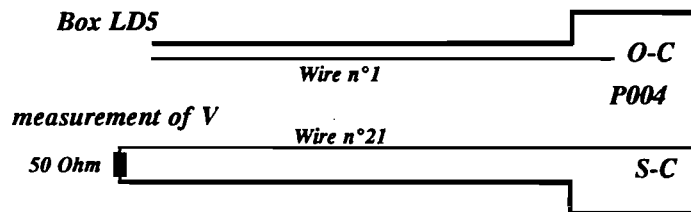
Fig. 4.7 Measurement of internal voltage

On fig 4.8, are represented the measured and simulated voltages on the inner conductor. From the comparison of both signals, we can say that the shielded cable model, when the structure was illuminated, reproduced correctly the coupling phenomenon.

Because of a lack of time, we were unable to do further simulation on the whole network A during the experiment in Albuquerque.
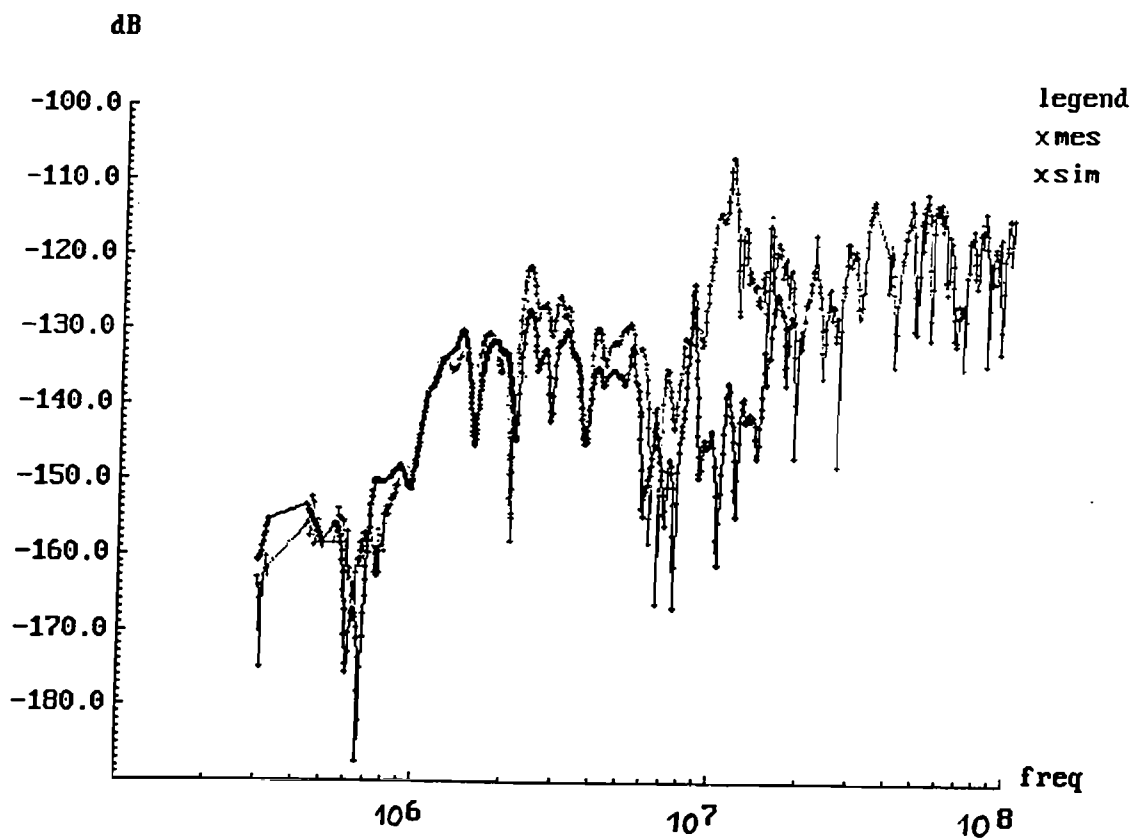
Fig. 4.8 Calculated and measured voltages on the inner conductor

dB=20.log(current in Ampere)

4.5) Conclusion of the experiment: Qualitative analysis

In the section related to the illumination of network B, the perturbation interfering bundles located in the lower volume came in 50% from the shielded cable and in 50% from the defects of the lower volume.

The main objective in this qualitative analysis is to evaluate the main point of entry of energy inside the structure. To achieve this purpose, two measurements have been made on one of the wires of the bundle connecting LD5 and LD7(Fig. 4.9):

1) Voltage measurement as described in fig. 4.7

2) Voltage measurement on the wire once the network is connected to the
   shielded cable

The first measurement represents the maximum voltage that can be induced by the external perturbation on the inner conductor. This assumption is correct in a low frequency domain, before the cables resonance.

The second measurement represents the effective voltage on the wire at box LD7.

After comparisons of both signals, we can see that the average level of the effective signal is much higher that the maximum voltage induced by the shielded cable.

Therefore, we can deduce that the perturbation induced on this wire at box LD7 does not come, mainly, from the shielded cable. This is easily explained by the fact the shielded cable presents a more efficient shielding level than the shielded cable used in network B.

We can conclude from this qualitative analysis that the shielding level of the lower volume is less important than the shielding level of the shielded cable located in the cockpit.
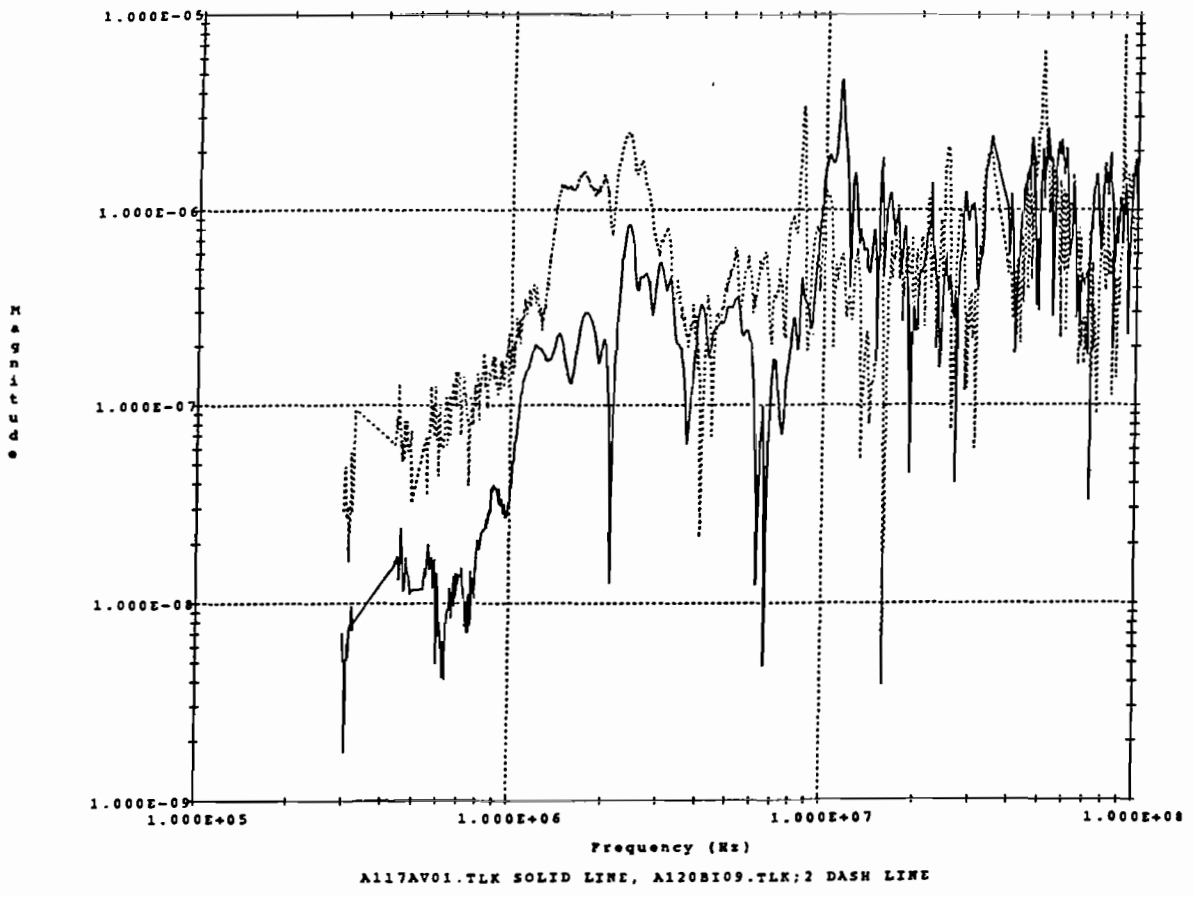
Fig. 4.9: Thevenin voltage measurement at P004 and effective voltage at LD5

4.6) Numerical simulations on network A

Back in France, we achieved further numerical simulations on the whole Network A, with a more powerful computer than the one we used during the experiment in Albuquerque. This computer allowed to treat all the network in quasi real time.

Several numerical simulations were done, showing the importance of the breakdown of the forward shielding volume in flatten an unflattened tubes. The configuration studied dealt with the disconnection of the shield in the cockpit volume, the only configuration for which measured signals were out of the noise level in the forward shielded volume. The method we adopted is similar to the one for Network B, that is to say:

- first, we calculated Thevenin equivalent generator vector at J004 level. The generators were determined thanks to a transfer function method.

- secondly, the Thevenin equivalent generator vector was applied to the sub network related to the forward shielded volume at the J004 level .

Further investigations on Network A would have been necessary to obtain more accurate calculations on Network A. In particular, we did not have enough time to characterize precisely the tubes of this network and we recall that the level of signal was not sufficient for us to be totally confident with their exactness. Nevertheless, the first numerical results we obtained, with no optimization, show a good agreement between the model and the experiment.

Figure 4.10 to 4.13 show a comparison of the simulated and computed current on 4 loads in LD7 (wire 1, wire 2, wire 8, wire 9).

Figure 4.14 to 4.17 show a comparison of the simulated and computed current on 4 loads in LD8 (wire 1, wire 2, wire 8, wire 9).

For both boxes, the signature of the current on wire 8 and wire 9 is proportional to the equivalent Thevenin generator applied on each wire at the level of J004 because these wires enter the shielded cable. From its side, the signature of the current is proportional to the derivative of the Thevenin equivalent generator. Because these wires do no enter the shielded cable, the coupling is made, in a differential way, with wires that belong to the shielded cable.
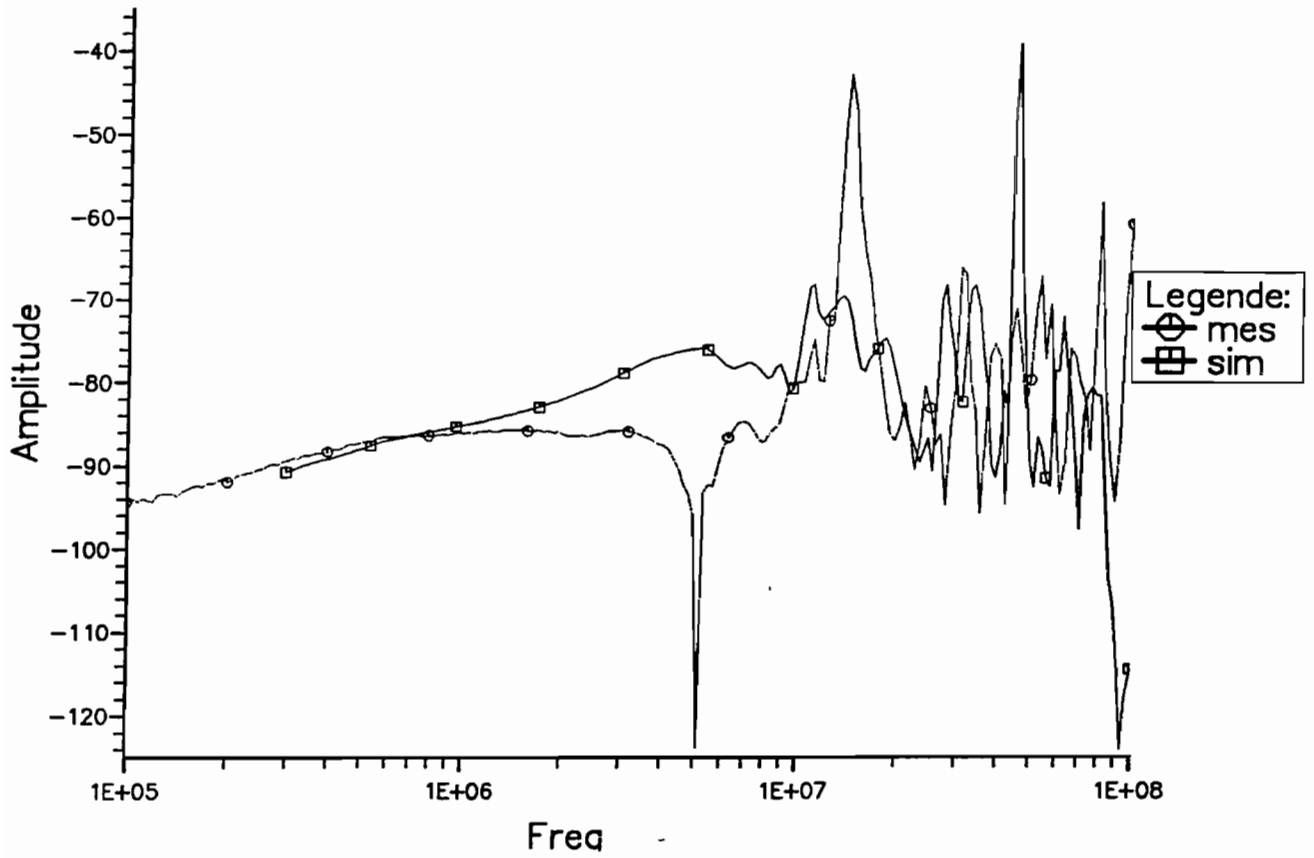
Fig. 4.10: current on wire 1 of LD7 box (Network A)

Amplitude=20 log (I in Ampere)
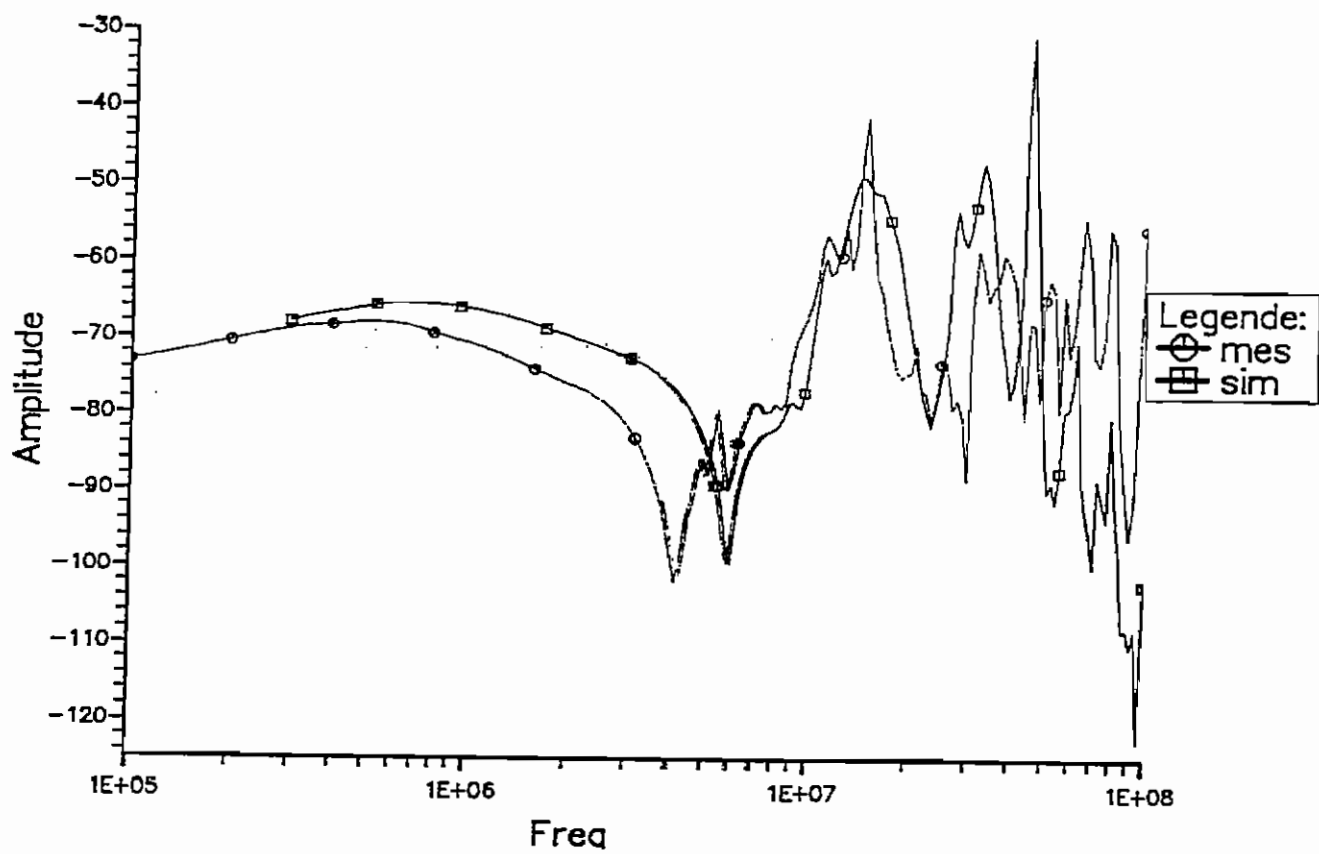
Fig. 4.11: current on wire 2 of LD7 box (Network A)

Amplitude = 20 log (I in Ampere)
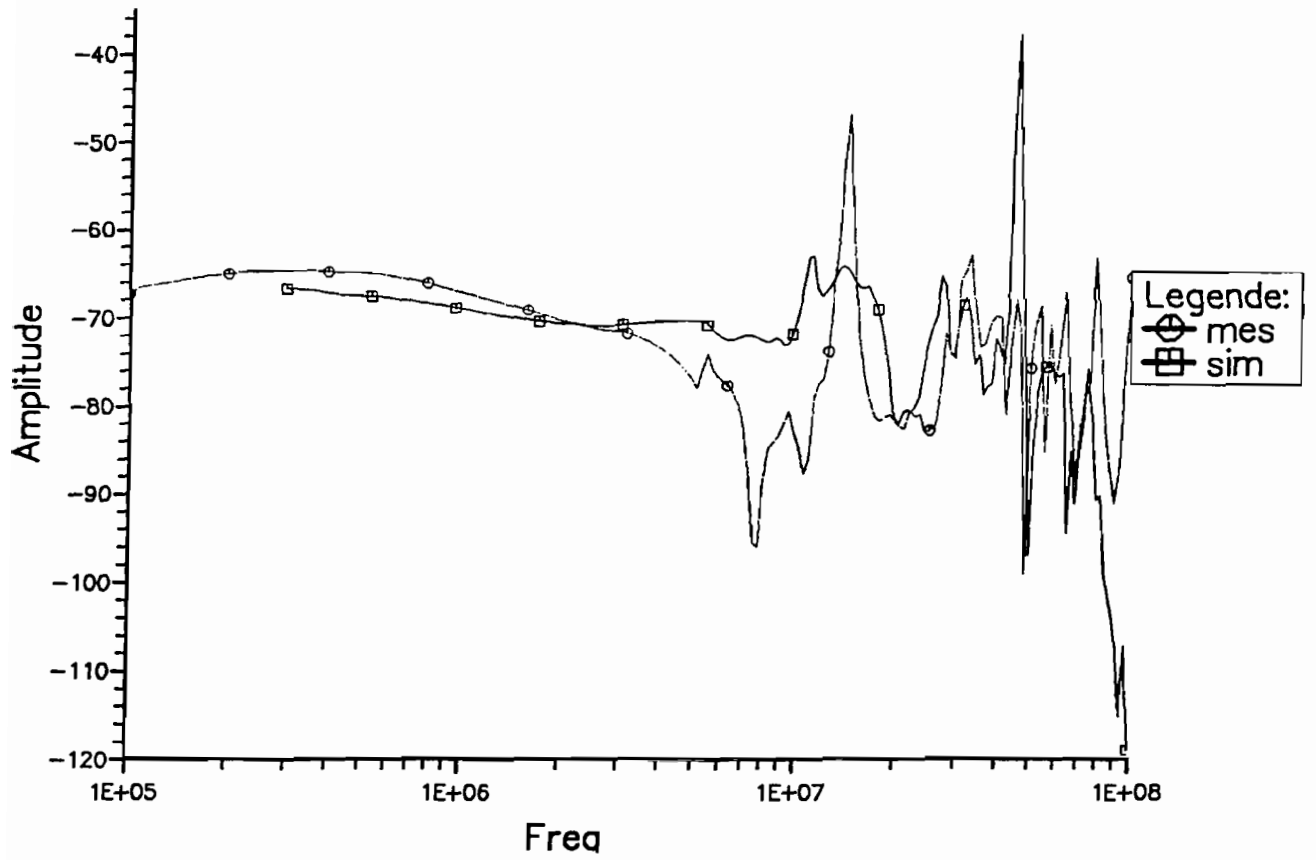
Fig. 4.12: current on wire 8 of LD7 box (Network A)

Amplitude = 20 log (I in Ampere)
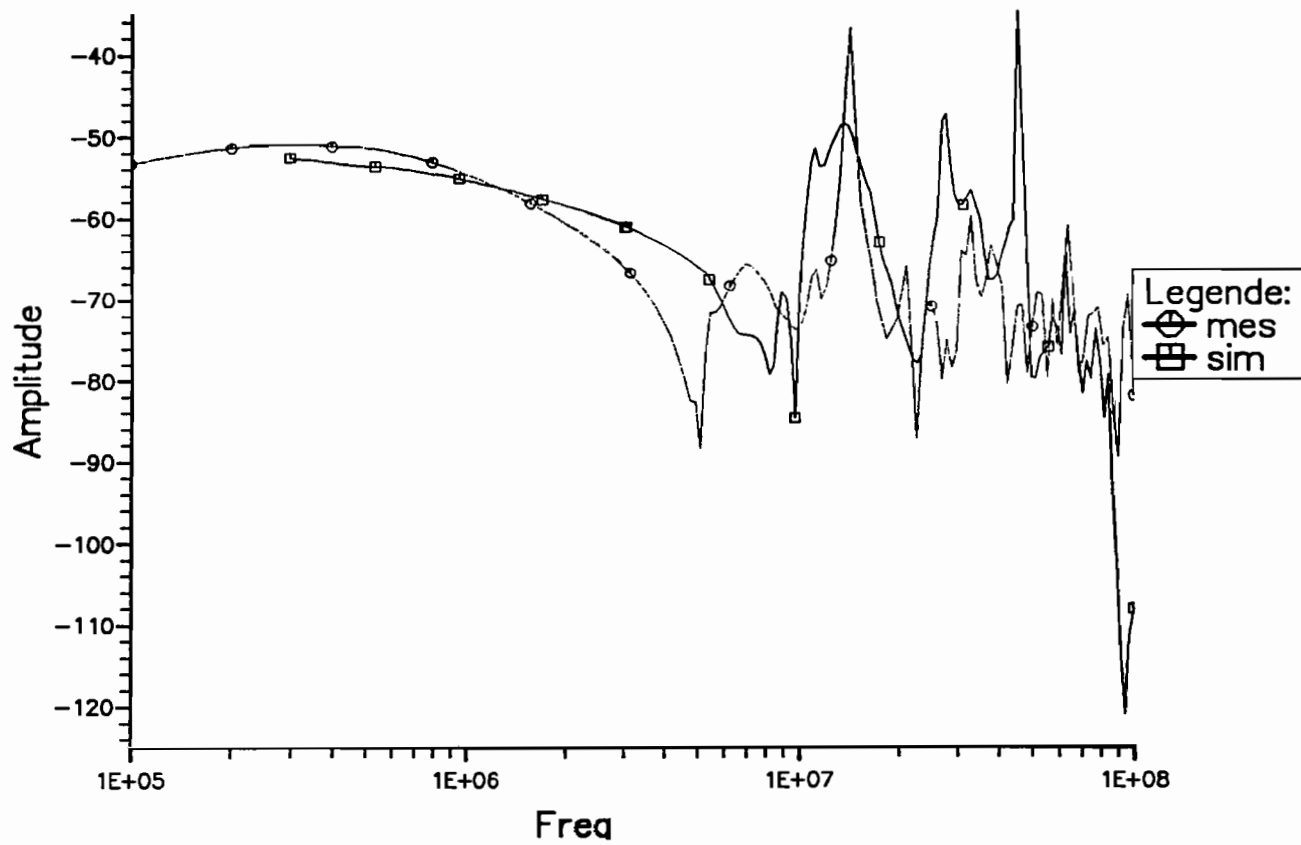
Fig. 4.13: current on wire 9 of LD7 box (Network A)

Amplitude=20 log (I in Ampere)
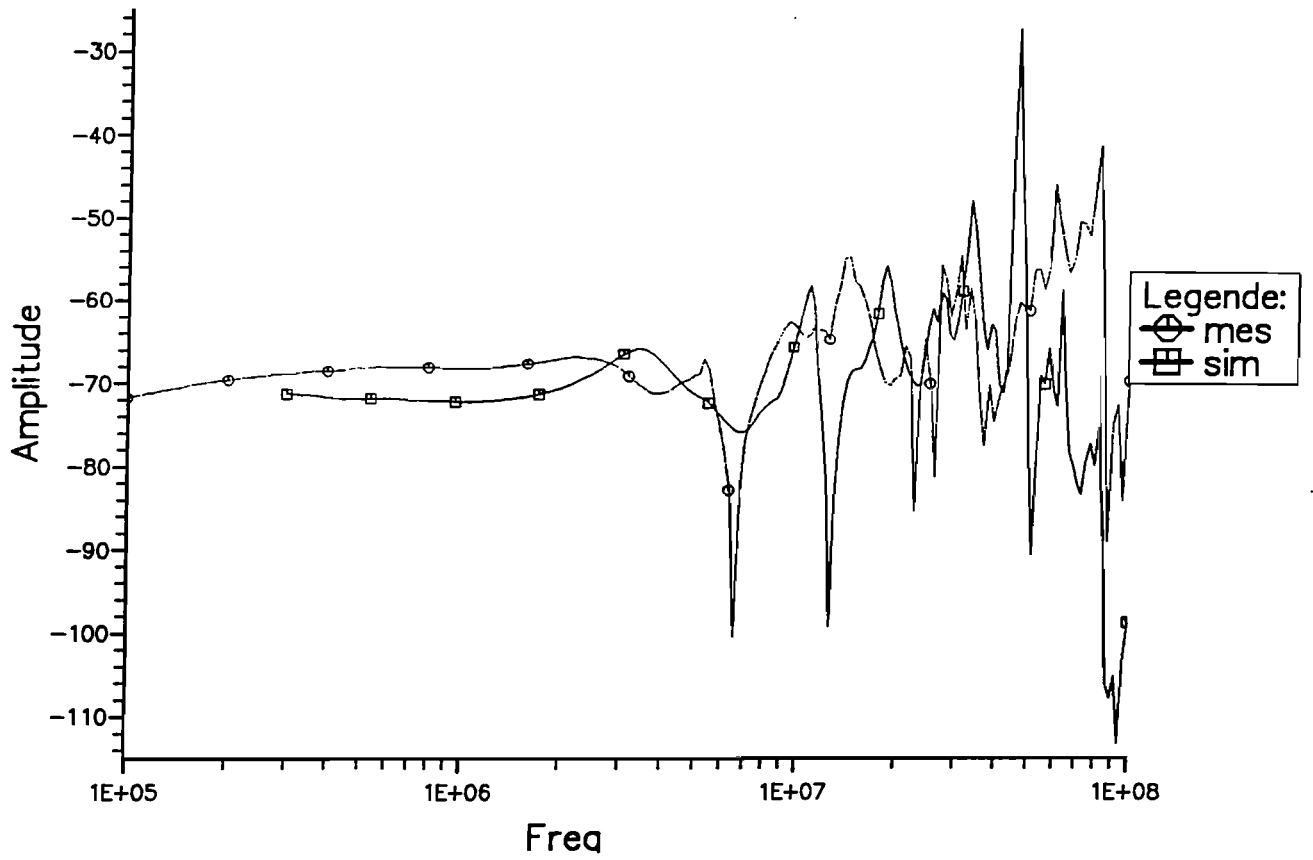
Fig. 4.14: current on wire 1 of LD8 box (Network A)

Amplitude=20 log (I in Ampere)
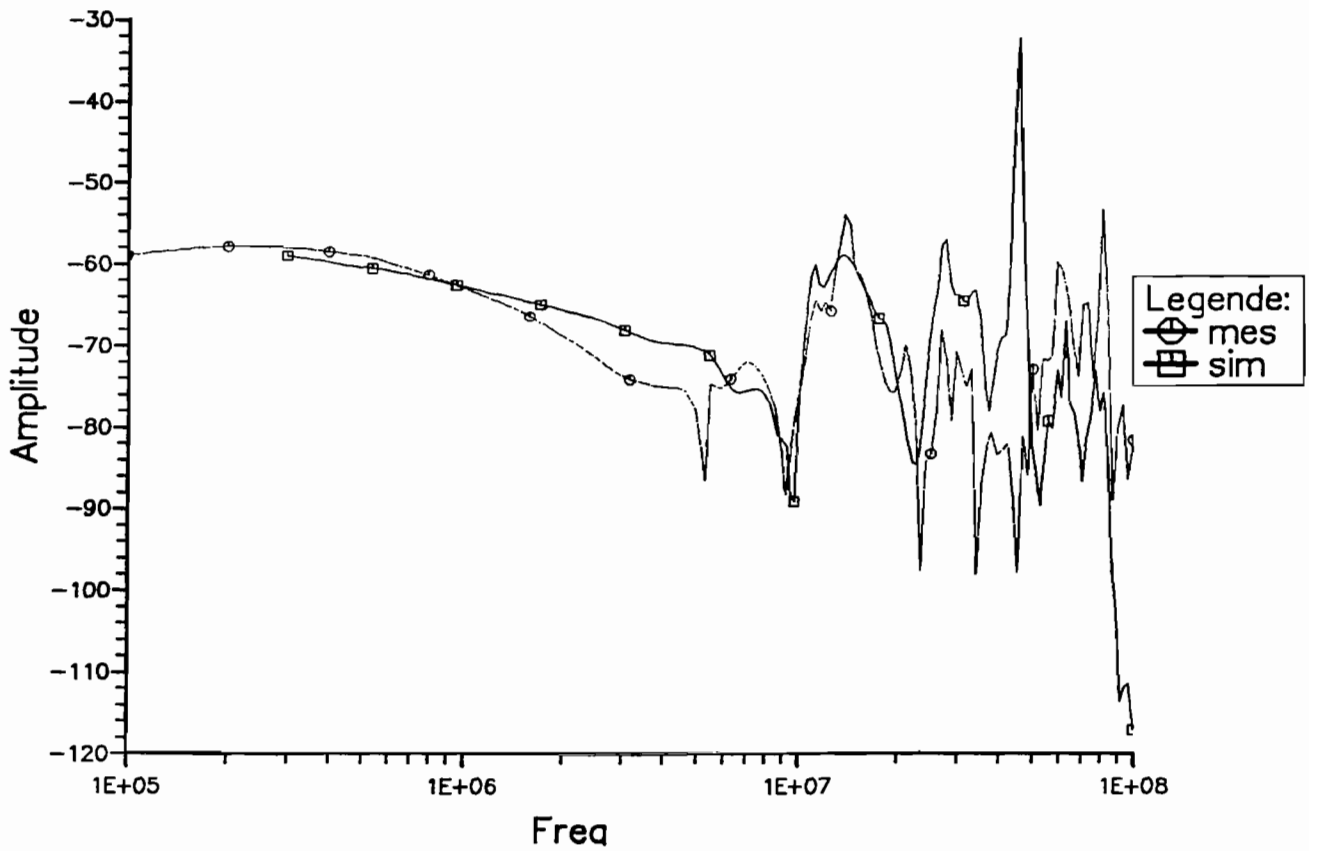
Fig. 4.15: current on wire 2 of LD8 box (Network A)

Amplitude=20 log (I in Ampere)
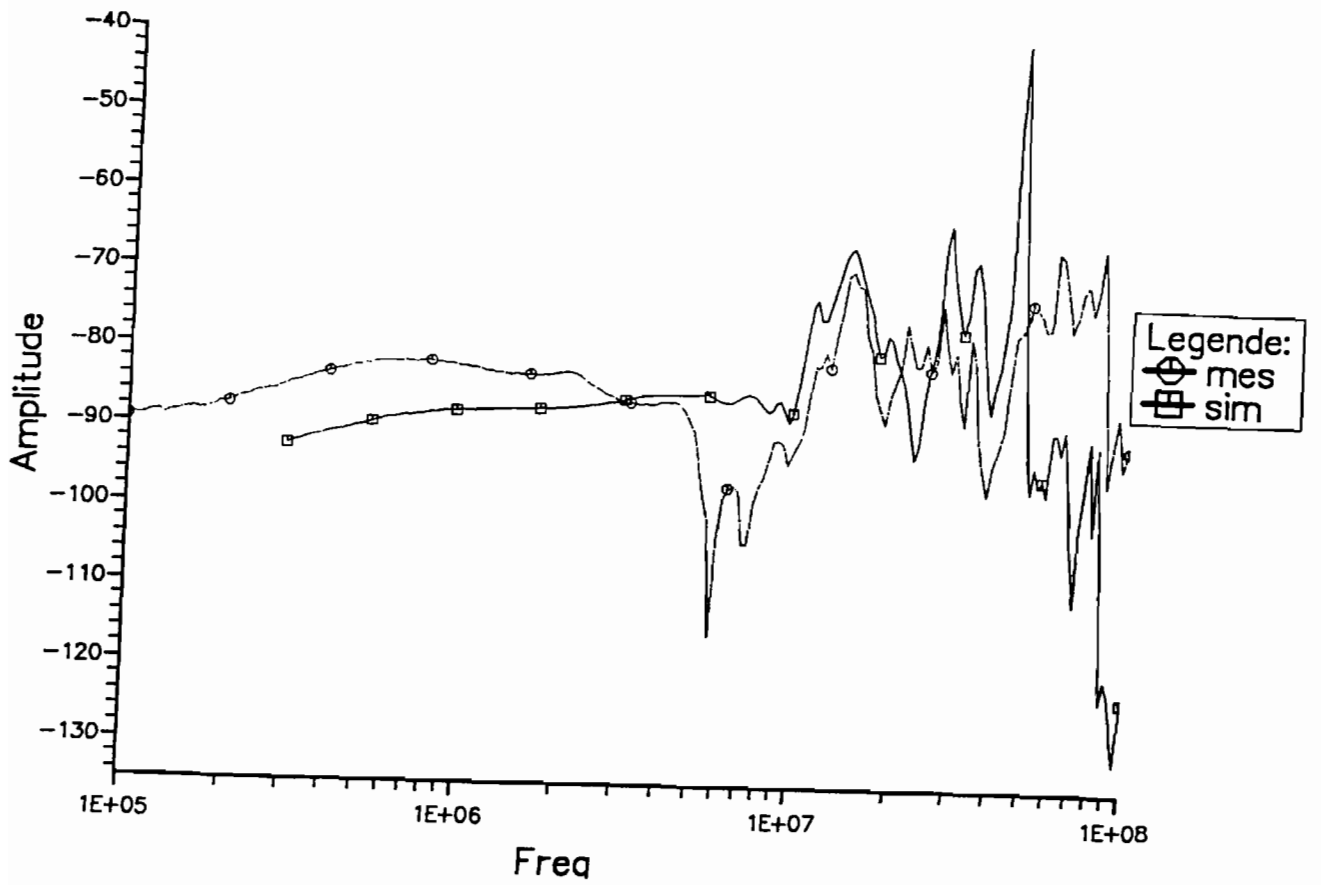
Fig. 4.16: current on wire 8 of LD8 box (Network A)

Amplitude=20 log (I in Ampere)
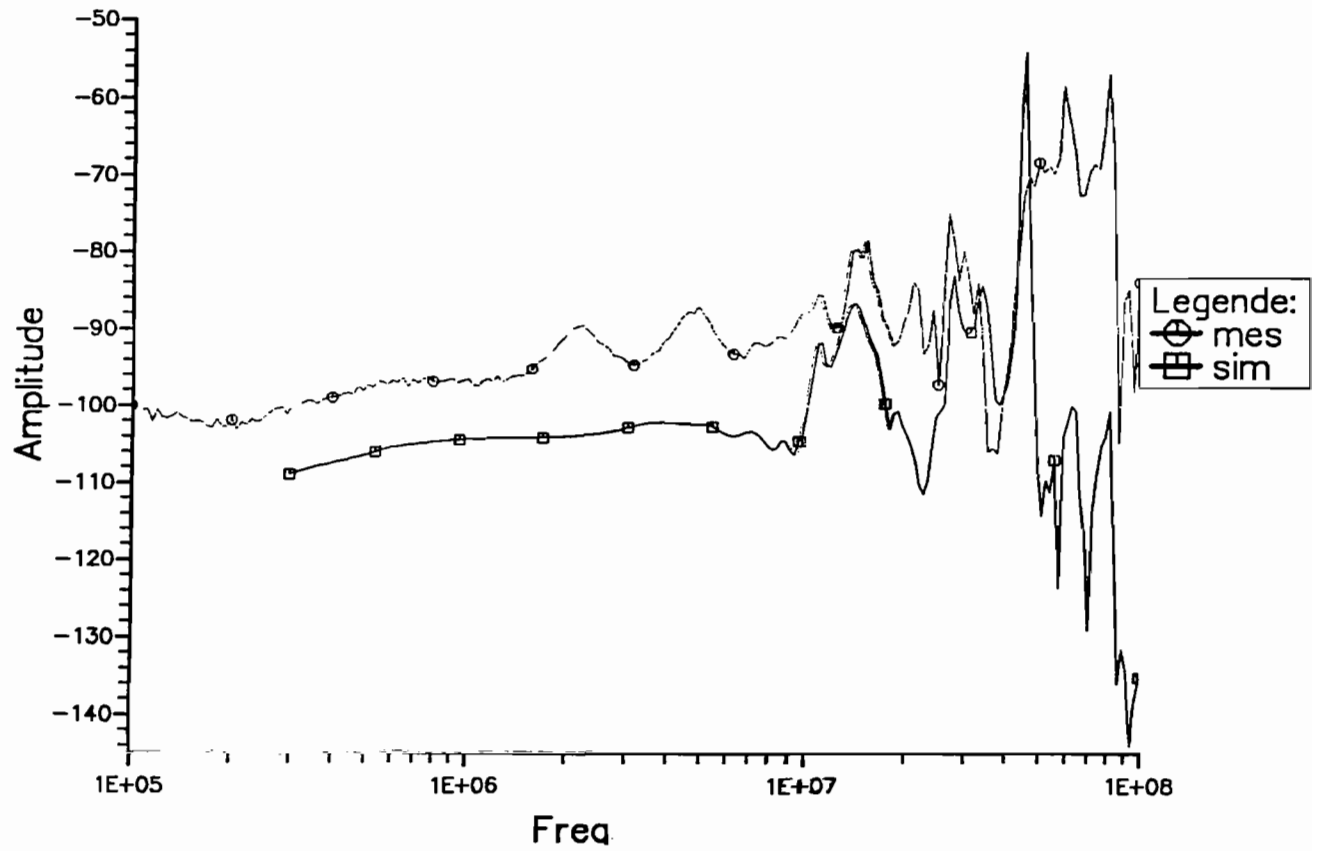
Fig. 4.17: current on wire 9 of LD8 box (Network A)
Amplitude = 20 log (I in Ampere)

5 - CONCLUSION

The experiment carried out in the Phillips Laboratory is a success. Most of the major purposes have been achieved. Among all the lessons brought by this experiment, two major ideas come out and new objectives can be foreseen:

- At first, this experiment enabled one to validate methods applying to the topological approach:

1) Thanks to the important preparation before the finale experiment itself, an a priori knowledge of the topology of the network under study has helped us to organize the research into interesting directions.

Because the characterization of network had been prepared in advance on a flat ground plane, where all the parameters where homogeneous, it has been possible to analyse the variation of the response of the network when installed in the EMPTAC. For a first approximation, the small differences between the two geometric configurations do not lead to large variation of the response of the structure to an illumination (less than a few dB depending on aspect considered, some variations appeared in the amplitude of the resonant frequencies).

To have a qualitative topological analysis that is to say an understanding of the most important path for EM perturbations, this is not really a problem.

If a more precise deterministic evaluation of the various levels is required, we have proved that an optimization of the electrical parameters of the network led to a best fit of the modelling compared to measurement. It is important to notice that to achieve this optimization, only geometrical considerations may be used. As an example, the optimization of the line constituted by the shield and the aircraft itself has been matched by measuring the average distances between the cable and the structure. The cable being divided into 8 tubes characterized by such approximate values, we have used our of cable parameter data base for various distances to a plane to determine the inductance and capacitance to introduce in the model (that is to say that no more calculation to determine tube parameters has been necessary). the quality of the results, in particular the fitting of the first resonant peaks is very encouraging for the future.

2) The interest of having studied two different EM sources is obvious:

With the local injection with a current probe, we perfectly know the propagation path of the energy. The various type of propagation can be analysed (direct transmission, mutual coupling, second order coupling). For the global illumination, the interpretation of the measurements is possible because of our confidence in the previous analysis

3) The modelling of the coupling on the shielded cable was performed in three different ways, introducing more or less complex procedures for this characterization.

The first one is based on an experimental study of the current injection probe and a confrontation with the topological modelling of the coupling. It leads to files containing the equivalent voltage generator to add on any transmission line to model the probe. With this method the coupling is quite independent of the wires under test. But it is necessary to consider the shield itself as a N+1 conductor. The problem which still remains, is that we must have a correct knowledge on the position of the shield near the return path.

With the transfer impedance concept, we just require the properties of the internal wires versus the shield. Because these parameters are independent of the position of the cable in the aircraft, this step has to be done once. The further information we need is the current distribution on the shield itself. We could get it by theoretical modelling (numerical code) or by direct measurement (as done in this campaign).

The third method is probably the most promising one. First, we calculate the current response on the shield for a unit generator disposed on each wire of the bundle. We normalise this transfer function with the actual current measured under the illumination simulator. We now have the generator that contains the information on the E and H field in the cockpit. Doing that we have used the shield as a sensor which response is analyzed by the topological tool.

For the three representations of the equivalent source applied on the wires, the most important point is that a single measurement or an only numerical calculation doesn't success. **The process is optimized because both measurement and modelling have been used together.**

- secondly, electromagnetic topology had been used to analyze quantitatively coupling phenomenon in the aircraft :

1) The interest of network B is that it enables us to simulate the coupling process with computation time generally less than 30 minutes. This a condition for a real time analysis. Moreover the interpretation of results being done so rapidly, it helped to lead the experimentation and to choose the required measurements.

Thus complementary of measurements and numerical simulations appeared during the whole experiment and contributed to its success.

2) During the campaign, the topological concept was present in each phase of the work. The break down of the aircraft into adjacent volumes (cockpit, lower shielded volume) was assimilated both for the experimental acquisition and the simulation. The proper use of Thevenin generator summarises the coupling between zones.

3) Thanks to possibilities of the topological code CRIPTE, the prediction and the interpretation of the observation is possible.

Among the results, we can extract an interesting conclusion. When the shield in the cockpit is short-circuited, the coupling on the terminal loads may come from the shielded cable or from fields inducing voltages directly on the wires of the lower shielded volume. If we try to analyze the shielding level between the Ellipticus antenna and these internal wires we find two ways. The perturbation may enter the cockpit by the window and arrive on the wire through the shield (level one).On the other hand, it can enter the lower shielded volume by some defects of the structure and directly couple on the wire that are not protected (level one again). This means that the topological shielding level is homogeneous along the wire. It is the reason why the order of magnitude of the voltage on the loads, on the whole network, changes significantly when the shielded cable is disconnected.

The topological CRIPTE code is now able to predict what happens when we change the level of protection (we have voluntary disconnected the shield at one of its end). Thus the voltage has increased (more than 40 dB at one frequency and the measurement confirm quantitatively and qualitatively the prediction).

4) Although Network B was simpler than actual Network A, it must be noticed that their topologies are quite similar: same length, same type of interaction, same proportion of crossing cable...

This means that the general conclusions obtained with the simpler network are not in contradiction with those related to network A ,even if some quantitative results are varying.

A fist qualitative analysis can be deduced. Indeed, when the shielded cable of network A, being of better quality than network B shielded cable, is not connected at one end, the interference coupling on the wires located in the lower volume is not induced by the shielded cable. In that case, the shielded cable and the lower volume don't have the same level of hardness.

- Perspectives:

1)The computing facilities available during this experiment limiting the numerical simulations, and a lack of time, did not enable us to achieve a complete quantitative analysis of network A "in situ".

Therefore in a short term, more numerical work must be done on network A to confirm the qualitative analyze developed during this experiment.

2)This experiment being limited to two volumes of the aircraft (cockpit and lower volume), and this first validation of the method on a piece of an aircraft being successful, this let us think that the topological approach can be applied to analyze the coupling on the global network running inside the whole EMPTAC.

3)Nevertheless, the problems of measurement met during the phase of illumination under Ellipticus antenna must be solved for future experiments. This requires one to develop and adapt the instrumentation in order to measure correctly low-level signals.

ANNEX A: NETWORK CHARACTERIZATION

A-1) Introduction

As previously described, cables of a network are characterized by parameters such as inductance matrices , capacitance matrices and resistive matrices. These parameters can be obtained from numerical simulations (if the network geometry is well known) or from measurements by means of an bridge impedance measurement apparatus (allowing only a low frequency approach) or by means of a network analyser.

This section describes how a network analyser can be used to measure the inductance and capacitance matrices, varying or not varying with frequency.

A-2) Determination of the inductance matrix

For a bundle having N elementary conductors of length l, the inductance matrix per unit length, based on a low-frequency model is defined as follows:

$$
\begin{bmatrix} V_1 \\ \vdots \\ V_N \end{bmatrix} = j\omega l \begin{bmatrix} L_{11} & \cdots & L_{1N} \\ \vdots & \ddots & \vdots \\ L_{N1} & \cdots & L_{NN} \end{bmatrix} \begin{bmatrix} I_1 \\ \vdots \\ I_N \end{bmatrix}
$$

where Vi and Ii are the ith conductor longitudinal voltage and current per unit length.

From this definition, the inductance, L_{ii}, can be derived: $L_{ii} = V_i / j\omega l I_i$, with Vk=0 for k different from j.

Applying this formula, the following principal scheme enables the determination of L_{ii} below the resonance domain:
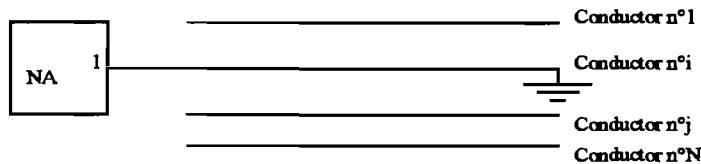
Fig. A1: direct measurement of $Z = 2\pi j f l L_{ii}$

From this definition the mutual inductance, L_{ij}, can be also derived: $L_{ij} = V_i / j\omega l I_j$ with Ik=0 for k different from j.

Applying this formula, the following principal scheme enables the determination of L_{ij} below the resonance domain:
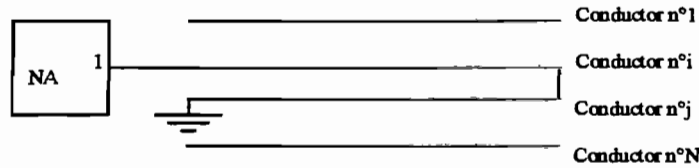
Fig. A2: direct measurement of $Z = 2\pi j f l\left(L_{ii} + L_{jj} - 2L_{ij}\right)$

L_{ij} can be derived from Z if all L_{ii} have previously been measured

A-3) Determination of the capacitance matrix

For a bundle having N elementary conductors of length l, the capacitance matrix per unit length, using a low-frequency model is defined as follow:

$$\begin{bmatrix} I_1 \\ \vdots \\ I_N \end{bmatrix} = j\omega l \begin{bmatrix} C_{11} & \cdots & -C_{1N} \\ \vdots & \ddots & \vdots \\ -C_{N1} & \cdots & C_{NN} \end{bmatrix} \begin{bmatrix} V_1 \\ \vdots \\ V_N \end{bmatrix}$$

where Vi and Ii are the ith conductor voltage and current .

From this definition the coupling capacitance, C_{ij}, can be derived : $C_{ij} = I_i / j\omega l V_j$ with Vk=0 for k different from j.

Applying this formula, the experimental scheme is:
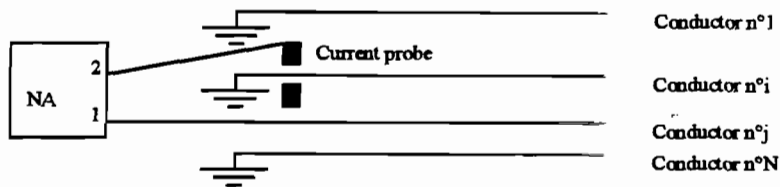
Fig. A3: measurement of $S_{21} = (V_{probe} - 50.I_{probe}) / (V_j + 50.I_j)$ with $V_{probe} = R.I_i$ and
$V_{probe} = -50.I_{probe}$ and $I_j = 0$ $S_{21} = 2RI_i / V_j$ thus $S_{21} = 2R 2\pi j f l C_{ij}$

84

Diagonal terms of the capacitance matrix can be derived from the following expression:

$$C_{ii} = C_{ie} + \sum_j C_{ij} \quad \text{where} \quad C_{ie} = C_{tot} / N$$

The following set-up enables us to measure C_{tot} :
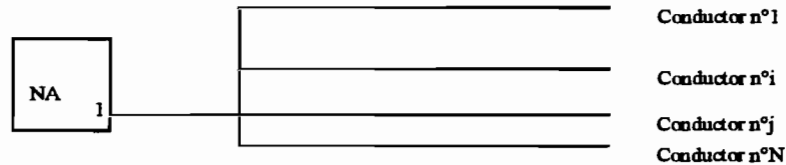
Fig. A4: direct measurement of $Y = j.2.\pi.f.l.C_{tot}$

A-4) Determination of frequency dependent parameters

A method to describe inductance, capacitance and resistive frequency-dependent matrices can be used. This approach is based on the measurements of S-parameters, seen at one end of the bundle, the other one being short-circuited or open-circuited. The matrixes are then derived from the theoretical expressions of these S-parameters assuming that the bundle does not have any discontinuity.

This method has successfully been applied to characterize network B during the pre-experiment held in France.

ANNEX B: SOURCE CHARACTERIZATION METHODS

This annex describes the various ways to characterize the different sources coupling on both network A and network B. The main penetration path to consider in the problem is the coupling on the shielded cable inside the cockpit volume. But other penetrations paths may also be considered:

- the coupling through the door of the lower shielded volume

- the coupling on the small fuselage shielded cable in the fuselage

The different models considered in our calculations are:

- the calculation of **Thevenin equivalent generators** deduced from measurements

- the calculation of internal sources inside the shielding cables thanks to the **Transfer impedance** concept.

- the precise modelling of the coupling of source terms on the shield and on wires in the case of the injection with current probes.

The two first methods can always be applied, whatever the geometry of the excited volume is. Nevertheless, the third one requires a very precise knowledge of the excited cable.

B-1) Calculation of the Thevenin equivalent generators deduced from measurements

The theory of Thevenin equivalent generator deals with the determination of the imput impedance of the excited volume and the measurement of a voltage vector at the output ports of this volume. With this approach, a volume can be reduced to the following model (Fig. 1):

- an input impedance containing all the topological information of the volume

- an equivalent generator characterizing the coupling of a given source in this volume
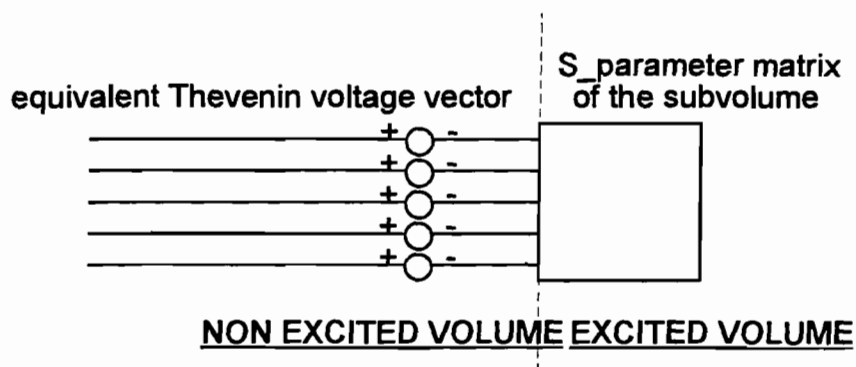
Fig. B1: equivalent Thevenin model of an excited volume

B-1-1) Application to the shielded cable of the cockpit (Network A and B)

The cockpit volume, because of the canopy wide aperture, is considered as an open volume. So the **first shielding level** (in the topological sense) cannot be made of the external

surface of this volume. The actual first shielding level in this problem is made of the shield of the cable. So this volume has 3 **output ports** for network B and 21 output ports for network A, dealing with the extremity of the inner wires of the shielding cable.

The geometry of this cable is very complex (fig 2) and it is not possible to consider it as an ideal transmission line over a ground plane. The equivalent voltage generator takes into account both:

- **the imperfections of the geometry** of the system thanks to the input **S-parameter matrix** of the volume. Its important to precise that this matrix doesn't depend on the source. That is to say it will be the same for all kinds of excitations (with a current probe or a global illumination)

- **the coupling of the sources on the network** thanks to the measurement of the vector composed of a resultant signal on each output port of the volume. This resultant signal may be a current (generally a short circuit current), or a voltage on given loads.

In the case of network B, voltages on 50 Ω loads are considered because they can be measured easily with a network analyser or with optical fibber links. Nevertheless, one must realize that the more convenient measurement is the open circuit voltage vector because it is directly equal to the Thevenin Equivalent Generator.

In the case of Network A, 21 output ports have to be considered. Its not possible to measure all the components of the 21x21 S-parameter matrix. But considering the wiring symmetry in the cable, only two measurements are necessary:

- a s_{11} measurement characterizing the reflection on 1 wire

- a s_{12} measurement characterizing the mutual coupling between two wires.

Afterwards, we suppose that all the S_{ii} and S_{ij} terms are identical in the matrix.

The measurement of all the voltages on 50 Ω may itself appear too much fastidious. Its the reason why only a bulk current measurement on a short-circuit is made. In low frequency, all the 21 equivalent voltage generators of our problem are equal on the inner wires of the shielded cable because this voltage is equal to Zt*Isc (Zt is the transfer impedance of the shield, Isc is the current on the shield). These generators may be deduced by:

Ethi = (Isc/n)/Ri

with   Ethi, equivalent voltage generator for wire i

        n, number of inner wires

        Ri, resistance load of the wire i

For higher frequencies, such an approximation is not still available, but a more accurate characterisation of the equivalent generators on network B cannot be undertaken in this experiment for lack of time.
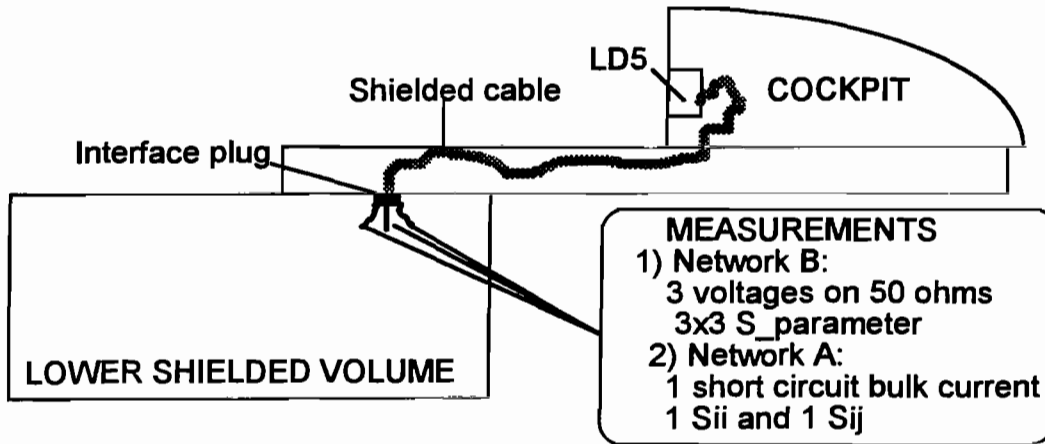
Fig. B2: determination of Thevenin equivalent model of the cockpit volume

B-1-2) Application to the fuselage shielded cable (network A)

These measurements are limited to Network A. 3 output ports are to be considered dealing with the extremities of the interface 3 wire shielded cables. Practically, the coupling on this cable may be neglected because this cable is less long (30 cm) than the cockpit one (6.1 m). The measurements are similar the cockpit previous ones (fig 3).
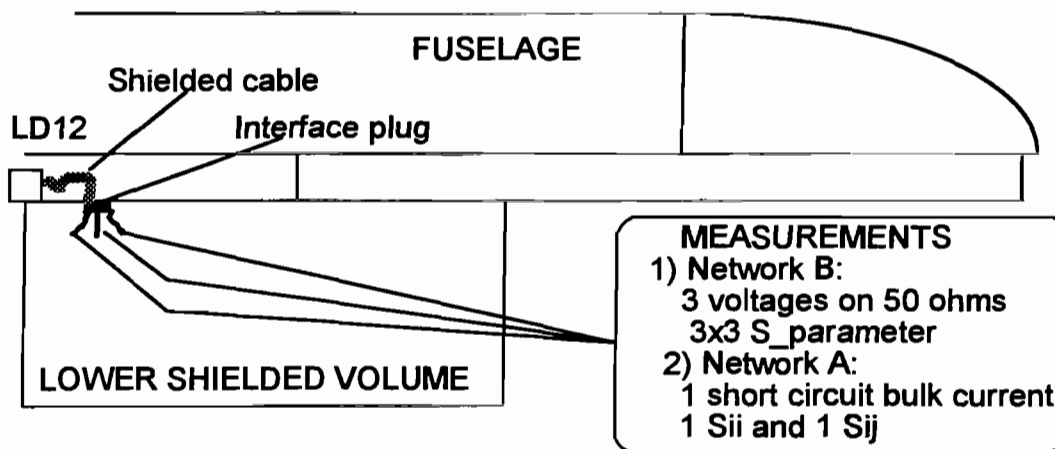
Fig. B3: determination of Thevenin equivalent model of the cockpit volume

B-1-3) Application to the lower shielded volume wiring (Network B)

The determination of the equivalent Thevenin model may be very useful for the lower shielded volume because they characterize the coupling due to the links through the door. In this problem, 9 output ports have to be considered (3 for each termination box). So a 9X9 S-parameter matrix an 9 voltages on 50 Ω have to be measured on network B (fig 4). In fact all the measurements will not be necessary. We must consider the fact that:

- wires connecting L55 and L75 on one side, L56 and L76 from the other side,

- wires connecting P65 and L85 from one side, P66 and L86 from the other side,

So, only 8 voltage measurements on 50 Ω loads and the measurement of a 8x8 S-parameter matrix can be considered on ports L59, L55, L79, L76, P65, P69, P85, P89.
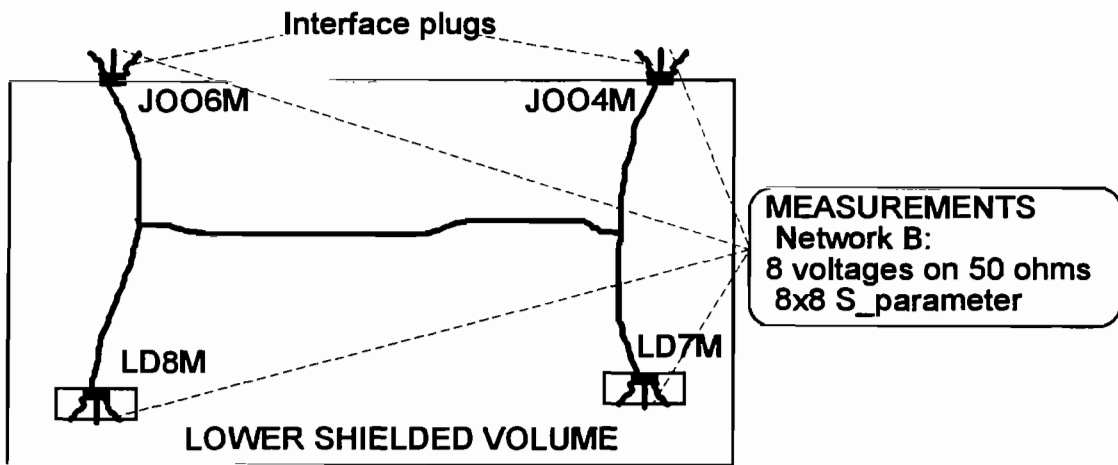
Fig. B4: determination of the Thevenin equivalent model for the lower volume

Due to a lack of time, this determination will not be undertaken on network A during this experiment.

B-2) Application of the transfer impedance concept on shielding cables

In theory, the method to determine Thevenin Equivalent model is totally exact. Nevertheless, these generators are sometimes technically difficult to obtain (theoretically n voltage measurements and $n.(n+1)/2$ measurements of S-parameters). This method supposes to be able to disconnect the network at the point where one wants to determine the generators. Moreover, problems of measurements may occur when the generators are measured with a network analyser. The problem happens when an interface plug is used: in this case the ground reference of the equipment (generally the network analyser) is not the same as the ground of the structure.

Applying the concept of transfer impedance would appear more convenient because it is based on the measurements of currents on shielded cables.

Two methods can be proposed for the concept of transfer impedance. The first one consists in introducing as sources terms different measurements of bulk currents on shielded cables, the other one is based on the knowledge of only one bulk current and on the application of transfer functions.

B-2-1) Direct introduction of several measurements of current on the shielded cable:

The principle is the following (fig 5):

It supposes that the shield of the cable is well connected to the ground of the boxes, itself connected to the structure. In this case the cable is decomposed in several sections on which the current due to an electromagnetic source is applied (a local injection with a current probe or a global excitation under simulator, in this experiment).

The distributed equivalent voltage generators induced in each section of the cable on the inner wires are calculated thanks to the transfer impedance per unit length, Zt.
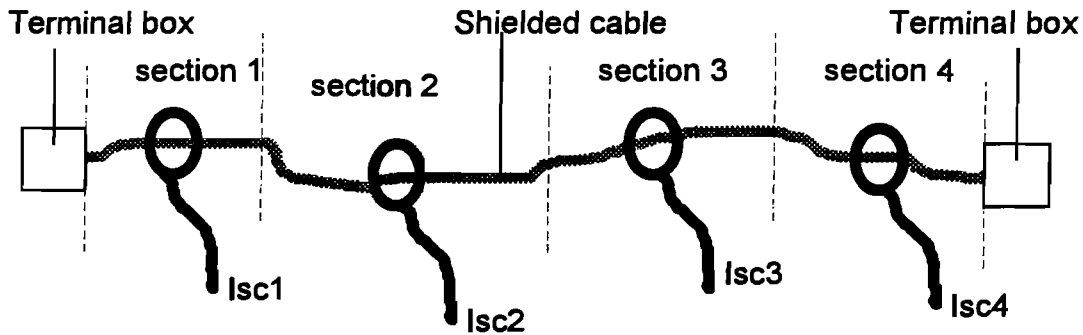
Fig. B5: measurement of currents on different sections of the shielded cable

The electrical model is presented on the Fig. 6. If in a section i, located between L_{i+1} and L_i, a shield current Isc_i has been measured, the total equivalent generator Vs_i induced on the inner wires is:

$$Vs_i = Zt.Isc_i.(L_{i+1}-L_i)$$

Of course because of the twisting of the inner wires, the transfer impedance is assumed equal for all the wires. It is supposed that Zt is the same all along the cable. Zt is in fact an average value of the Zt all along the cable.

As for the Thevenin model, an advantage of this method is that it doesn't depend on the running of the cable. Nevertheless, the accuracy of the calculation depends on the number of current measurements which have been measured and introduced in the model. In the experiment, it has been shown that 3 measurements of Isc could give a good numerical simulation including the two first resonance peaks.

Terminal box   Shield of the cable   Terminal box

| section 1 | section 2 | section 3 | section 4 |
| Isc1 | Isc2 | Isc3 | Isc4 |

-○+   -○+   -○+   -○+

Zt.Isc1(L1) Zt.Isc2(L2-L1) Zt.Isc3(L3-L2) Zt.Isc4(L4-L3)

0   L1   L2   L3   L4
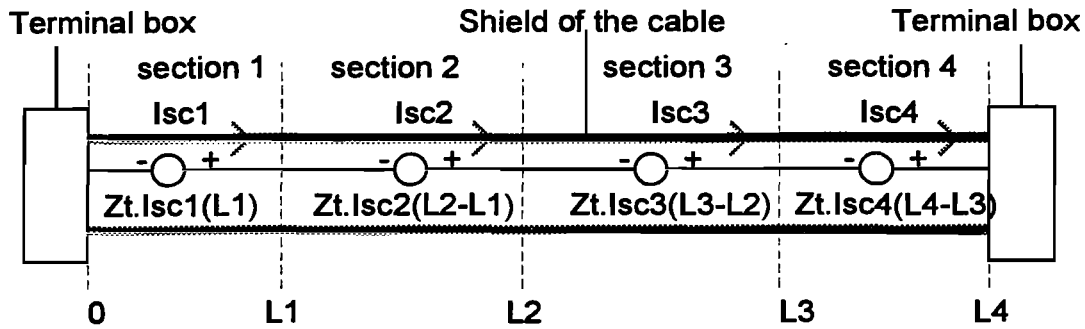
Fig. B6: electrical modelling of the coupling on shielded cable with the Zt concept

B-2-2) Indirect method of sources terms characterization using transfer impedance concept

In some cases, the measurements of the currents distribution along the shielded cable is quite impossible due to its running inside the aircraft. Thus the problem, now, is to characterize correctly the excitation and its propagation on the shield assuming that the current on the shielded cable can be measured at only one location and that the coupling on the internal wires is correctly characterized by the transfer impedance concept described in the previous section.

It is obvious that the aggression and its propagation along the shielded cable depends on the running of this cable inside the structure. Thus the cable shielding is split up in different tubes derived from an analysis based on reflectometry, representative of its running. To determine the sources that have to be introduced on the wires of the network, we have to think of a direct derivation of the general antenna theory. More precisely, the **induction theorem** proves that the current induced on a structure can be determined knowing the incident field (defined as the field when the structure is removed). In our case, the incident field is the field in the EMPTAC without the shielded cable. Note that the consequence of this discussion is that this incident field is independent of the properties of the studied cable. To apply correctly the induction theorem, we are supposed to introduce a distributed voltage generator all along the cable. For practical reasons, we decided to introduce an only generator distributed on the section of the shielded cable that is directly illumined that will represent the total contribution of the incident field. Doing this, it can be shown that the integration process removes a part of the contribution of the charges. This is not too important for a shielded cable because we have supposed that the transfer admittance is negligible. Thus the problem is now to determine the equivalent generator to be put on each wire of the bundle.

We now apply in the numerical model of the cable (topological network) a Voltage generator equal to 1V distributed on the portions of the cable directly illuminated (portions located in the cockpit). This generator has to be applied on all the parallel wires including the shield itself.

This voltage generator equal to 1V induces a current distribution along the shield. Thus we can now compare the current measured at one location and the one induced by a 1V

91

generator at the same point. Assuming linearity, the Voltage generator to be applied in order to describe correctly the current distribution on the shield is:

$$V_{eq} = I_{measured} \ / \ I_{induced \ by \ a \ 1V \ generator}$$

We can now apply this equivalent Voltage generator on the shielded cable and the coupling on the internal wires will be correctly described thanks to the transfer impedance model.

Of course, this method could be extended to several points where the current had been measured. In that case the principle of superposition of voltage generator can be applied and different transfer functions between measured currents and simulated currents induced by a 1V voltage generator will be introduced as equivalent voltage generators. The more we measure some currents on the shielding, the more accurate the simulation is in higher frequency. In our case, the equivalent voltage had been determined using only one measured current on the shielding.

In theory, the equivalent generator evaluated as previously is independent of the cable. A determination with the network B (which is easier to perform) can be used for network A ,if the position of both network is the same.

B-3) Modelling of the injection with the current probe

In some canonical geometrical excitations the source can be modelled very precisely. As an example, it is the case of localized injections on lines. The following injections may be considered as localized injections:

- current or voltage generator injections at the extremity of wires

- coupling through small apertures

- injection with current probes

In this experiment we'll consider local injections with current probes. This way is a very convenient way for testing a network because the insertion of the probe doesn't require to disconnect the cables such as in the voltage or current injection on wires.

The characterization of the current probe is made by measuring the coupling S-parameters S_{12} and S_{13} on a small test wire (fig B7). It can be shown that the coupling on the wire can described as a serial voltage generator Vs given by:

$$Vs = (S_{12} - S_{13}) \ / \ 2$$

The scattering parameters may include the amplifier gain necessary to obtain enough level on the lines. The calibration of the device is made in the reference plane of the two input and output ports.
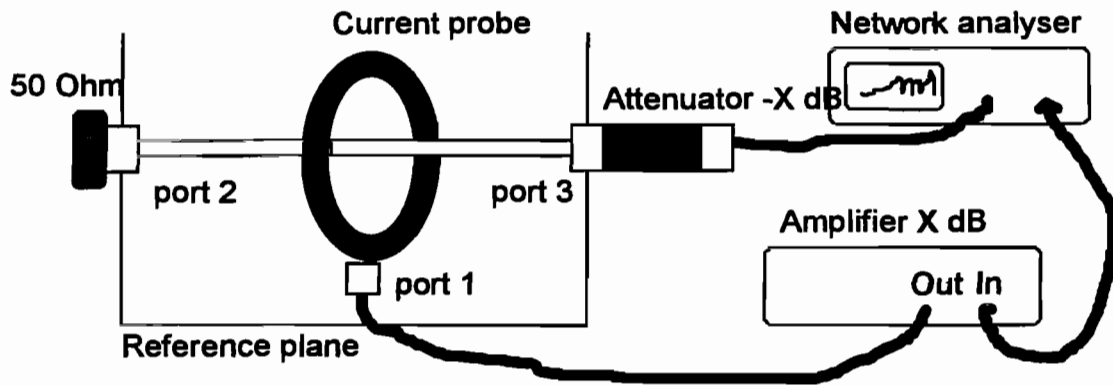
Fig. B7: example of the measurement of S31 on the probe taking into account an the gain of an amplifier

The modelling of the coupling on a cable deals to introduce a serial voltage Vs on all the wires at the location of the current probe. In the case where the cable is shielded, this voltage has also to be applied on the wire made by the shield (figure B8).

This method lends itself perfectly for shields parallel to the ground plane and which can be also treated as transmission lines. In this case, an advantage of this method is that it predicts the behaviour of the current all along the shield. It has been successfully applied in the pre-experiment held in France on a metallic ground plane.
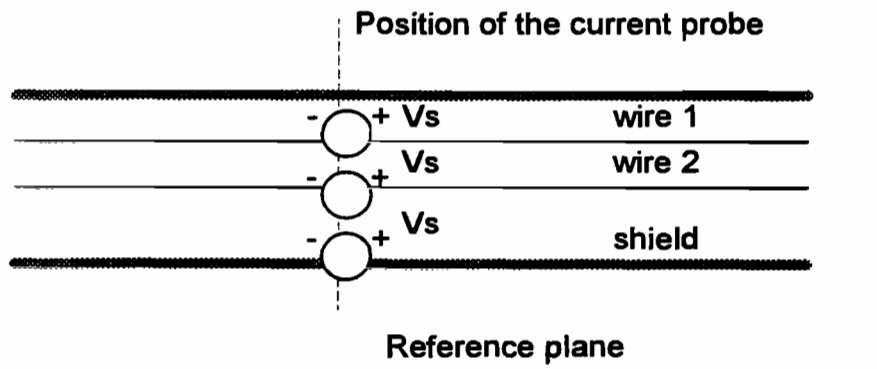
Fig. B8: modelling of the coupling with a current probe on a shielded transmission line

93

ANNEX C: RECENT DEVELOPMENTS IN E.M TOPOLOGY

Jean Philippe Parmantier

Office National d'Etudes et de Recherches Aérospatiales
29, avenue de la division Leclerc
BP n° 72, 92320 Chatillon Cedex, FRANCE
tel: (1) 46-23-50-64
FAX: (1) 46-23-50-61

Abstract

This paper presents the recent developments in Electromagnetic Topology since the main principles had been presented at the last ESA workshop held in ESTEC (1989). The objective is to show that topological concepts begin to be successfully applied on complex EM problems. After a brief recall on the qualitative EM topology theory and its adaptation to real problems, the use of Multiconductor Line Network formalism as a EM quantitative Topology method is then discussed. Particularly some applications of CRIPTE computer code derived from this formalism and developed at ONERA are presented. It is shown how data for tubes and junctions are nowadays determined numerically and experimentally to characterise the elements of networks. The input of sources is illustrated thanks to the description of an experiment carried out by ONERA and Centre d'Etudes de Gramat on a test-bed modular caisson. Different techniques for localised and large penetration paths are illustrated with experiments performed in time and frequency domain. Other more ambitious works undertaken since 1993 are presented to prove the powerfulness of the method: an experiment on a Mirage III wing, an experiment on the EMPTAC aircraft, the numerical simulation for a subway train. As a conclusion, it is mentioned that future developments would lead to statistical studies.

1 Introduction

Electromagnetic Topology (EMT) is a Method developed through the seventies in the USA by C.E Baum and al [1]. Unlike studying coupling on structures in a numerical way (by solving Maxwell's equations on an entire meshing of the structure), or in an experimental way (by setting a realistic scale model of the structure under an antenna), this method proposes a modular approach. It will be shown that EMT proposes a complementary approach of expemental and numerical methods. The aim of EMT is to break down the structure in elementary volumes. The coupling in each volume is then characterised by applying in them arbitrary sources. Finally, the art of EMT is to build the solution of the whole problem by linking the individual E.M characterisations in each volume.

2 Recalls on qualitative EMT

The first step in the topological approach of a problem is always to perform what is called "Qualitative EM Topology". This phase of the study deals in fact with an analysis of the geometry of the problem to help for future quantitative treatments concerning the determination or the reduction of EM interference on the structure. Subvolumes are so defined as respect to the different shields and walls existing in the structure. The "shielding order" of a given subvolume is the minimum number of shields one external wave must cross from the outside to the volume into study. As respect to the "good shielding approximation" principle, equivalent sources induced in one volume are related to the signal in upper volumes (volumes having a lower shielding order) but are independent from the signal in volumes having the same or a higher shielding order [2].

The second step of the EMT qualitative analysis is then to transcript the previous breakdown in a Topological diagram. This diagram may be considered as an abstract representation of the geometry of the problem taking into account EM interactions between each volume. Every volumes are labelled as respect to their shielding level.

The last step of the qualitative analysis is to design a graph derived from the topological diagram and called "topological interaction diagram sequence". In this diagram, each volume is represented as a node and all existing paths between volumes are represented as oriented branches. Several branches may be associated to the same surface, related to the type of coupling path (coupling through apertures, coupling on wires ...). At this time, some studies have been carried out to try to compute an automatic graph for the design of structures at their conception phase [3].

One must notice that the usual graph derived from qualitative analysis on actual structures such as aircraft barely look like the ideal theoritical tree graph, representing the fact that many volumes included one into each others may exist. Generally only two main shields may be distinguished: one made by the skin of the structure and one made by the internal cable

network. Its the reason why coupling on cables has a so great importance in EM problems.

3 Qualitative EM Topology and Multiconductor Transmission Line formalism

The step following the qualitative analysis is the Quantitative EMT analysis in which one tries to predict the value of induced signals at each node. In a general way, this work may be performed by defining sets of observables at each node (EM fields on apertures, currents and voltages on wires ...) and to relate them by transfer functions associated to the branches of the interaction diagram sequence. This can be done easily for tree graphs for which edges are directed from the outside to the inside. But, these transfer functions are much more difficult to derive when both directed edges exists between volumes having the same shielding levels. Nevertheless, in the relevant case of volumes associated with cable networks, this can be done with the Multiconductor Transmission Line (MTL) Network formalism [4].

In this formalism, a topological network is made of tubes linked by junctions (figure 1). Tubes represent homogeneous sections of harness described as MTL. Junctions represent terminal load sets, branching of cables in different directions. On tubes, wave vectors depending on voltages and currents on elementary wires are defined. At each extremity of tubes, waves are related thanks to a propagation matrix $\Gamma_{i,j}$ deduced from the characteristic distributed impedance and admittance parameters of the associated MTL, defining so a propagation equation. A source wave vector term Ws_j may be added to the equation. Ws_j is calculated from the distributed voltage and current equivalent generators describing external coupling on cables in MTL model. For each tube, the propagation equation may be written in the following form:

$$W_i = \Gamma_{i,j} W_j + Ws_j \qquad (1)$$

At each junction a scattering equation can be defined, relating incoming and outgoing waves thanks to a scattering matrix $S_{i,j}$:

$$W_i = S_{i,j} W_j \qquad (2)$$

One may have the idea to combine all the incoming and outgoing waves to define great supervectors for the entire network. The same combination can be done for a Ws supervector. One can then derive a single propagation supermatrix Γ and a single scattering supermatrix S, deduced from (1) and (2).

By eliminating incoming wave supervectors in (1) and (2) one can then write the famous BLT equation:

$$(1 - S \Gamma) W = S \, Ws \qquad (3)$$

"BLT" comes from "Baum, Liu and Tesche" the authors of the equation.

From a topological point of view, tubes and junctions are in fact topological subvolumes having the same shielding level. The Γ and S matrices represent their

both side directed transfer function. The Ws source term on each tube may be calculated thanks to the transfer function from an outer volume.
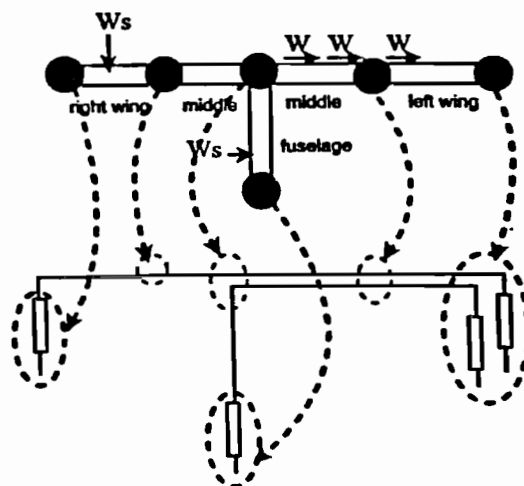
Figure 1: example of a topological network

4 CRIPTE code

4-1 Description of the computer code

A computer code inspired from the MTL network formalism and including topological concepts have been developed at ONERA to help the prediction of EM interference in a frequency range from several kHz to about 500 MHz (range including lightning and EMP phenomena and for which coupling on cables remains still predominant for the internal response of the structure) [5].

As a topological tool dedicated to the prediction and the optimisation of internal interference CRIPTE code may give an helpful answer to some typical questions as:

- What will be the signal at the input port of a given electrical device ?

- Is it possible to make a sensible cable run under one given aperture or even inside a given harness ?

- What is the relative influence of different coupling paths on the global response at the input port of an electrical device ?

Written in FORTRAN language, CRIPTE code is decomposed in several menus describing the previous mentioned qualitative and quantitative phases of the topological study of a problem.

The first menu of the qualitative part deals with the graph definition of the problem in which the operator defines the different tubes and junctions of its cable network. In the future, we hope that this network topology will be extracted from data available in

industrial companies in charge of the wiring of structures.

The second menu of the qualitative part deals with the introduction of the electrical intrinsic parameters for each volume, that is to say distributed impedance and admittance parameters for tubes, scattering parameters for junctions. Data can come even from models, even from measurements.

In the quantitative part, CRIPTE code may provide three types of calculations.

The first calculation deals of course with the computation of the basic BLT equation which may give current and voltage everywhere on the network.

The second calculation deals with Ws vector terms. As described latter, Ws calculation may be very long because it is based on an integration of voltage and current generators all along one given tube. Moreover, these generators may be provided in time domain. This imposes a Fourier Transform for each generator. In some applications, it may be very useful to determine this Ws term once: a typical case is when one wants to optimise the running of a cable bundle and has to make several BLT resolutions by modifying only parameters of tubes and junctions.

The third calculation is totally dedicated to topological considerations. It deals with the determination of equivalent scattering parameter of subnetworks, what allows the operator to concatenate a part of network made of several tubes and junctions as a single junction. If the subnetwork is entirely enclosed into a subvolumes, the equivalent parameters are those of a black box. By this way, one can then reach the general formulation of BLT equation in which the length of tubes is shrunk to zero and for which only junctions of subvolumes have to be considered [6].

4-2 The input data of CRIPTE code

4-2-1 Junctions

Junctions are characterised by their scattering parameters (S-parameters). In the theory of MTL network, S-parameters depend on the characteristic impedance (Zc) matrix of tubes connected to it. But they may be easily related to other circuit type matrices (impedance Z-parameters or admittance Y-parameters). Particularly, they are also related to S-parameters determined on a 50 Ω reference load, called S50-parameters [7]. One advantage of such parameters is that they can be calculated thanks to powerful circuit computer codes (CRIPTE code is coupled with Touchstone code). The other advantage is also that a very convenient way to characterise experimentally a junction is to use a network analyser, equipment dedicated to the measurements of S50-parameters.

Nevertheless, in the case of ideal junctions including open circuits, short-circuits the deduction of topological S-parameters from S50-parameters is not always possible. For this, special treatments have been developed dealing with a direct determination of S-parameters [8].

4-2-2 Tubes

Tubes are one of the specificity of CRIPTE code. Some analytical formula exist to calculate the distributed impedance and admittance of MTL model (in fact, only resistance, inductance and admittance terms are generally significant). Nevertheless these expressions are not still true in the case of harnesses in which wires are very close to each other and close to their reference plane. Particularly, the presence of dielectric is predominant to determine the different propagation modes of the transmission line.

The more precise way to determine R, L, C matrices is to measure them. Direct measurements can be performed with impedance-meters applying specific conditions of loads at the extremity of the MTL (short and open circuits) and give quite accurate results in general cases [9].

For more precise simulations one has to take into account the frequency variation of R, L, C parameters. One of the most well-known is the increasing variation of the resistance due to the skin effect phenomenon. These results can be nowadays obtained by making S50-parameter measurements at one extremity of the MTL, the other being loaded with short and open circuits [10]. One interest of this method is that the treatment of S50-parameters gives at the same time these following matrix terms with their frequency variation: propagation, characteristic impedance, resistance, inductance, capacitance, propagation speed. This method, well suited to an automatic acquisition of parameters, could be applied advantageously in the future to characterise shielded liaisons with specified immunity. Moreover, the frequency variation of line parameters is nowadays introduced in CRIPTE code.

But a disadvantage of experimental methods is due to the fact that it is necessary to be able to disconnect or to reproduce in laboratory the geometry of the tube. It may be more useful to be able to predict the value of the parameters. This nowadays can be done with a computer code based on method of moments calculating capacitance and inductance matrices by meshing different sections of MTL (figure 2) [11].

Practically, for big harnesses post-treatments of the results obtained are necessary. In experimental methods, only a set of limited coefficients between characteristic wires is measured and the global matrix is then generated with respect to symmetry considerations. In the numerical method, an average of the coefficients is calculated to take into account the fact that several groups of wires are twisted. In parallel to these treatments, a statistical approach is developed, based on the data bank made of experimental and numerical results. Particularly; until now the

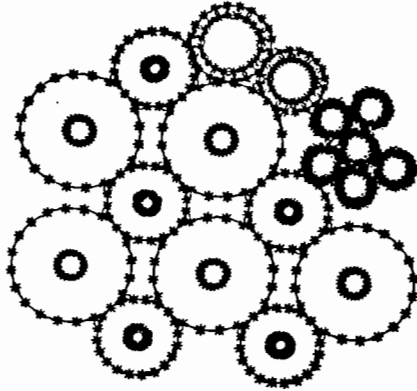prediction of the value of the parameters as respect to the height of the cable have been investigated [12].

Figure 2: typical meshing of the section of a MTL for the calculation of capacitance and inductance matrices

4-2-3 Sources

The way to introduce sources in CRIPTE code depends on the type of penetration paths in the structure.

Both localised and large penetration paths have to be distinguished. Localised penetrations represent small apertures, joints or direct excitations at one extremity of a cable. Large penetrations deals essentially with large apertures. Different models to introduce source terms have been investigated in an experiment carried out in time and frequency domain as a collaboration between ONERA and Centre d'Etudes de Gramat (CEG) [13].

Description of the test-bed caisson:

The object under study was a caisson having the shape of a cross with an average dimension of 4 meters per 4 meters (figure 3). This caisson was conceived in a modular way. It was composed of 5 volumes: a "source" volume, a "terminal" volume, a "middle" volume, a "left wing" and a "right wing" volumes. Small apertures could be opened in it, but also large apertures by removing panels on the different volumes. One of the main specificity of this caisson dealt with its internal topology. It was made of a complex cable network for which we tried to take into account different topological aspects. For example, in the right wing, a trifilar was laying on a metallic plate, then separated in a monofilar connecting one side edge of the volume and a bifillar. In the left wing, a metallic tube, not directly connected to the electrical network, could be excited under a small aperture; then itself could excite the trifilar running along its opposite side and connected to one side edge of the volume. A last example deals with the middle volume in which a shielding level equal to 2 had been respected to define

a clean zone. This was achieved with coaxial cables connecting the other four volumes to a black box containing an arbitrary circuit made of lumped elements.
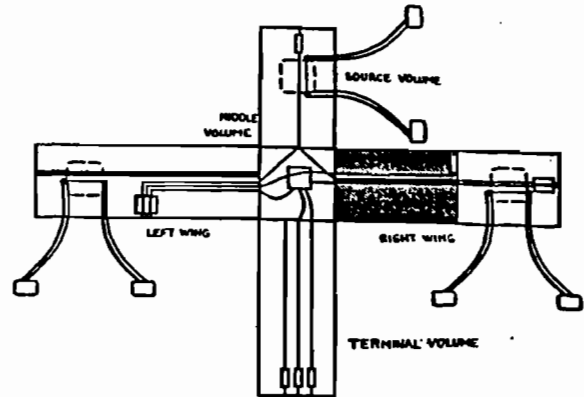

Figure 3: electrical scheme of the test-bed caisson

Modelling localised penetrations:

Localised penetrations coupling on lines may be modelled with single current or voltage generators. This is the typical case of coupling through small apertures. It is well known now that this coupling deals with applying on the line one current and one voltage generators, Vs and Is, depending on the short circuit electromagnetic fields on the aperture, Esc and Hsc:

$$Vs = \alpha \, Hsc \qquad\qquad (4)$$
$$Is = \beta \, Esc \qquad\qquad (5)$$

The main problem is to determine α and β coefficients. For this one can perform a simple experiment by exciting the small aperture with a plane wave provided by a strip line located on the aperture and respecting a 50 Ω characteristic impedance. The open circuit voltage and short circuit current can be measured and related to the input voltage on the strip line. Simple considerations on the plane wave allow to relate this voltage on short-circuited EM fields on the aperture. An equivalent way is also to calculate α and β by making the S50-parameter measurement of the 4 port system constituted by the strip-line and the internal line[14].

Figure 4 presents a comparison of two simulations performed with CRIPTE code (the caisson was located under an EMP simulator) on a voltage in the right wing volume; in the first one, short-circuited fields have been measured, in the second, they have been computed with a 3D computer code based on a finite difference method considering all the apertures were closed. This results show in fact that source terms can efficiently be predicted thanks to other codes. In this problem, an external and internal problems could have successively been treated because of the small size of apertures.

97
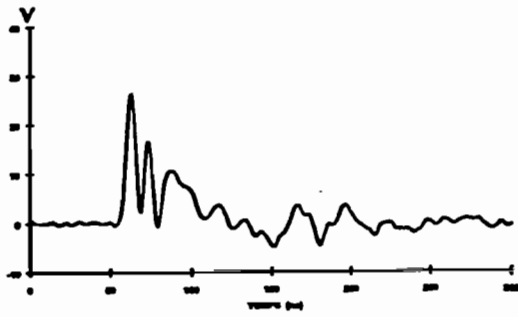
b - CRIPTE simulation with measured Esc and Hsc
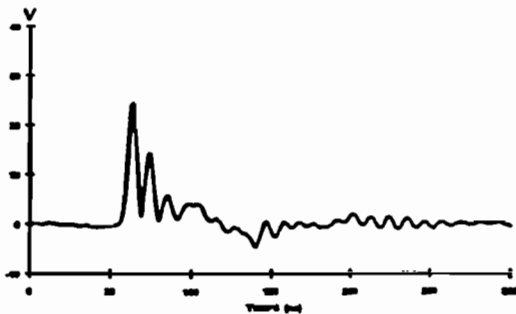
a - CRIPTE simulation with computed Esc and Hsc

Figure 4: two comparisons of a voltage on a monofilar in the source volume

Modelling large penetration paths with Thevenin model:

In the case of large apertures, the problem cannot be decomposed as previously in an external problem and an internal problem. Or the volume containing the large penetration path must be considered as belonging to the external problem. A typical example of large penetration paths is provided by large apertures. In the general case, without any knowledge on their size, all types of apertures can be considered as large apertures. In this case, the coupling is modelled with current and source voltages distributed all along the internal wires of the excited volume. The determination of all these parameters may be considered too much time consuming. Its the reason why one could prefer to model the coupling as a set of a Thevenin equivalent voltage vector, Vth, and a Thevenin input impedance matrix, Zth, located at each output port of the volume. Figure 5 gives an equivalent model in the case of the coupling through a large aperture in the source volume.
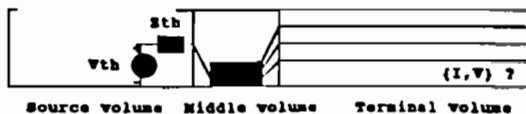

Figure 5: equivalent model of the coupling through large apertures

Zth is calculated by determining the S50 input parameter at each output port of the volume. This can be done easily with a measurement with a network analyser, or with the calculation of the equivalent S-parameters of the subnetwork (if the topology of the internal wiring is known).

Vth is calculated by determining the voltage at the output ports loaded with the same impedance. 50 Ω is a good value because it is well suited to measurements and CRIPTE simulations (indeed, this voltage can also be calculated with a BLT resolution).

Figure 5 illustrates a comparison of measured and simulated voltages obtained at one port of the caisson excited with a log-periodic antenna working in time domain. An interesting aspect of this result is that the agreement between both curves remains still very good up to 500 Hz. This promising result could make one think that CRIPTE code could be used in the future for much higher frequencies, despite the fact the MTL model cannot rigorously be applied.
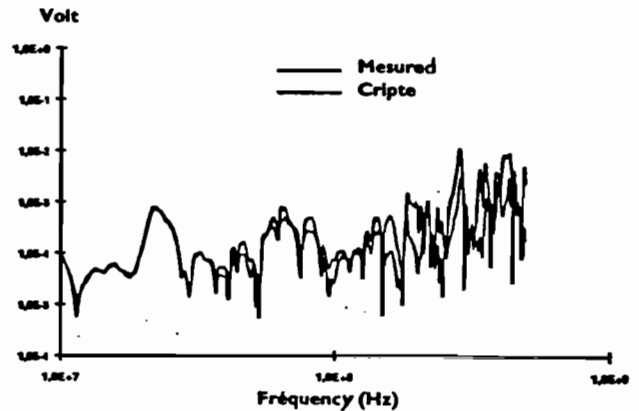

Figure 6: induced voltage on the monofilar of the right wing when a large aperture is opened in the source volume

Modelling large penetration paths in the general case:
One of the main drawback of the previous equivalent model approach is that one loses all the information concerning induced signal inside the excited volumes (only signals at output ports are available). The only way to accede this information is to calculate the distributed equivalent generators thanks to 3D computer codes. This calculation must be performed on a meshing of the structure which doesn't include wires. The calculation of fields at the virtual running way of wires allows to calculate the generators. Depending of the 3D code, 3 types of models can be introduced. The normal electric and the transverse magnetic fields give voltage and current generators of the general MTL model. The tangential electric field can also be determined providing voltage distributed generators (the complete model must then include voltages at each extremity of the tube, due to the

98

height of wires) [15]. This work has begun to be developed at ONERA on canonical geometric configurations (wires in a parallelepiped shape volume, wires on metallic planes [16]), but remains to be applied to more complex geometrical configurations such as aircraft. Nevertheless, this approach presents two advantages in comparison with the direct calculation of currents on wires in 3D codes. First, MTL can be taken into account whereas only single wires can be taken into account in 3D codes. Secondly, with interpolations of EM fields, lines can be located very near from their reference plane, whereas in 3D codes this location is limited to the size of the elementary mesh. Yet, 3D codes remain essential for determining the distributed generators on wires.

5 Application of EM Topology to industrial type problems

All the work we performed in laboratory and on the caisson test-best was useful to validate CRIPTE code and to define methods to characterise a network in a topological sense. But these studies were always made the same reproach: global problems treated until now were to far from complex industrial problems. It is the reason why, the treatment of more ambitious problems have been investigated since this year.

5-1 Experiment on a Mirage III aircraft

As a carrying out of the collaboration between ONERA and CEG, it has been decided to undertake a topological study on an entire scale 1 Mirage III aircraft. The project would last for several years. For the present year, the work has begun with the characterisation of the left wing, as the first topological subvolume.

A self made harness has been constituted and tested on a metallic plane and inside the wing. It is made of aeronautical cables providing real functions. The cable bundle is made of:
- 1 coaxial cable providing an antenna function
- 6 monofilars for 2 lights and 1 dc supply functions
- 1 shielded bifilar for a weapon system function
- 5 pairs of trifilars and bifilars for flight control wiring functions

All wires run from the socket of the wing and separate from the harness to connect black boxes representing equipments (figure 7). These boxes are made of realistic loads such as differential loads for flight control systems.
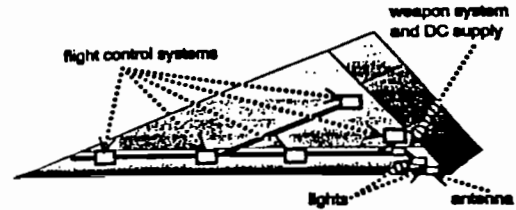

Figure 7: running of the harness in the Mirage III wing

Wires providing the same electrical function have been gathered, making themselves sub-harnesses. In one sense, the total harness is made of 13 sub-harnesses, weakly twisted as it is commonly the case in aeronautics.

The noticeable point in the electrical characterisation of the harness is that only a set of representative R, L, C measurements have been made on the big socket tube. The other terms of matrices have been extrapolated on this big tube, but also on all other thinner tubes thanks to this reduced set of parameters. These representative measurements are mainly made of the coupling between cables of two different sub-harnesses and the coupling between two wires inside a sub-harness. Figure 8 shows that such a very simple approach may give good results.
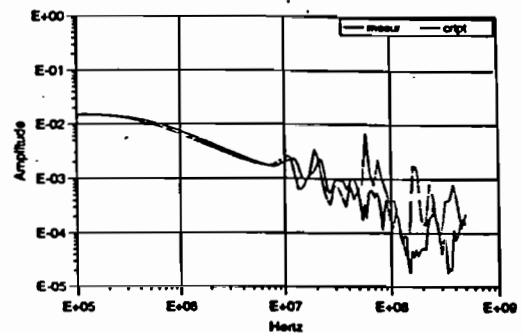
Figure 8: global current at the socket tube, for a global current excitation between two flight control systems.

The experimental program on the wing will be achieved at the end of 1993. All the present results obtained for local excitations have not been yet exploited. The last part of the experiment deals with a global excitation of the wing, putting it under an EMP simulator. All these results will be presented in the next Bordeaux EUROEM meeting, in June 1994.

5-2 Experiment on EMPTAC aircraft

ONERA and CEG have also been contacted by The Philipps Laboratory, in Albuquerque, New Mexico, to perform a topological experiment on their EMP Test Aircraft (EMPTAC). This aircraft is conceived in a topological way: two volumes, the forward shielded volume and the aft shielded volume are connected with an over shielded cable liaison, performing a sensible electrical function (figure 9). All other cables have been re-routed in the outside of both volumes to avoid unexpected wire penetrations paths into them. A first experiment, taking place at the beginning of November 1993, is going to characterise the coupling into the forward shielded volume.
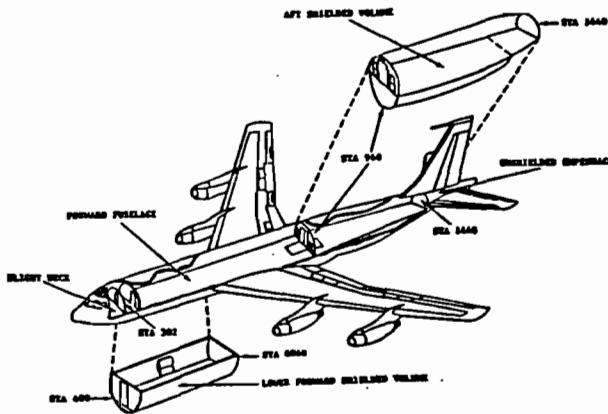

Figure 9: scheme of EMPTAC aircraft

6 Numerical calculation of EM interference in industrial programs

6-1 Study of the performances of the underframe wiring of a subway train

This work, supported by GEC Alsthom and Labinal companies, is the first industrial project in which topological concepts have been applied until now. The objective was to calculate induced currents on sensible cables, due to high, medium and low voltage transients into internal electrical devices of a subway train which is planed to be in exploitation in Paris in 1995. All the underframe wiring of motor and slip coaches have been modelled with tubes and junctions.

One interesting point of the study is that the work could not have been performed by applying direct circuit calculation without any topological considerations. Indeed, after simplifications, the global problem was made of about 900 wires, decomposed in about 150 tubes and junctions. This network could not be computed on common computers. What has really been done deals with a concatenation of subnetworks applying the calculation of equivalent S-parameters

and Thevenin equivalent model. By this way the size of the problem was reduced to about 170 wires, with about 30 tubes and junctions.

Such a study was an evidence that EM Topology could, from now on, be used for the conception of a structure in industrial problems. In the future, the introduction of normalised data, organised in data banks, would make the simulation process more convenient.

6-2 Study of the performances of a sensible wiring of a satellite

This work, supported by CNES, concerned the prediction of induced electrical signals into a network made of individual shielded cables running in a satellite. This will be dealt with in the lecture entitled "A numerical Approach in EMC at system level" in session B of this symposium.

7 Conclusion: future developments in EM Topology

Based on Multiconductor Line formalism, CRIPTE computer code applies EM Topology concepts on cable networks. It may be efficiently applied to lightning and EMP problems but some results higher than 100 MHz are promising. From now on, it gives helpful results:
- to analyse experimental data
- to predict and understand EM interference in internal problems
- to take elementary decisions on the shielding or the running of a harness.

The input data can be numerical or experimental. To apply EM Topology to complex industrial programs, the previous deterministic approaches developed on canonical structures become more and more statistical when applied on industrial type vehicles. But improvements are still necessary to apply it to big systems. The following improvements are already developed and validated at ONERA:
- iterative resolution methods of the BLT equation
- the coupling with 3D codes
- the numerical calculation of cable parameters
- the automatic experimental acquisition of cable parameters.

Until now, main studies dealt with the prediction of the exact value of a signal in one given geometrical configuration. With all the mentioned improvements, the objective of future work on EM Topology at ONERA, will be to use more statistics, giving an average value of a signal, or its probability of occurrence for several topologies.

References

[1] C.E. Baum: " The Theory of EM Interference Control", Interaction Notes, Note 478, December 28, 1989.

[2] J.P. Parmantier, G. Labaune, J.C. Alliot, P. Degauque: "EM Topology on complex systems: Topological Approach", La Recherche Aerospatiale, 1990, n°5, pp.57-70 (Interaction Note 488)

[3] J.L. Vetri, G.I. Costache: "An EM Interaction Modelling Advisor", IEEE Trans on EMC, Vol. 33, August 1991, pp. 241-251

[4] C.E. Baum, T.K. Liu, F.M. Tesche: "On the Analysis of General MTL Networks", Interaction Notes, Note 461, January 1988.

[5] J.P. Parmantier: "Approche topologique pour l'étude des couplages EM", Rapport de thèse de l'USTL, December 20, 1991.

[6] J.P. Parmantier: "Topologie EM: calcul des paramètres-S d'un sous-réseau", Proceedings du 6ème CEM symposium, Ecully, June 2-4, 1992, pp. 366-371

[7] J.P. Parmantier, G. Labaune, J.C. Alliot, P. Degauque: "EM Topology: Junction Characterisation Methods", La Recherche Aerospatiale, 1990, n°5, pp.71-82 (Interaction Note 489)

[8] P.Besnier: "Etude des couplages EM sur des réseaux de lignes de transmission non uniformes à l'aide d'une approche topologique", Rapport de Thèse de L'USTL, January 26, 1993.

[9] F. Issac: "Etude de la Topologie EM: application à une expérience sur caisson modulaire", Rapport Technique ONERA n°2/6727PY, October 1992, pp. 15-22

[10] J.P. Parmantier, P. Besnier, V. Gobin, B. Michielsen: "Etude des couplages sur avion par Topologie EM", Rapport final ONERA n°6/6727PY, pp. 58-70

[11] J.C. Clements, C.R. Paul, A. T. Adams: "Computation of the Capacitance Matrix for Systems of Dielectric-Coated Cylindrical Conductors", IEEE Trans. on EMC, Vol. 17, n°4, November, 1975

[12] M. Lemistre, J.P. Aparicio: "Caractérisation de câbles multiconducteurs: application au code de Topologie", Proceedings du 6ème CEM symposium, Ecully, June 2-4, 1992, pp.366-371

[13] V. Gobin, F. Issac, J.P. Aparicio, J. P. Parmantier, I. Junqua, A. Madore, D. Gautier:" Validation des concepts de Topologie EM sur une structure complexe", Proceedings du 6ème CEM symposium, Ecully, June 2-4, 1992, pp.366-371

[14] J.P. Parmantier, J.P. Aparicio: "EM Topology: Coupling of Two Wires Through an Aperture", Proceedings of the Zürich EMC symposium, March 1991, pp. 595-600

[15] A.K. Agrawal; H.J. Price, S.H. Gurbaxani: "Transient response of a MTL excited by a non uniform EM field", IEEE Trans. on EMC, Vol. 22, 1980

[16] J. Grando, V. Gobin, J.P. Parmantier, X. Ferrières: "Optimisation des codes numériques 3D", Rapport final ONERA n°10/6161PY, June 1993